arXiv:1411.7903v4 [hep-th] 11 Jul 2017

5d E_n Seiberg-Witten curve via toric-like diagram

Sung-Soo Kim, Futoshi Yagi

School of Physics,
Korea Institute for Advanced Study,
85 Hoegiro, Dongdaemun-gu
Seoul 130-722, Korea

E-mail: sungsoo.kim@kias.re.kr, fyagi@kias.re.kr

ABSTRACT: We consider 5d $Sp(1)$ gauge theory with E_{N_f+1} global symmetries based on toric(-like) diagram constructed from (p,q)-web with 7-branes. We propose a systematic procedure to compute the Seiberg-Witten curve for generic toric-like diagram. For $N_f = 6, 7$ flavors, we explicitly compute the Seiberg-Witten curves for 5d $Sp(1)$ gauge theory, and show that these Seiberg-Witten curves agree with already known $E_{7,8}$ results. We also discuss a generalization of the Seiberg-Witten curve to rank-N cases.

Contents

1   Introduction

Various aspects of supersymmetric gauge theories have been studied via branes, and rich physics associated with branes has been revealed. Wide class of four-dimensional $\mathcal{N} = 2$ supersymmetric gauge theories are given by D4-NS5 brane setup, whose asymptotic distance of the NS5 branes gives 1-loop correction to the gauge coupling constant. The condition that NS5 branes do not intersect gives the asymptotic free/conformal condition of the gauge theory. Furthermore, the M-theory uplift of the corresponding brane setup gives Seiberg-Witten (SW) curve [1].

Five-dimensional uplift of this derivation of SW curve from branes was studied in [2] for the case with simple Lie groups like SU, SO, Sp, and extended to more general setup by using (p, q) 5-brane web in [3]. The method with (p, q) 5-brane web gives a systematic and simple procedure to derive the SW curve, using the dual graph of the 5-brane web whose vertices correspond to the non-vanishing coefficients of the polynomial describing the curve. In [3], it was discussed that five-dimensional $Sp(1)$ ($\simeq SU(2)$) gauge theories could be studied up to four flavors by this (p, q) 5-brane web[1]. As five-dimensional theories are given as natural uplift of four-dimensional gauge theories, studying the case with more than four flavors via the (p, q) 5-branes seemed not so straightforward. As discussed, for example, in [5], more flavors lead to the intersection of NS5-branes analogously to the four-dimensional case, which makes it hard to interpret.

On the other hand, five-dimensional $Sp(1)$ gauge theory with N_f flavors is expected to have nontrivial UV fixed point up to [2] $N_f \leq 7$ [6], where the global symmetry enhancement

---

[1]In this paper, we do not consider O-planes. If one introduces it, 5-brane web can describes up to six flavors [4].

[2]UV fixed point of the five-dimensional $Sp(1)$ theory with eight flavors is believed to be six-dimensional. Although this case is also interesting, we do not study in this paper.

to E_{N_f+1} group is realized. Such class of isolated conformal field theories (CFT) has been studied in various different methods. Recently, the global symmetry enhancement was explicitly checked in [7] by computing the superconformal index (up to $N_f = 5$), and confirmed later up to $N_f = 6, 7$ in [8]. It was also shown that the Nekrasov partition function is invariant under the enhanced E_{N_f+1} symmetry when one expands it in terms of the properly redefined Coulomb moduli parameter [9], where fiber-base duality [3, 10–12] plays an important role.

The SW curves for corresponding four-dimensional theory with $E_{6,7,8}$ global symmetries were studied in [13, 14]. These curves were obtained from dimensional analysis and symmetry argument without referring to specific field theory description at UV. Uplift of the SW curves to five dimensions [15] and to six dimensions [16, 17] was performed via the effective action of the E-string theory, which is obtained by compactification to the corresponding local del Pezzo surface or half K3 manifold. When the geometry is toric, the corresponding SW curve can be computed also from the toric diagram which can be reinterpreted as the dual graph of the (p,q) 5-brane web [18]. It followed that the SW curve for five-dimensional $Sp(1)$ gauge theory with $N_f \leq 4$ flavors was reproduced as mirror curve of the corresponding Calabi-Yau geometry [19]. While it can be toric for $N_f \leq 5$, the corresponding local del Pezzo surfaces for $N_f = 6, 7$ are non-toric, and thus there have been difficulties finding corresponding (p,q) 5-brane web diagrams.

Such obstacles seem avoidable in the brane setup introduced in [20] which thus opens up a possibility to analyze the $Sp(1)$ gauge theory with more than four flavors in the (p,q) 5-brane setup. It is $[p,q]$ 7-branes at infinity that resolve the non-toric nature of dual diagrams, each of which binds an arbitrary number of (p,q) 5-branes. Some of the bound 5-branes "jump over" other 5-branes in such a way not to break the s-rule. The brane setup in [20] was originally introduced as a five-dimensional uplift of isolated CFTs discussed in [21]. It includes five-dimensional CFT of E_6, E_7 and E_8 global symmetries, which are expected to be identified as the UV fixed point of the $Sp(1)$ gauge theories with five, six and seven flavors, respectively.

It was known that the five-dimensional $Sp(1)$ gauge theory with N_f flavors can be realized by adding N_f D7-branes inside the 5-brane loop of the pure $Sp(1)$ brane setup, and that the global symmetry enhancement to E_{N_f+1} can be shown from the monodromy properties of 7-branes [22, 23]. More intuitive and relevant explanation connecting D7-branes inside the 5-brane loop to 7-branes at infinity leading to E_6 symmetry was presented in [24] for $N_f = 5$ where the brane setup with E_{N_f+1} symmetry studied in [20] can be derived by properly pulling out all the 7-branes outside by the Hanany-Witten effect.

With this brane setup, the SW curve for $Sp(1)$ with five flavors was computed in [20, 24] and is in agreement with the aforementioned result [15–17]. Moreover, by generalizing the relation between toric (p,q) 5-brane web and toric diagram discussed in [18], the superconformal index/Nekrasov partition function in [7, 8] were reproduced from the computations of topological string partition function [24–26]. Throughout this paper, such dual graph of the original (p,q) 5-brane web diagram, introduced in [20], we call "toric-like diagram" as the counterpart of the toric diagram. In this paper, we develop a systematic way of computing the SW curve for the five-dimensional theory with $N_f = 6, 7$ flavors

based on the toric-like diagram.

The rest of this paper is organized as follows: In section 2, we review the derivation of SW curve of five-dimensional $Sp(1)$ gauge theory with $N_f = 5$ flavors [24], which is identified as five-dimensional T_3 theory. Throughout this review, we clarify generic procedure to compute SW curve from toric-like diagram. In section 3 and 4, we compute the SW curve for the theory with $N_f = 6$ and $N_f = 7$ flavors, respectively. We present the SW curves obtained based on three representative web diagrams which are related by the Hanany-Witten transitions, and then show that each of these curves is obtained from another one simply by taking a proper coordinate transformation, thus demonstrating that the Hanany-Witten transition is realized in the SW curve as a coordinate transformation. We also show that the obtained curves agree with the known results [15–17]. In section 5, we study mass decoupling limit to reproduce the SW curve for lower flavors from the curve for higher flavors, especially from $N_f = 7$ to $N_f = 6$. In section 6, we consider the SW curve obtained from the toric-like web diagram corresponding to higher rank E_n theory given in [20] and shows that the rank-2 curve actually factorizes into the two copies of the SW curve for the rank-1 E_n theory. We then conclude and discuss the observed relation[3] analogous to the special case of $\mathcal{N} = 2$ dualities [21]. In Appendices, we give various complimentary computation and results of the SW curves for $Sp(1)$ theory with N_f flavors.

2   5d Seiberg-Witten curve from toric-like diagram

In this section, after reviewing the SW curve of the 5d T_3 theory which is identified as 5d $Sp(1)$ theory with five flavors, we propose a procedure to derive the SW curve from generic toric-like diagram.

2.1   5d T_3 theory

5d version of 4d T_N theories was studied based on the web or dual toric diagrams [20] where it describes M-theory compactified on a non-compact CY threefold. The dual toric diagram is obtained by associating a vertex to each face of 5-brane junctions. For a single junction, T_1, it corresponds to $\mathbb{C}^3$ and for multi-junctions, T_N, it corresponds to $\mathbb{C}^3/(\mathbb{Z}_N \times \mathbb{Z}_N)$. Upon compactification on S^1, it gives rise to 4d T_N constructed in [21].

We now briefly review 5d T_3 theory in relation with its SW curve. A detail analysis for T_3 theory has been done in [24]. Rather than summarizing the result of [24], we here point out salient features of the analysis and then use this T_3 theory to give an intuitive idea on how the SW curves for E_7 and E_8 can be derived.

As shown in [20], the 5d uplift of rank-1 4d T_N theories well fits into the multi-junction of the 5d (p, q) web. 4d Minahan-Nemenschansky's isolated superconformal theories with the exceptional E_n symmetry can be uplifted and studied in this framework. For instance, in 5d, the $N_f = 5$ superconformal theory with E_6 global symmetry at the UV fixed point

---

[3]Although this relation should be closely related to [27], we give slightly different interpretation. Our observation is closer to the one in [24].

corresponds to T_3 theory; the $N_f = 6, 7$ superconformal theory with E_7, E_8 global symmetry corresponds to a Higgsed T_4, T_6 (to keep one Coulomb modulus) theory, respectively.

E_n symmetries realized in the framework is not manifest, only subgroup of E_n is manifest. As an instructive example, we consider T_3 theory. It has the following web diagram or corresponding dual toric diagram:
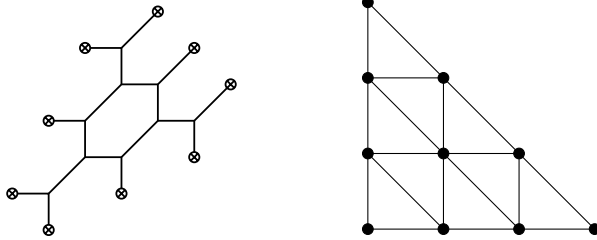

Figure 1. A toric diagram for E_6

As the diagram indicates, it has manifest $SU(3)^3$ global symmetry which is a maximal compact subgroup of E_6

$$E_6 \supset SU(3) \times SU(3) \times SU(3). \tag{2.1}$$

Using the Hanany-Witten transition (as well as monodromy of 7-brane branch cut), we can explain that this diagram is related to the diagram of five flavors ($N_f = 5$). In the (p, q) 5-brane web configuration, the matters are represented by semi-infinite $(1, 0)$ 5-branes. We introduce $[p, q]$ 7-branes such that (p, q) 5-branes can end without breaking supersymmetry. See Figure 2.
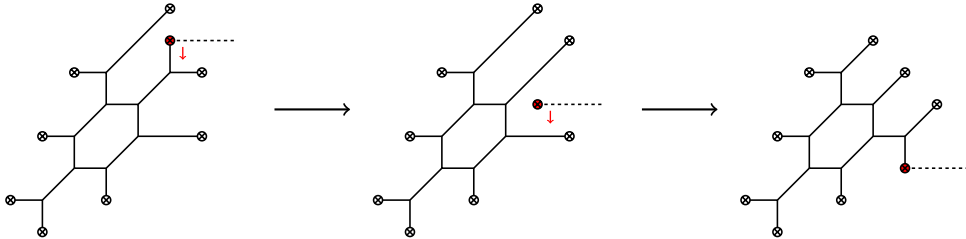
Figure 2. A brane configuration with five flavors leading to T_3-diagram.

Let us imagine a web diagram with five $(1, 0)$ 5-branes ending on 7-branes (denoted by $\otimes$). For convenience, we put three on the left and two on the right. This is the leftmost web diagram configuration in Figure 2. In order to avoid colliding of 7-branes, we bring down the $[0, 1]$ 7-brane filled in red. Recall that this $[0, 1]$ 7-brane has a branch cut denoted by the dashed line. When the $[0, 1]$ 7-brane passes through a (p, q) 5-brane, the charge of the 5-brane changes as it experiences monodromy due to the $[0, 1]$ 7-brane. For instance, as depicted in the middle of Figure 2, $(1, 0)$ 5-brane charge is altered to $(1, 1)$ as the $[0, 1]$ 7-brane passes through it. As it is brought to further down, the web configuration becomes the web diagram of T_3, which is the rightmost Figure 2.

It is interesting to see what happens to the web diagram if one pushes up the $[0,1]$ 7-brane rather than bringing it down. See Figure 3.
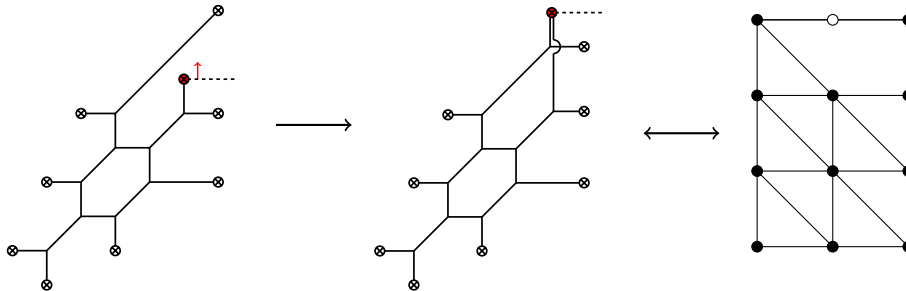

Figure 3. A brane configuration with five flavors leading to a toric-like diagram.

As explained in [20], the $[0,1]$ 7-brane jumps over the $(1,1)$ 5-brane when crossing, and another $(0,1)$ 5-brane is created to attach to the $[0,1]$ 7-brane (the Hanany-Witten effect). The resultant dual toric-like diagram involves a new kind of dot (white dot) to indicate this jumping phenomenon associated with binding multiple 5-branes attached to a single 7-brane. In this way, the number of the Coulomb moduli remains unaltered. This dual toric-like diagram was called a dot diagram in [20].

If the white dot above were a black dot, it would increase the number of both the dimension of the Coulomb moduli and triangulation, hence it would be a toric diagram for $SU(3)$ gauge theory. Notice that in this specially tuned web diagram or toric-like diagram in Figure 3, it appear to have six flavors coming from six $(1,0)$ 5-branes. This implies that the manifest global symmetry is no longer $SU(3)^3$ but it is $S[U(3) \times U(3)] \times SU(2)$. Turning a black dot into a white dot can be interpreted as a procedure of Higgsing. But we call it a special tuning, as the it can be understood as a procedure keeping dimension of the Coulomb moduli to be one. We then say that it provides a dual picture of the $SU(2)$ theory of E_6 symmetry as a special tuning of $SU(3)$ gauge theory with six flavors.

It is clear that the toric diagram for the T_3 theory can be given in a different way through the Hanany-Witten transition as explained. This means that as one writes the SW curve based on a toric diagram, two SW curves obtained from two different toric diagrams should be related by the Hanany-Witten effect. We emphasize that the way that the Hanany-Witten effect is realized in the SW curve is a coordinate transformation. It is also worth noting that as a toric diagram shows manifest global symmetry, one can find different manifest symmetry by the Hanany-Witten transition. As we will show later, we find that the Hanany-Witten transition on a given (tuned) T_N theory gives rise to different compact subgroups of E_n symmetry.

We now consider the construction of the SW curve. For this, we compactify the theory on a circle, and T-dualize it to become IIA theory, and then we uplift it to M-theory. The curve then describes M5 brane configuration embedded in $\mathbb{R}^2 \times T^2$. Given a toric diagram, say Figure. 1, the SW curve takes the form as

$$\sum_{ij} c_{ij} \, t^i \, w^j = 0, \tag{2.2}$$

with the SW one-form

$$\lambda_{SW} = \log t \; \mathrm{d}(\log w). \tag{2.3}$$

Here, c_{ij} in (2.2) is the non-vanishing coefficient that corresponds to the (i,j) dot in the toric diagram.
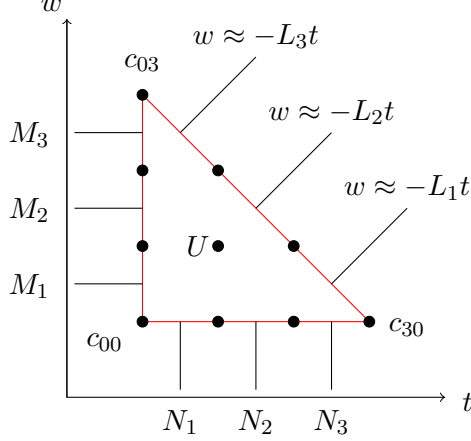

Figure 4. The configuration for the SW curve of T_3 toric diagram

For instance, consider the configuration for the T_3 toric diagram given in Figure 4. There are 10 coefficients c_{ij} which can be determined from the boundary conditions. Here, we impose the following boundary condition

$$
\begin{aligned}
t &= N_1, N_2, N_3 \quad \text{as} \quad w \to 0 \\
w &= M_1, M_2, M_3 \quad \text{as} \quad t \to 0 \\
w &= -L_1 t, -L_2 t, -L_3 t \quad \text{as} \quad |t| \sim |w| \to \infty,
\end{aligned}
\tag{2.4}
$$

where the first, second and third lines in Figure 4 correspond to three NS5-branes, three D5-branes and three (1,1) 5-branes, respectively, in the original type IIB picture. These conditions yield the constraints to the coefficients:

$$
\begin{aligned}
\sum_{i=0}^{3} c_{i0} t^i &= c_{30}(t - N_1)(t - N_2)(t - N_3), \\
\sum_{j=0}^{3} c_{0j} w^j &= c_{03}(w - M_1)(w - M_2)(w - M_3), \\
\sum_{j=0}^{3} c_{i,3-i} t^i w^{3-i} &= c_{03}(w + L_1 t)(w + L_2 t)(w + L_3 t),
\end{aligned}
\tag{2.5}
$$

which enables us to express the coefficients c_{ij} in terms of L_i, M_i, and N_i. In order for these conditions to be consistent, we find that the following compatibility conditions are necessary

$$M_1 M_2 M_3 = N_1 N_2 N_3 \cdot L_1 L_2 L_3. \tag{2.6}$$

This means that one of the constraint equations in (2.5) is used not to determine the coefficient but to determine this compatibility condition. Since the SW curve does not change when we multiply an identical constant to all the coefficients, this degree of freedom can be also used to determine one coefficient as we like. Including this, we can determine 9 coefficients out of 10 in (2.2). The undetermined coefficient c_{11} corresponds to the internal dot in the toric diagram in Figure 4 and is not affected by the boundary condition. This coefficient c_{11} is interpreted as the Coulomb moduli parameter and we denote it as U.

Using the degrees of freedom of rescaling t and w, we can further impose the conditions on N_i and M_i. Together with the compatibility condition, it is convenient to impose

$$M_1 M_2 M_3 = N_1 N_2 N_3 = L_1 L_2 L_3. \tag{2.7}$$

It is then straightforward to find the curve corresponding to the toric diagram, Figure 4:

$$w^3 - \sum_i M_i w^2 + \sum_i L_i w^2 t + \sum_i M_i^{-1} w + Uwt$$
$$+ \sum_i L_i^{-1} wt^2 - 1 + \sum_i N_i^{-1} t - \sum_i N_i t^2 + t^3 = 0. \tag{2.8}$$

The procedure to move from the diagram in Figure 4 to the one in Figure 3 by moving the [0,1] 7-brane in Figure 4 at $t = N_3$ upward by using Hanany-Witten effect can be realized by the coordinate transformation

$$w = W(t - N_3). \tag{2.9}$$

With this transformation, the SW curve (2.8) can be expressed as

$$(t - N_3)^2 W^3 + (t - N_3) \left(\sum_i L_i t - \sum_i M_i \right) W^2$$
$$+ \left(\sum_i L_i^{-1} t^2 + Ut + \sum_i M_i^{-1} \right) W + (t - N_1)(t - N_2) = 0, \tag{2.10}$$

where we have divided entire equation by the factor $(t - N_3)$. Although the corresponding diagram in Figure 3 includes a white dot, every dots correspond to non-vanishing coefficients of the SW curve. However, compared to the SW curve corresponding to the usual toric diagram, we find that the coefficients are tuned to be specific values. That is, some extra conditions are imposed to this SW curve due to the white dot. Writing the left hand side of (2.10) as $\sum_{i,j} c_{ij} t^i W^j$, it is straightforward to see that this SW curve satisfies the
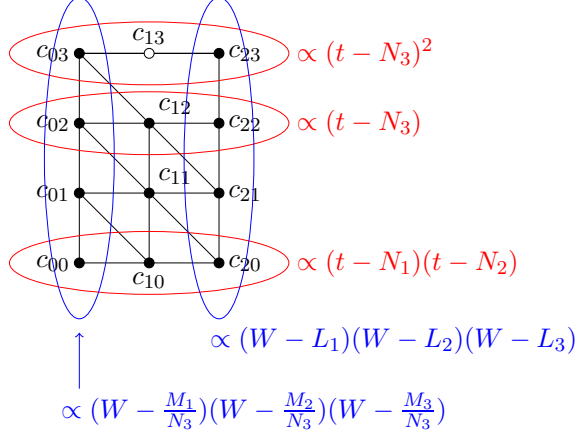
Figure 5. The boundary conditions toric-like diagram for E_6.

following relation:

$$\sum_{i=0}^{2} c_{i3} t^i \propto (t - N_3)^2, \qquad \sum_{i=0}^{2} c_{i2} t^i \propto (t - N_3),$$

$$\sum_{i=0}^{2} c_{i0} t^i \propto (t - N_1)(t - N_2),$$

$$\sum_{j=0}^{3} c_{2j} W^j \propto (W - L_1)(W - L_2)(W - L_3),$$

$$\sum_{j=0}^{3} c_{0j} W^j \propto \left(W - \frac{M_1}{N_3}\right)\left(W - \frac{M_2}{N_3}\right)\left(W - \frac{M_3}{N_3}\right), \tag{2.11}$$

which we interpret as the constraints coming from the boundary conditions.

As depicted in Figure 5, the white dots in the toric-like diagram is associated with the first line of (2.11). The first relation, which gives the leading behavior at $W \to \infty$, is consistent with the two NS5-branes are coincident, bound by one [0,1] 7-brane. Furthermore, as for the second relation, which gives the subleading contribution in the region $W \to \infty$, we would like to interpret that this is the consequence that one out of two coincident NS5-branes jumps over the other 5-brane. The remaining three relations from the third to the fifth are more straightforward to give the interpret. They correspond to the boundary conditions for two NS5-branes at $W \to 0$, three external D5-branes at $t \to \infty$, and three more external D5-branes at $t \to 0$.

It is worth noting that these boundary conditions (2.11) together with our convention (2.7) are enough to reproduce the SW curve (2.10). This example gives us an intuition of what kind of boundary condition we should impose, if we have white dots in a generic toric-like diagram. In the following, we discuss how the boundary conditions yields the SW curve in more details.

2.2 General procedure

Based on the computation of the SW curve for E_6 theory, we propose a systematic procedure of deriving the SW curve from any given toric-like diagram.

If all the vertices are black dots, it is a usual toric diagram and thus the SW curve is given by

$$\sum_{(i,j)\in\text{vertices}} c_{ij}t^i w^j = 0, \tag{2.12}$$

where (i,j) are summed over all the vertices in the diagram. The coefficients c_{ij} corresponding to the dots on the boundary edge of the toric diagram are determined by the boundary condition for the external (p,q) 5-branes. These boundary conditions are given in the form

$$w^p t^{-q} \sim \tilde{m}_n^{(p,q)} \qquad \text{at} \qquad |w|^q \sim |t|^p \to \infty, \tag{2.13}$$

where this $\tilde{m}_n^{(p,q)}$ corresponds to the "mass parameter"[4]. For example, the first line in (2.4) is obtained by identifying $p = 0$, $q = -1$ and $\tilde{m}_n^{(-1,0)} = N_n$. These boundary conditions give the constraints

$$\sum_{\substack{(ij)\\ ip+jq=N_{i,j}}} c_{i,j}t^i q^j \propto \prod_n (w^p - \tilde{m}_n^{(p,q)}t^q), \tag{2.14}$$

where $N_{i,j}$ is the maximum of the value $ip + jq$ among all the combination of (i,j) corresponding to the vertex in the toric diagram. In other words, the (i,j) is summed over the vertex on the boundary edge which is perpendicular to the considered (p,q) 5-brane. We impose this boundary condition corresponding to all the external (p,q) 5-branes and solve for $c_{i,j}$. Note that in order for a solution to exist, there must be one constraint among all the mass parameters.

Generic toric-like diagram is obtained by converting some of black dots into white dots in toric diagram. This procedure corresponds to the tuning of the coefficients c_{ij}. Therefore, the SW curve is still the same form as (2.12) but more conditions are added to the coefficients. Suppose that n-th (p,q) 7-brane binds k_n external (p,q) 5-branes. In this case, the boundary conditions are of the following sets of constraint

$$\sum_{\substack{(ij)\\ ip+jq=N_{i,j}}} c_{i,j}t^i q^j \propto \prod_n (w^p - \tilde{m}_n^{(p,q)}t^q)^{k_n},$$

$$\sum_{\substack{(ij)\\ ip+jq=N_{i,j}-1}} c_{i,j}t^i q^j \propto \prod_n (w^p - \tilde{m}_n^{(p,q)}t^q)^{\max(k_n-1,0)},$$

$$\dots$$

$$\sum_{\substack{(ij)\\ ip+jq=N_{i,j}-\ell}} c_{i,j}t^i q^j \propto \prod_n (w^p - \tilde{m}_n^{(p,q)}t^q)^{\max(k_n-\ell,0)},$$

$$\dots \tag{2.15}$$

---

[4]The "mass parameter" here is not physical mass of the gauge theory. It is typically the exponential of some linear combination of masses and inverse gauge coupling with some shift.

These sets of constraints are understood as natural generalization of the first two conditions in (2.11).

2.3 Comment on general procedure

In the previous subsection, we proposed the procedure to derive SW curve from generic toric-like diagram. In this subsection, we discuss that this procedure can be understood as a natural 5d uplift of the SW curve for the following D4-NS5 brane setup with flavor D6-branes [1].

To begin with, we review the related result in [1]. Suppose that we have $n + 1$ NS5-branes labeled by $\alpha = 0, 1, \cdots, n$. Between α-th NS5-brane and $(\alpha - 1)$-th NS5-brane, k_α color D4 branes are suspended ($\alpha = 1, \cdots, n$). Moreover, $(i_\alpha - i_{\alpha-1})$ D6-branes exist between α-th NS5-brane and $(\alpha - 1)$-th NS5-brane at the place $v = e_a$ with $a = i_{\alpha-1} + 1, \cdots, i_\alpha$, where we set $i_0 = 0$. In this setup, no D4-branes are attached to any of the D6-branes. The D6-branes are uplifted to the Taub-NUT space in the M-theory, which is defined by

$$\frac{y}{z} = \prod_{a=1}^{i_n}(v - e_a) = \prod_{s=1}^{n} J_s(v), \tag{2.16}$$

embedded in $\mathbb{C}^3$ with three complex coordinates[5] y, z, and v, where we put

$$J_s(v) = \prod_{a=i_{s-1}+1}^{i_s}(v - e_a). \tag{2.17}$$

It is known that the SW curve is given in the following form:

$$y^{n+1} + g_1(v)y^n + g_2(v)J_1(v)y^{n-1} + g_3(v)J_1(v)^2 J_2(v)y^{n-2}$$
$$+ \cdots + g_\alpha(v)\prod_{s=1}^{\alpha-1} J_s(v)^{\alpha-s} \cdot y^{n+1-\alpha} + \cdots + f\prod_{s=1}^{n} J_s(v)^{n+1-s} = 0, \quad (2.18)$$

where $g_\alpha(v)$ are polynomials of degree k_α. Or, if we change the coordinate from y to z by using (2.16), it reads

$$\prod_{s=1}^{n} J_s^s \cdot z^{n+1} + g_1(v)\prod_{s=2}^{n} J_s^{s-1} \cdot z^n + g_2(v)\prod_{s=3}^{n} J_s^{s-2} \cdot z^{n-1}$$
$$+ \cdots + g_\alpha(v)\prod_{s=\alpha+1}^{n} J_s^{s-\alpha} \cdot z^{n+1-\alpha} + \cdots + g_{n-1}(v)J_n(v)z + f = 0. \quad (2.19)$$

In order to connect this results to our proposal, we reinterpret this in a slightly different way. Instead of placing the D6-branes between the NS5-branes without any D4 branes attached, we can move these D6-branes horizontally to infinity using the Hanany-Witten effect. Suppose that we move all the D6-branes to the direction of the outside of the 0-th

---

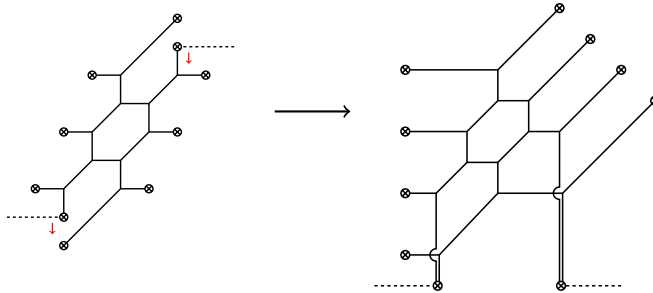[5]Our z corresponds to z^{-1} in [1].

Figure 6. $N_f = 6$ brane configuration (left) and a tuned T_4 diagram after Hanany-Witten transitions (right).

NS5-brane. Through this process, the $(i_\alpha - i_{\alpha-1})$ D6-branes originally placed between α-th NS5-brane and $(\alpha - 1)$-th NS5-brane pass through NS5-branes α times, and thus each D6 brane binds α D4-branes. The bound D4-branes jump over NS5-branes properly in such a way to avoid breaking the s-rule. In this setup, since D6-branes are placed at infinity, the space is not Taub NUT space anymore but just flat $\mathbb{C}^2$.

We reinterpret (2.19) as the M5-brane configuration for this situation, where the space is now flat $\mathbb{C}^2$ spanned by the two coordinates v and z. All the D6-branes now exist at the region $z \to \infty$, and the first term in (2.19) is consistent with the situation that $(i_s - i_{s-1})$ D6-branes bind s D4-branes each. The second term has also the factor J_s but with one power less. As we decrease the power of z, the power of J_s also reduces one by one. We claim that this is the counterpart of our proposal (2.15). What is generalized in our proposal is that we consider not only for $D7$-branes but also for arbitrary $[p,q]$ 7-branes. This generalization appears only when we uplift to five dimensions.

We note that with this reinterpretation, we find that (2.16), which originally defines the multi Taub NUT space, can be seen as the coordinate transformation to move the external D4-branes from one side to the other side by the Hanany-Witten transition, which is the analogue of (2.9). Then, the curve (2.18) is also consistent with this interpretation, where the $(i_\alpha - i_{\alpha-1})$ D6-branes originally placed between α-th NS5-brane and $(\alpha - 1)$-th NS5-brane bind $n + 1 - \alpha$ D4-branes each. An analogous consistency check is also possible for our examples dealt in this paper. That is, even after such coordinate transformation, our proposal (2.15) is still satisfied.

3 E_7 Seiberg-Witten curve

In this section, we compute the Seiberg-Witten curve for 5d Sp(1) theory $N_f = 6$ flavor based on toric-like diagram. After constructing the corresponding toric-like diagram, we compute the SW curve using the technique developed in the previous section. Then, we check that it is consistent with the known expression written in E_7 invariant manner [16, 17]. We also study the 4d limit of the 5d SW curve and show that it reproduces the expected curve [21].

3.1 Construction of the toric-like diagram

Let us first start by adding one more flavor to the brane configuration for $N_f = 5$, for instance, the first diagram of Figure 6. As shown for the $N_f = 5$ case leading to T_3 diagram, it is then straightforward to obtain a tuned T_4 diagram, via successive use of the Hanany-Witten transition.
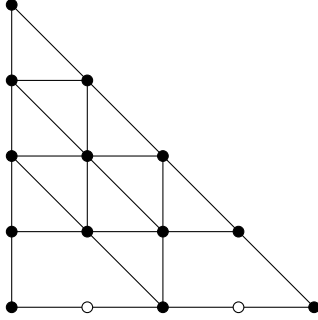

Figure 7. A toric-like diagram for the $SU(2)$ theory with $N_f = 6$ flavors. It can be viewed as a tuned T_4 diagram. It has manifest $SU(4) \times SU(4) \times SU(2)$ symmetry, but it is invariant under which E_7 symmetry

The corresponding toric-like diagram is given in Figure 7. This is a T_4 diagram that is specially tuned to have only one Coulomb modulus. It has manifest global symmetry $SU(4) \times SU(4) \times SU(2)$, which is a maximal compact subgroup of E_7.

As discussed in section 2.1, the curve can be seen in various ways through the Hanany-Witten transition. For instance, one can push a 7-brane upward instead of bringing it downward. This gives a rectangular shape toric-like diagram, which has manifest $S[U(4) \times U(4)]$ symmetry. See Figure 8. It follow from the figure that the $SU(2)$ theory with $N_f = 6$ flavors can be viewed as a a special case of toric diagram for $SU(4)$ gauge theory with $N_f = 8$ flavors.
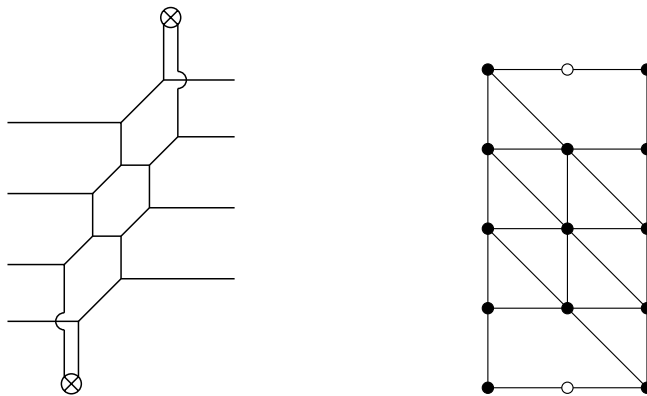

Figure 8. Left: Another web diagram for the $SU(2)$ theory with $N_f = 7$ flavors. We use $\otimes$ to denote the 7-brane that combine 5-branes. Right: Another toric-like diagram for E_7. It has manifest $S[U(4) \times U(4)]$ symmetry. This can be viewed as a tuned toric diagram for $SU(4)$ gauge theory with eight flavors.
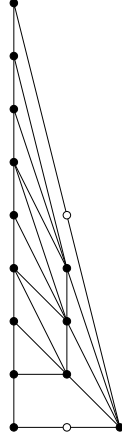
Figure 9. A toric-like diagram for the $SU(2)$ theory with $N_f = 6$ flavors. It has manifest $SU(8)$ symmetry

We can further apply the Hanany-Witten to other 7-branes. For instance, let us move all the $[1,0]$ 7-branes on the right hand sides of Figure 8 to the left. We then obtain the toric-like diagram given in Figure 9. This toric-like diagram has manifest $SU(8)$ symmetry, which is again a maximal subgroup of E_7.

3.2 $N_f = 6$ Seiberg-Witten curve from M-theory

We now have at least three toric-like diagrams describing the $SU(2)$ theory with $N_f = 6$ flavors. Let us call the diagrams as the tuned T_4 digram for Figure 7, the rectangular diagram for Figure 8, and the long triangle diagram for Figure 9. In this subsection, we compute the SW curve for each diagram following the procedure discussed in section 2.2. We then explicitly show that the curves are related by a proper coordinate transformation confirming that the Hanany-Witten transition is realized as a coordinate transformation in the SW curve.

3.2.1   Seiberg-Witten curve from the tuned T_4 diagram

Before computing the SW curve from Figure 7, we first briefly mention the curve for T_4 theory, which corresponds to the diagram obtained by replacing all the white dots into black dots in Figure 10. The SW curve is written in the form.

$$\sum_{\substack{p \geq 0, q \geq 0 \\ p+q \leq 4}} c_{pq} t^p w^q = 0. \tag{3.1}$$

We then impose the following conditions. The polynomial at asymptotic region behaves

$$t \sim w \to \infty \quad : \quad \sum_{p=0}^{4} c_{p,4-p} t^p w^{4-p} = c_{04} \prod_{i=1}^{4} (w + L_i t),$$

$$t \to 0 \quad : \quad \sum_{q=0}^{4} c_{0q} w^q = c_{04} \prod_{i=1}^{4} (w - M_i),$$

$$w \to 0 \quad : \quad \sum_{p=0}^{4} c_{p0} t^p = c_{40} \prod_{i=1}^{4} (t - N_i), \tag{3.2}$$

from which we can obtain the T_4 SW curve. The coefficients c_{11}, c_{12}, and c_{21} are not determined from the above conditions and are treated as the Coulomb moduli parameters. This T_4 theory corresponds to the 5d uplift of sphere with three full punctures in 4d setup [21].
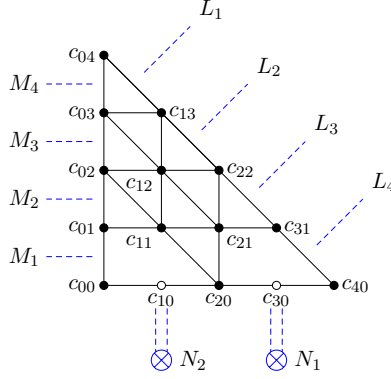
Figure 10. Coefficients in the tuned T_4 diagram

Now, we move on to the SW curve for the $SU(2)$ theory with $N_f = 6$ flavors. In 4d, E_7 theory is obtained by replacing one of the full punctures with the degenerate one. In 5d, it is equivalent to replacing some of the black dots into the white dots in the toric-like diagram as in Figure 10. Let us apply the generic procedure discussed in section 2.2. Structurally, the SW curve is still of the form (3.1), but the conditions (3.2) are replaced by the following ones:

$$t, w \to \infty \quad : \quad \sum_{p=0}^{4} c_{p,4-p} t^p w^{4-p} = c_{0,4} \prod_{i=1}^{4} (w + L_i t),$$

$$t \to 0 \quad : \quad \sum_{q=0}^{4} c_{0,q} w^q = c_{0,4} \prod_{i=1}^{4} (w - M_i),$$

$$w \to 0 \quad : \quad \sum_{p=0}^{4} c_{p,0} t^p = c_{4,0} \prod_{i=1}^{2} (t - N_i)^2, \qquad \sum_{p=0}^{4} c_{p,1} t^p \propto \prod_{i=1}^{2} (t - N_i). \tag{3.3}$$

This amounts not only to put $N_3 = N_1$, $N_4 = N_2$ but also gives rise to to one more condition which is the last condition in (3.3) This extra condition enables us to determine c_{11} and

c_{21} in terms of physical parameters. Recall that these coefficients are the Coulomb moduli parameters in T_4 case, and tuning the T_4 keeping only one modulus, these coefficients are no longer Coulomb moduli parameters. This is the effect of "degenerating puncture".

The next thing we do is to determine the coefficients c_{ij} from the boundary conditions (3.3). There are 15 dots in the toric-like diagram in Figure 10, which means that we have 15 non-zero coefficients in the SW curve (3.1). Naive counting says that the conditions (3.3) give 14 relations between the coefficients c_{ij} and the parameters L_i, M_i, N_i. However, not all the relations are independent. For instance, three relations including c_{00}, c_{04}, c_{40} are given as

$$c_{40} = c_{04} \prod_i^4 L_i, \qquad c_{00} = c_{04} \prod_i^4 M_i, \qquad c_{00} = c_{40} \prod_i^2 N_i{}^2, \tag{3.4}$$

which lead to one compatibility condition on the parameters L_i, M_i, N_i

$$\prod_{i=1}^4 M_i = \prod_{j=1}^4 L_j \cdot \prod_{k=1}^2 N_k{}^2. \tag{3.5}$$

That is, one out of the 14 relations gives this compatibility condition rather than determining the coefficients. It means out of the 15 coefficients, one can determine 13 coefficients. Two remaining undetermined coefficients can be identified as follows: one can be identified as an overall constant and the other plays a role of the Coulomb modulus U of the theory which is the black dot in the middle of the toric diagram, c_{11}.

As shifting along the t- and w-axes is irrelevant, one can say that there are three rescaling degrees of freedom one can freely choose (overall constant, shifts in t and w coordinates). For an overall constant, we choose

$$c_{04} = 1. \tag{3.6}$$

With the rescaling of t and w, we can choose, $N_1 N_2 = 1$ and $\prod_{i=1}^4 M_i = 1$, respectively. Together with the compatibility condition (3.5), we obtain

$$\prod_{i=1}^4 L_i = \prod_{i=1}^4 M_i = \prod_{i=1}^2 N_i = 1. \tag{3.7}$$

The resulting Seiberg-Witten curve is then written as

$$w^4 + (\chi_1(L)t - \chi_1(M)) w^3 + (\chi_2(L)t^2 + c_{12}t + \chi_2(M)) w^2$$
$$+ (t - N_1)(t - N_2) (\chi_3(L)t - \chi_3(M)) w + (t - N_1)^2 (t - N_2)^2 = 0, \tag{3.8}$$

where, $\chi_i(X)$ is the character of $SU(4)$ defined as

$$\chi_n(X) = \sum_{1 \leq i_1 \leq i_2 \leq \cdots \leq i_n \leq 4} X_{i_1} X_{i_2} \cdots X_{i_n}. \tag{3.9}$$

As the SW curve is obtained from the tuned T_4 diagram in Figure 10, manifest symmetry is $SU(4) \times SU(4) \times SU(2)$ and the curve is the curve is expressed in terms of the characters of $SU(4) \times SU(4) \times SU(2)$.
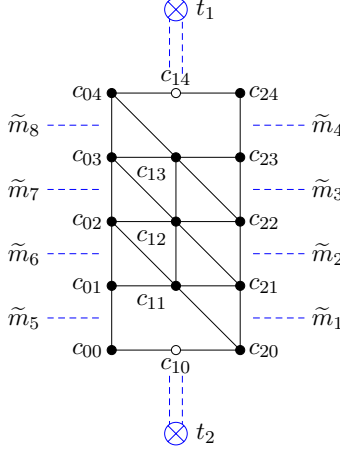
Figure 11. Coefficients in the rectangular diagram

3.2.2 Seiberg-Witten curve from the rectangular diagram

We now discuss the SW curve corresponding to the diagram in Figure 8. This rectangular diagram is obtained by moving one of the $[0, 1]$ 7-brane in Figure 7 to upward by Hanany-Witten transition. As mentioned in section 2.2, such Hanany-Witten transition can be realized by the coordinate transformation

$$w \to w(t - N_1), \tag{3.10}$$

which moves $[0, 1]$ 7-brane at $t = N_1$ upward. By substituting (3.10) to (3.8) and by multiplying the factor $(t - N_1)^{-2}$, we obtain

$$(t - N_1)^2 w^4 + (t - N_1) \left(\chi_1(L)t - \chi_1(M) \right) w^3 + \left(\chi_2(L)t^2 + C_{12}t + \chi_2(M) \right) w^2$$
$$+ (t - N_2) \left(\chi_3(L)t - \chi_3(M) \right) w + (t - N_2)^2 = 0. \tag{3.11}$$

It is also possible to obtain the SW curve from the rectangular diagram in Figure 8 or Figure 11 directly. The curve should take the form of the polynomial

$$\sum_{i=0}^{2} \sum_{j=0}^{4} c_{ij} t^i w^j = 0, \tag{3.12}$$

with the boundary conditions given as follows

$$
\begin{aligned}
t \to 0 \quad &: \quad \sum_{j=0}^{4} c_{0j} w^j = c_{04} \prod_{j=5}^{8} (w - \widetilde{m}_j), \\
t \to \infty \quad &: \quad \sum_{j=0}^{4} c_{2j} t^2 w^j = c_{24} t^2 \prod_{j=1}^{4} (w - \widetilde{m}_j), \\
w \to 0 \quad &: \quad \sum_{i=0}^{2} c_{i0} t^i = c_{20}(t - t_2)^2; \qquad \sum_{i=0}^{2} c_{i1} t^i \propto (t - t_2), \\
w \to \infty \quad &: \quad \sum_{i=0}^{2} c_{i4} t^i w^4 = w^4 c_{24}(t - t_1)^2; \qquad \sum_{i=0}^{2} c_{i3} t^i \propto (t - t_1).
\end{aligned} \tag{3.13}
$$

By using the rescaling of t, we set $t_1 = 1$. With the rescaling of w, we set the center of mass position of m_i's to be unity

$$\prod_{i=1}^{8} \widetilde{m}_i = 1. \tag{3.14}$$

The compatibility condition corresponding to (3.5) is given as

$$\frac{t_2^2}{t_1^2} = \frac{\prod_{i=5}^{8} \widetilde{m}_i}{\prod_{j=1}^{4} \widetilde{m}_j}, \tag{3.15}$$

which leads to $t_2 = \prod_{i=5}^{8} \widetilde{m}_i$. With a little calculation, one finds that the SW curve is given by

$$\prod_{i=1}^{4} (w - \widetilde{m}_i)\, t^2 + k(w)\, t + \prod_{i=5}^{8} (w - \widetilde{m}_i) = 0, \tag{3.16}$$

where

$$k(w) = -2w^4 + \chi_{\mu_1}^{SU(8)}\, w^3 + U\, w^2 + \chi_{\mu_7}^{SU(8)}\, w - 2. \tag{3.17}$$

Up to the rescaling of the coordinates

$$t \to N_1^{-1} t, \qquad w \to -N_1^{\frac{1}{2}} w, \tag{3.18}$$

we find that this curve is exactly the same as (3.11), where the parameters are related by

$$\widetilde{m}_i = N_2^{\frac{1}{2}} L_i, \qquad \widetilde{m}_{i+4} = N_1^{\frac{1}{2}} M_i, \quad (i = 1, 2, 3, 4), \qquad U = c_{12}. \tag{3.19}$$

Therefore, we find that the SW curve computed from the tuned T_4 diagram and the one computed from the rectangular diagram is indeed related by a simple coordinate transformation (3.10).

3.2.3 Seiberg-Witten curve from the long triangle diagram

Finally, we move to the SW curve corresponding to Figure 9. Here we used the choice (3.14) enabling us to express in terms of χ_{μ_i}, the characters of the fundamental weights μ_i of $SU(8)$,[6]

$$\chi_{\mu_i}^{SU(8)} \equiv \sum_{k_1 < k_2 < \cdots < k_i}^{8} \widetilde{m}_{k_1} \widetilde{m}_{k_2} \cdots \widetilde{m}_{k_i}. \tag{3.20}$$

---

[6]Dynkin diagram for $SU(8)$ is given by

$$\circ \!\!-\!\!\!- \circ \!\!-\!\!\!- \circ \!\!-\!\!\!- \circ \!\!-\!\!\!- \circ \!\!-\!\!\!- \circ \!\!-\!\!\!- \circ$$
$$\mu_1 \quad \mu_2 \quad \mu_3 \quad \mu_4 \quad \mu_5 \quad \mu_6 \quad \mu_7$$

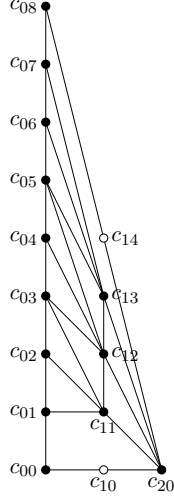and μ_i are the fundamental weight corresponding to the Dynkin label.

Figure 12. Coefficients in the long triangle diagram

By performing the coordinate transformation

$$t \to \frac{T}{\prod_{i=1}^{4}(w - \widetilde{m}_i)}, \tag{3.21}$$

we can write the SW curve in an $SU(8)$ manifest way as

$$T^2 + k(w)\,T + \prod_{i=1}^{8}(w - \widetilde{m}_i) = 0, \tag{3.22}$$

or

$$
\begin{aligned}
&T^2 + (-2w^4 + \chi_{\mu_1}\,w^3 + U\,w^2 + \chi_{\mu_7}\,w - 2)T \\
&+ w^8 - \chi_{\mu_1}w^7 + \chi_{\mu_2}w^6 - \chi_{\mu_3}w^5 + \chi_{\mu_4}w^4 - \chi_{\mu_5}w^3 + \chi_{\mu_6}w^2 - \chi_{\mu_7}w + 1 = 0, \tag{3.23}
\end{aligned}
$$

where we have dropped the superscript of the characters, $\chi_{\mu_i} \equiv \chi_{\mu_i}^{SU(8)}$. The coordinate transformation (3.21) is interpreted as the Hanany-Witten to obtain the diagram in Figure 9 from that in Figure 8.

Again, we can obtain (3.23) directly from the diagram in Figure 9 or Figure 12 by considering the polynomial

$$\sum_{\substack{p \geq 0, q \geq 0 \\ 4p + q \leq 8.}} c_{pq} T^p w^q = 0 \tag{3.24}$$

– 18 –

with the boundary conditions given as follows

$$
T \to 0 \quad : \quad \sum_{q=0}^{8} c_{0q} w^q = c_{08} \prod_{q=1}^{8} (w - \widetilde{m}_q),
$$

$$
w \to 0 \quad : \quad \sum_{p=0}^{2} c_{p0} t^p = c_{20}(T-1)^2; \qquad \sum_{p=0}^{2} c_{p1} t^p \propto (T-1),
$$

$$
w^4 \sim T \to \infty \quad : \quad \sum_{p=0}^{2} c_{p,8-4p} T^p w^{8-4p} = c_{20}(T - w^4)^2;
$$

$$
\sum_{p=0}^{1} c_{p,7-4p} T^p w^{7-4p} \propto (T - w^4). \tag{3.25}
$$

3.3 E_7 invariance

In this subsection, we discuss E_7 symmetry of the SW curve with six flavors. The curve (3.23) that we obtained for the $N_f = 6$ case is manifestly $SU(8)$ invariant, which is a maximal compact subgroup of E_7, and is expected to be E_7 invariant. One way to check the E_7 invariance is to check whether the curve (3.23) is invariant under the Weyl invariance of E_7. This can be done, but in practice it is not so straightforward because it involves mixing of coordinate transformations. Another way, which is more direct, is to compare (3.23) to the curve which is written in a E_7 manifest way [15–17] by examining the modular function called j-invariant of the elliptic curve.

To this end, we rewrite the $SU(8)$ invariant curve (3.23) in a form that is easier to extract the j-invariant

$$
y^2 = \left(-4U + \chi_{\mu_1}^2 - 4\chi_{\mu_2}\right) w^4 + (2U\chi_{\mu_1} + 4\chi_{\mu_3} - 4\chi_{\mu_7}) w^3 \tag{3.26}
$$
$$
+ \left(U^2 + 2\chi_{\mu_1}\chi_{\mu_7} - 4\chi_{\mu_4} + 8\right) w^2 + (2U\chi_{\mu_7} - 4\chi_{\mu_1} + 4\chi_{\mu_5}) w - 4U - 4\chi_{\mu_6} + \chi_{\mu_7}^2
$$

where

$$
y = T - w^4 + \frac{1}{2}\chi_{\mu_1} w^3 + \frac{1}{2}U w^2 + \frac{1}{2}\chi_{\mu_7} w - 1. \tag{3.27}
$$

The E_7 manifest curve [16, 17], that we want to compare, is of the following form

$$
y^2 = 4x^3 + (-u^2 + 4\chi_{\mu_1}^{E_7} - 100)x^2 + \left((2\chi_{\mu_2}^{E_7} - 12\chi_{\mu_7}^{E_7})u + 4\chi_{\mu_3}^{E_7} - 4\chi_{\mu_6}^{E_7} - 64\chi_{\mu_1}^{E_7} + 824\right)x
$$
$$
+ 4u^4 + 4\chi_{\mu_7}^{E_7} u^3 + (4\chi_{\mu_6}^{E_7} - 8\chi_{\mu_1}^{E_7} + 92)u^2 + (4\chi_{\mu_5}^{E_7} - 4\chi_{\mu_1}^{E_7}\chi_{\mu_7}^{E_7} - 20\chi_{\mu_2}^{E_7} + 116\chi_{\mu_7}^{E_7})u
$$
$$
+ 4\chi_{\mu_4}^{E_7} - \chi_{\mu_2}^{E_7}\chi_{\mu_2}^{E_7} + 4\chi_{\mu_1}^{E_7}\chi_{\mu_1}^{E_7} - 40\chi_{\mu_3}^{E_7} + 36\chi_{\mu_6}^{E_7} + 248\chi_{\mu_1}^{E_7} - 2232,
$$
$$
\tag{3.28}
$$

where $\chi_{\mu_i}^{E_7}$ is the character of the fundamental weight μ_i of E_7 which is associated to the node of the E_7 Dynkin diagram as
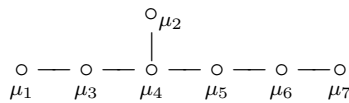
Expressed in the standard Weierstrass form, this E_7 manifest curve is of degree three polynomial in x. On the other hand, the our $SU(8)$ manifest curve is quartic in w. In order to compare both, we use the j-invariant of elliptic curve

$$j = \frac{g_2^3}{g_2^3 - 27g_3^2}.$$ (3.29)

For generic cubic and quartic polynomials, the forms of g_2 and g_3 are given in Appendix C

We first compare the massless case by taking all the mass parameters $\widetilde{m}_i$ to unity $(\widetilde{m}_i = e^{-\beta m_i} \to 1)$. This means that the character of the fundamental weights becomes the dimension of the corresponding fundamental weights: For E_7,

$$\chi_{\mu_1}^{E_7} \to 133, \quad \chi_{\mu_2}^{E_7} \to 912, \quad \chi_{\mu_3}^{E_7} \to 8645,$$
$$\chi_{\mu_4}^{E_7} \to 365750, \quad \chi_{\mu_5}^{E_7} \to 27664, \quad \chi_{\mu_6}^{E_7} \to 1539, \quad \chi_{\mu_7}^{E_7} \to 56.$$ (3.30)

and the curve (3.28) is written as

$$y^2 = 4x^3 + \left(432 - u^2\right)x^2 + (1152u + 20736)x + 4u^4 + 224u^3 + 5184u^2 + 69120u + 442368.$$ (3.31)

The corresponding j-invariants is given by

$$\frac{(u - 36)^3}{1728(u - 52)}.$$ (3.32)

For $SU(8)$, the characters again become the dimensions of the representations

$$\chi_{\mu_1} = \chi_{\mu_7} \to 8, \quad \chi_{\mu_2} = \chi_{\mu_6} \to 28, \quad \chi_{\mu_3} = \chi_{\mu_5} \to 56, \quad \chi_{\mu_4} \to 70,$$ (3.33)

and the curve (3.26) is written as

$$y^2 = (U + 12)\left[-4w^4 + 16w^3 + (U - 12)w^2 + 16w - 4\right].$$ (3.34)

The corresponding j-invariants for this is given by

$$\frac{(U - 36)^3}{1728(U - 52)},$$ (3.35)

which coincide with that of E_7 manifest curve. From this, we can identify the Coulomb moduli parameter U with u used in [17].

With this identification of the Coulomb modulus and agreement of the j-invariant for massless case, one can check a generic massive case. Although it is tedious, it is straightforward to see that the j-invariant for the E_7 manifest curve (3.28) exactly coincides with the j-invariant for the $SU(8)$ manifest curve (3.26) by implementing the decomposition of the E_7 fundamental weights into the $SU(8)$ fundamental weights listed in Appendix D.1. (We list the form of g_2 and g_3 for the $SU(8)$ manifest curve (3.26) in Appendix D.) Therefore, our expression (3.26) of the SW curve for $N_f = 6$ flavors describes the E_7 curve, although it is not manifestly E_7 invariant.

3.4 4d limit of 5d E_7 Seiberg-Witten curve

From the 5d curve (3.16)

$$\prod_{i=1}^{4}(w - \widetilde{m}_i)\, t^2 + \left(-2w^4 + \chi_{\mu_1}^{SU(8)}\, w^3 + U\, w^2 + \chi_{\mu_7}^{SU(8)}\, w - 2\right) t + \prod_{i=5}^{8}(w - \widetilde{m}_i) = 0, \quad (3.36)$$

whose corresponding toric-like diagram is of rectangular shape given in Figure 8, we discuss 4d limit of 5d theory which is to take zero radius limit of the compactified circle. We associate the radius of the circle β and then the 5d coordinate w and mass parameters $\widetilde{m}_i$ are related to the 4d coordinate v and masses m_i as

$$w = e^{-\beta v}, \quad \text{and} \quad \widetilde{m}_i = e^{-\beta m_i}. \quad (3.37)$$

To take zero size limit of the radius β, we expand the Coulomb moduli parameter U in five dimensions as

$$U = \sum_{k=0}^{\infty} u_k \beta^k. \quad (3.38)$$

Expansion of the curve (3.36) leads to consistent conditions determining the expansion coefficient of the 5d Coulomb moduli parameter U, and non-trivial relation occurs at order β^4 which gives rise to 4d SW curve

$$t^2 \prod_{i=1}^{4}(v - m_i) + t\left(-2v^4 - D_2\, v^2 + D_3\, v + u\right) + \prod_{i=5}^{8}(v - m_i) = 0, \quad (3.39)$$

where $D_n \equiv \sum_{i_1 < \cdots < i_n}^{8} m_{i_1} \cdots m_{i_n}$ are the symmetric product and the 4d Coulomb moduli parameter u appears at order β^4 in the expansion of U

$$U = -12 + 2D_2\, \beta^2 + \left(u + \frac{1}{6}(2D_2 - D_2)\right)\beta^4 + \mathcal{O}(\beta^5). \quad (3.40)$$
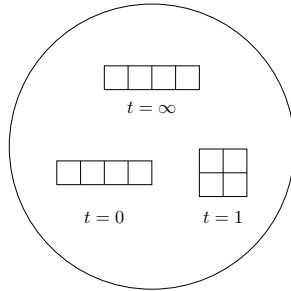

Figure 13. Sphere with three punctures which corresponds to E_7 CFT.

In the following, we check that the 4d SW curve (3.39) is exactly the SW curve for the 4d E_7 CFT found in [20, 21], which is given by the quadruple cover of the sphere with

three punctures with specific type. See Figure 13. For later convenience, we reparametrize the mass parameters as

$$m = \frac{1}{4} \sum_{i=1}^{4} m_i = -\frac{1}{4} \sum_{i=5}^{8} m_i,$$

$$\hat{m}_i = m_i - m \quad (i = 1, 2, 3, 4), \qquad \hat{m}_i = m_i + m \quad (i = 5, 6, 7, 8) \tag{3.41}$$

By changing the coordinate as

$$v = xt + m\frac{t+1}{t-1}, \tag{3.42}$$

we can write the curve in the way

$$x^4 + \sum_{n=2}^{4} \phi_n(t) x^{4-n} = 0, \tag{3.43}$$

with SW one-form $\lambda = x dt$. Here, $\phi_n(t)$ has poles at $t = 0, 1, \infty$ where the three punctures exist. The residues at each pole are given by

$$\begin{aligned} \{\hat{m}_5, \hat{m}_6, \hat{m}_7, \hat{m}_8\} &\quad \text{at} \quad t = 0, \\ \{-2m, -2m, 2m, 2m\} &\quad \text{at} \quad t = 1, \\ \{\hat{m}_1, \hat{m}_2, \hat{m}_3, \hat{m}_4\} &\quad \text{at} \quad t = \infty, \end{aligned} \tag{3.44}$$

which we identify as mass parameters. This is consistent with the type of each puncture. The type of each puncture can be further checked by looking at the order of the pole of ϕ_n at each puncture when we turn off the mass parameters associated with the corresponding puncture. The expected order of ϕ_n are given by "$n-$(height of the n-th boxes)", where we label the boxes in the Young diagram in such a way that the height of the box does not decrease. See [21] for detail. Denoting the order of the pole of ϕ_n as p_n, we can explicitly check

$$\begin{aligned} (p_2, p_3, p_4) = (1, 2, 3) &\quad \text{at} \quad t = 0 \quad \text{when} \quad \hat{m}_5 = \hat{m}_6 = \hat{m}_7 = \hat{m}_8 = 0, \\ (p_2, p_3, p_4) = (1, 1, 2) &\quad \text{at} \quad t = 1 \quad \text{when} \quad m = 0, \\ (p_2, p_3, p_4) = (1, 2, 3) &\quad \text{at} \quad t = \infty \quad \text{when} \quad \hat{m}_1 = \hat{m}_2 = \hat{m}_3 = \hat{m}_4 = 0. \end{aligned} \tag{3.45}$$

This is again consistent with the type of punctures. Thus, we have checked that our 4d curve (3.39) agree with that of the 4d E_7 CFT.

4 E_8 Seiberg-Witten curve

In this section, we consider the SW curve for $Sp(1)$ gauge theory with $N_f = 7$ flavors. The construction of the toric-like diagram, the computation of the corresponding SW curve, the comparison with the known curve, and the 4d limit can be studied analogously to the previous section.
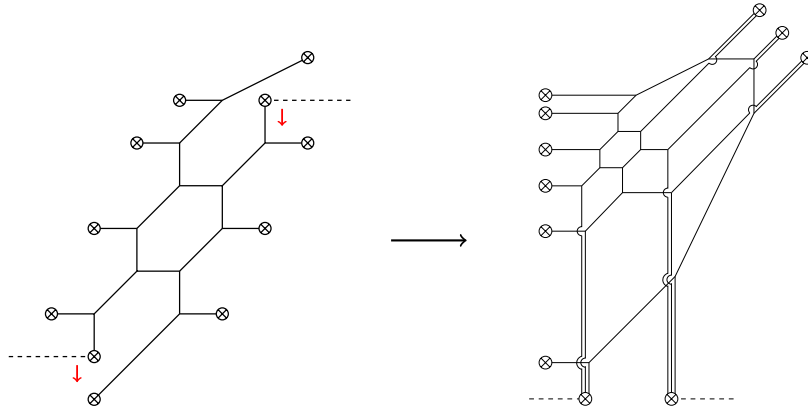
Figure 14. $N_f = 7$ brane configuration (left) and tuned T_6 diagram after Hanany-Witten transitions (right)

4.1 Constructing toric-like diagram

We begin by adding one more flavor brane to the $N_f = 6$ brane configuration. Via successive applications of the Hanany-Witten transition, it is straightforward to see that it leads to a tuned T_6 diagram as in Figure 14. The corresponding toric-like diagram is given in Figure 15.
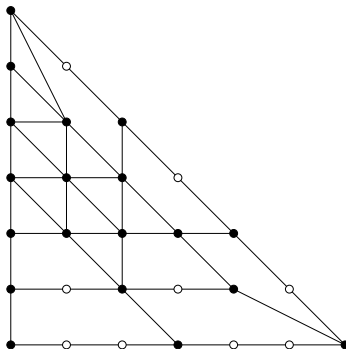

Figure 15. A toric-like diagram with E_8 symmetry. It can be viewed as a tuned T_6 diagram.

As this toric-like diagram is a tuned T_6 diagram,[7] it has manifest symmetry of $SU(6) \times SU(3) \times SU(2)$ which is a maximal compact subgroup of E_8. As explained earlier, by performing the Hanany-Witten transition, the manifest symmetry structure is changed to another subgroup of E_8. For instance, if we perform the Hanany-Witten transition on one of 7-branes combining three 5-branes on the bottom of the toric-like diagram, Figure 15, we get the corresponding toric-like diagram of a rectangular shape, Figure 16. The diagram shows manifest symmetry of $S[U(6) \times U(3)]$.

---

[7]We note that although this toric-like diagram is a tune T_6, the number of white dots inside is different from the tuned T_6 in [20]. Depending on how one triangulates while keeping one Coulomb modulus, an interior black dot near the boundary can be turned to a white dot.
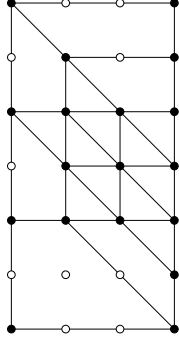
Figure 16. A rectangular toric like diagram for E_8

We can further move all the $[1,0]$ 7-branes on the right hand sides to the left by Hanany-Witten transition. Then, we obtain the toric-like diagram in Figure 17.
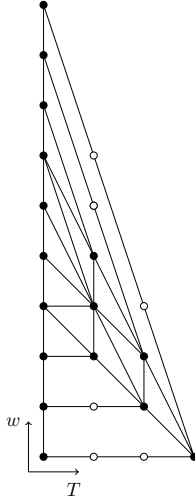
Figure 17. A toric-like diagram for E_8 with manifest $SU(9)$ symmetry

This toric-like diagram has manifest $SU(9)$ symmetry, which is the maximal subgroup of E_8. Again, the SW curve can be computed from either of these three toric diagrams shown above.

4.2 $N_f = 7$ Seiberg-Witten curve from M-theory

In the following, we compute the SW curve based on toric-like diagram of $N_f = 7$. We start from the diagram in Figure 15 and obtain the SW curve corresponding to the other diagrams by coordinate transformation. Since the computation and the logic are quite parallel to section 3.2, we summarize the computation briefly.

The SW curve is given by the special case of T_6 curve

$$\sum_{\substack{p \geq 0, q \geq 0 \\ p+q \leq 6}} c_{pq} t^p w^q = 0. \tag{4.1}$$

We impose the following conditions

$$w, t \to \infty \quad : \quad \sum_{p=0}^{6} c_{p,6-p} t^p w^{6-p} = c_{06} \prod_{i=1}^{3} (w + L_i t)^2,$$

$$\sum_{p=0}^{5} c_{p,5-p} t^p w^{5-p} \propto \prod_{i=1}^{3} (w + L_i t), \tag{4.2}$$

$$t \to 0 \quad : \quad \sum_{q=0}^{6} w^q = c_{06} \prod_{i=1}^{6} (w - M_i), \tag{4.3}$$

$$w \to 0 \quad : \quad \sum_{p=0}^{6} c_{p0} t^p = c_{60} \prod_{i=1}^{2} (t - N_i)^3, \qquad \sum_{p=0}^{6} c_{p1} t^p \propto \prod_{i=1}^{2} (t - N_i)^2,$$

$$\sum_{p=0}^{6} c_{p2} t^p \propto \prod_{i=1}^{2} (t - N_i). \tag{4.4}$$

This leads to the SW curve as

$$
\begin{aligned}
0 = \quad & w^6 - (S_1' t - 2T_1') w^5 + \Big(S_2 t^2 - (S_1' T_1' + S_5' + R_1 T_2') t + (T_1'^2 + 2T_2') \Big) w^4 \\
& - \Big(S_3' t^3 - U' t^2 + (S_1' T_2' + S_5' T_1' + 3R_1 + R_1 T_1' T_2') t - (2T_1' T_2' + 2) \Big) w^3 \\
& + (t^2 - R_1 t + 1)\Big(S_4' t^2 - (S_1' + S_5' T_2' + R_1 T_1') t + (T_2'^2 + 2T_1') \Big) w^2 \\
& - (t^2 - R_1 t + 1)^2 (S_5' t - 2T_2') w + (t^2 - R_1 t + 1)^3,
\end{aligned}
\tag{4.5}
$$

where we defined the characters of $SU(6)$, $SU(3)$, and $SU(2)$ as

$$S_n' = \sum_{1 \le i_1 \le i_2 \le \cdots \le i_n} M_{i_1} M_{i_2} \cdots M_{i_n}, \quad (n = 1, \cdots, 5)$$

$$T_n' = \sum_{1 \le i_1 \le i_2 \le \cdots \le i_n} L_{i_1} L_{i_2} \cdots L_{i_n}, \quad (n = 1, \cdots, 2)$$

$$R_1 = N_1 + N_2, \tag{4.6}$$

and we also have imposed

$$\prod_{i=1}^{3} L_i = \prod_{i=1}^{6} M_i = \prod_{i=1}^{2} N_i = 1, \tag{4.7}$$

by using the rescaling of t and w together with the compatibility condition.

Let us consider the coordinate transformation

$$w \to w(t - N_1) \tag{4.8}$$

which corresponds to the Hanany-Witten transition enabling us to obtain the toric-like diagram in Figure 16. After further scalings[8] of w and t, and introducing new parameter,

---

[8] $t \to N_1^{-1} t$ and $w \to N_1^{-4/3} w$.

we obtain

$$(t - S_6)^3 w^6 - S_1(t - S_6)^2(t - 2T_1 S_6 S_1^{-1})w^5$$

$$+ S_2(t - S_6)\Big(t^2 - S_2^{-1}(S_1 S_6 T_1 + S_5 + S_6 T_2 + S_6^2 T_2)t + S_2^{-1} S_6^2(T_1^2 + 2T_2)\Big)w^4$$

$$+ \Big(-S_3 t^3 + U t^2 - \big[S_1 S_6^2 T_2 + S_5 S_6 T_1 + 3S_6 + 3S_6^2 + S_6^2 T_1 T_2 + S_6^3 T_1 T_2\big]t + 2S_6^3 T_1 T_2 + 2S_6^2\Big)w^3$$

$$+ S_4(t - 1)\Big(t^2 - S_4^{-1}[S_1 S_6 + S_5 S_6 T_2 + S_6 T_1 + S_6^2 T_1]t + S_4^{-1} S_6^2(S_6 T_2^2 + 2T_1)\Big)w^2$$

$$- S_5(t - 1)^2(t - 2S_5^{-1} S_6^2 T_2)w + S_6(t - 1)^3 = 0, \tag{4.9}$$

where we introduced

$$S_n = N_1^{\frac{n}{3}} S_n', \quad (n = 1, \cdots, 5), \qquad S_6 = N_1{}^2,$$
$$T_n = N_1^{-\frac{2n}{3}} T_n', \quad (n = 1, 2), \qquad T_3 = N_1^{-2}. \tag{4.10}$$

We note that this curve is invariant under $S[U(6) \times U(3)]$. This curve is again also directly obtained from the diagram in Figure 16. In terms of the fugacities associated with the mass parameters, S_n and T_n can be written as follows:

$$S_1 = \sum_{i=1}^{6} \widetilde{m}_i, \quad S_2 = \sum_{i,j=1, i<j}^{6} \widetilde{m}_i \widetilde{m}_j, \quad S_3 = \sum_{i_1, i_2, i_3}^{6} \widetilde{m}_{i_1} \widetilde{m}_{i_2} \widetilde{m}_{i_3}, \quad \cdots, \quad S_6 = \prod_{i=1}^{6} \widetilde{m}_i,$$

$$T_1 = \sum_{i=7}^{9} \widetilde{m}_i, \quad T_2 = \sum_{i,j=7, i<j}^{9} \widetilde{m}_i \widetilde{m}_j, \quad T_3 = \widetilde{m}_7 \widetilde{m}_8 \widetilde{m}_9, \quad S_6 T_3 = 1.$$

Introducing the characters of the fundamental weights of $SU(9)$ [9]

$$\chi_n = \sum_{i=0}^{n} S_{n-i} T_i \qquad (S_0 = 1 = T_0, \quad S_{n>6} = 0 = T_{n>3}, \quad \chi_9 = S_6 T_3 = 1), \tag{4.11}$$

the curve (4.9) is expressed in a simple form as

$$\Big[\prod_{i=1}^{6}(w - \widetilde{m}_i)\Big]t^3 - S_6\Big[3w^6 - 2\chi_1 w^5 + (\chi_2 + \chi_8)w^4 + U w^3 + (\chi_1 + \chi_7)w^2 - 2\chi_8 w + 3\Big]t^2$$

$$+ S_6^2\Big[(3w^3 - \chi_1 w^2 + \chi_8 w - 3)\prod_{j=7}^{9}(w - \widetilde{m}_j)\Big]t - S_6^3 \prod_{i=7}^{9}(w - \widetilde{m}_i)^2 = 0. \tag{4.12}$$

We now take a further coordinate transformation

$$t \to -S_6 \frac{\prod_{i=7}^{9}(w - \widetilde{m}_i)}{T}.$$

---

[9] Dynkin diagram for $SU(9)$ is given by

and μ_i are the fundamental weight associated with the Dynkin label.

This corresponds to the Hanany-Witten transition that enables us to obtain the toric-like diagram in Figure 17. We then obtain an $SU(9)$ manifest curve

$$
\begin{aligned}
&T^3 + \Big(3w^3 - \chi_1 w^2 + \chi_8 w - 3\Big)T^2 \\
&+ \Big(3w^6 - 2\chi_1 w^5 + (\chi_2 + \chi_8)w^4 + Uw^3 + (\chi_1 + \chi_7)w^2 - 2\chi_8 w + 3\Big)T \\
&+ w^9 - \chi_1 w^8 + \chi_2 w^7 - \chi_3 w^6 + \chi_4 w^5 - \chi_5 w^4 + \chi_6 w^3 - \chi_7 w^2 + \chi_8 w - 1 = 0. \quad (4.13)
\end{aligned}
$$

Again, this diagram can be also obtained directly from Figure 17.

4.3 E_8 invariance

We now compare the $SU(9)$ manifest SW curve for the $N_f = 7$ case to the known E_8 manifest curve [16, 17] to check E_8 invariance of the curve (4.13). To this end, with

$$
\widetilde{T} = \frac{1}{w}\Big(T - w^3 + \frac{1}{3}\chi_1 w^2 - \frac{1}{3}\chi_8 w + 1\Big), \tag{4.14}
$$

we rewrite (4.13) as

$$
\begin{aligned}
&\widetilde{T}^3 + \Big[\Big(-\frac{\chi_1^2}{3} + \chi_2 - \chi_8\Big)w^2 + \Big(U + \frac{2\chi_1\chi_8}{3} + 6\Big)w - \frac{\chi_8^2}{3} - \chi_1 + \chi_7\Big]\widetilde{T} \\
&+ \Big(-U - \frac{2}{27}\chi_1^3 + \frac{1}{3}\chi_2\chi_1 - \frac{1}{3}\chi_8\chi_1 - \chi_3 - 3\Big)w^3 \\
&+ \Big(\frac{U}{3}\chi_1 + \frac{2}{9}\chi_8\chi_1^2 + \chi_1 + \frac{\chi_8^2}{3} + \chi_4 - \chi_7 - \frac{\chi_2\chi_8}{3}\Big)w^2 \\
&+ \Big(-\frac{1}{3}U\chi_8 - \frac{1}{3}\chi_1^2 - \frac{2}{9}\chi_8^2\chi_1 + \frac{1}{3}\chi_7\chi_1 + \chi_2 - \chi_5 - \chi_8\Big)w \\
&+ U + \frac{2\chi_8^3}{27} + \frac{\chi_1\chi_8}{3} - \frac{\chi_7\chi_8}{3} + \chi_6 + 3 = 0. \tag{4.15}
\end{aligned}
$$

Observe that this curve is of mutually degree 3 polynomials in $\widetilde{T}$ and w. One can convert this into the standard Weierstrass form which makes it easier to compare to the known E_8 manifest curve (For an explicit coordinate transformation to the Weierstrass form, see, for example, [28]).

The E_8 manifest curve [16, 17] is given by

$$
\begin{aligned}
y^2 = 4x^3 &+ \left[-u^2 + 4\chi^{E_8}_{\mu_1} - 100\chi^{E_8}_{\mu_8} + 9300 \right]x^2 + \left[(2\chi^{E_8}_{\mu_2} - 12\chi^{E_8}_{\mu_7} - 70\chi^{E_8}_{\mu_1} + 1840\chi^{E_8}_{\mu_8} - 115010)u \right. \\
&+ 4\chi^{E_8}_{\mu_3} - 4\chi^{E_8}_{\mu_6} - 64\chi^{E_8}_{\mu_1}\chi^{E_8}_{\mu_8} + 824(\chi^{E_8}_{\mu_8})^2 - 112\chi^{E_8}_{\mu_2} + 680\chi^{E_8}_{\mu_7} + 8024\chi^{E_8}_{\mu_1} - 205744\chi^{E_8}_{\mu_8} + 9606776 \Big] x \\
&+ 4u^5 + \left(4\chi^{E_8}_{\mu_8} - 992 \right)u^4 + \left(4\chi^{E_8}_{\mu_7} - 12\chi^{E_8}_{\mu_1} - 680\chi^{E_8}_{\mu_8} + 93620 \right)u^3 \\
&+ \left(4\chi^{E_8}_{\mu_6} - 8\chi^{E_8}_{\mu_1}\chi^{E_8}_{\mu_8} + 92(\chi^{E_8}_{\mu_8})^2 - 28\chi^{E_8}_{\mu_2} - 540\chi^{E_8}_{\mu_7} + 2320\chi^{E_8}_{\mu_1} + 30608\chi^{E_8}_{\mu_8} - 3823912 \right)u^2 \\
&+ \left(4\chi^{E_8}_{\mu_5} - 4\chi^{E_8}_{\mu_1}\chi^{E_8}_{\mu_7} - 20\chi^{E_8}_{\mu_2}\chi^{E_8}_{\mu_8} + 116\chi^{E_8}_{\mu_7}\chi^{E_8}_{\mu_8} + 8(\chi^{E_8}_{\mu_1})^2 - 52\chi^{E_8}_{\mu_3} - 416\chi^{E_8}_{\mu_6} + 1436\chi^{E_8}_{\mu_1}\chi^{E_8}_{\mu_8} \right. \\
&\quad \left. - 17776(\chi^{E_8}_{\mu_8})^2 + 4180\chi^{E_8}_{\mu_2} + 16580\chi^{E_8}_{\mu_7} - 182832\chi^{E_8}_{\mu_1} + 1103956\chi^{E_8}_{\mu_8} + 18130536 \right)u \\
&+ 4\chi^{E_8}_{\mu_4} - (\chi^{E_8}_{\mu_2})^2 + 4(\chi^{E_8}_{\mu_1})^2\chi^{E_8}_{\mu_8} - 40\chi^{E_8}_{\mu_3}\chi^{E_8}_{\mu_8} + 36\chi^{E_8}_{\mu_6}\chi^{E_8}_{\mu_8} + 248\chi^{E_8}_{\mu_1}(\chi^{E_8}_{\mu_8})^2 - 2232(\chi^{E_8}_{\mu_8})^3 \\
&+ 2\chi^{E_8}_{\mu_1}\chi^{E_8}_{\mu_2} - 232\chi^{E_8}_{\mu_5} + 224\chi^{E_8}_{\mu_1}\chi^{E_8}_{\mu_7} + 1124\chi^{E_8}_{\mu_2}\chi^{E_8}_{\mu_8} - 6580\chi^{E_8}_{\mu_7}\chi^{E_8}_{\mu_8} - 457(\chi^{E_8}_{\mu_1})^2 + 4980\chi^{E_8}_{\mu_3} \\
&+ 8708\chi^{E_8}_{\mu_6} - 88136\chi^{E_8}_{\mu_1}\chi^{E_8}_{\mu_8} + 1129964(\chi^{E_8}_{\mu_8})^2 - 146282\chi^{E_8}_{\mu_2} + 66612\chi^{E_8}_{\mu_7} + 6123126\chi^{E_8}_{\mu_1} \\
&- 104097420\chi^{E_8}_{\mu_8} + 2630318907,
\end{aligned}
$$

(4.16)

where the characters of E_8, $\chi^{E_8}_i$, are associated with the fundamental weights μ_i assigned to the E_8 Dynkin diagram as follows:

We first check the j-invariant for massless cases, where the character becomes the dimension of the representation. For the E_8 manifest curve, it reads

$$
\begin{aligned}
y^2 = 4x^3 &- \left(u^2 + 14968 \right)x^2 + 8(41644u + 1022767)x \\
&+ 4u^5 - 76392u^3 + 9420308u^2 - 777374372u + 12225915472.
\end{aligned}
$$

(4.17)

The j-invariant is then

$$
\frac{u^2}{1728(u - 432)}.
$$

(4.18)

For the $SU(9)$ manifest curve, the corresponding curve is expressed as

$$
t^3 + (U + 60)wt - (U + 60)w^3 + 3(U + 60)w^2 - 3(U + 60)w + (U + 60) = 0,
$$

(4.19)

and the corresponding j-invariant is

$$
\frac{(U + 60)^2}{1728(U - 372)}.
$$

(4.20)

Note that two j-invariants, (4.18) and (4.20), look different, but a shift in the Coulomb moduli parameter can make them coincide with each other. In fact, if one checks the j-invariant for the case with generic masses, in order to compare two curves, one needs to

shift the Coulomb moduli parameters by a constant [10]

$$U \to u - 60.$$

With this shift of the Coulomb moduli parameter, one can write (4.15) in the standard Weierstrass form

$$y^2 = 4x^3 - g_2^{SU(9)}x - g_3^{SU(9)}, \tag{4.21}$$

where

$$
\begin{aligned}
g_2^{SU(9)} &= \frac{1}{12}u^4 - \frac{2}{3}\big(2349 + \chi_1\chi_2 - 27\chi_3 + \chi_1\chi_5 - 27\chi_6 + \chi_2\chi_7 - 25\chi_1\chi_8 \\
&\quad + \chi_4\chi_8 + \chi_7\chi_8\big)u^2 + \mathcal{O}(u), \\
g_3^{SU(9)} &= \frac{1}{216}u^6 - 4u^5 - \frac{1}{18}\big(-15579 + \chi_1\chi_2 + 45\chi_3 + \chi_1\chi_5 + 45\chi_6 + \chi_2\chi_7 \\
&\quad + 47\chi_1\chi_8 + \chi_4\chi_8 + \chi_7\chi_8\big)u^4 + \mathcal{O}(u^3).
\end{aligned}
\tag{4.22}
$$

The complete expressions of g_2 and g_3 are complicated and long, so we list them in Appendix E, from which one can compute the j-invariant. As the global symmetry for $N_f = 7$ flavors is expected to be E_8, this j-invariant should coincide with that from the E_8 manifest curve [17, 28]

$$y^2 = 4x^3 - g_2^{E_8}x - g_3^{E_8}, \tag{4.23}$$

where

$$
\begin{aligned}
g_2^{E_8} &= \frac{1}{12}u^4 - \Big(\frac{2}{3}\chi_1^{E_8} - \frac{50}{3}\chi_8^{E_8} + 1550\Big)u^2 + \mathcal{O}(u), \\
g_3^{E_8} &= \frac{1}{216}u^6 - 4u^5 - \Big(\frac{1}{18}\chi_1^{E_8} + \frac{47}{18}\chi_8^{E_8} - \frac{5177}{6}\Big)u^4 + \mathcal{O}(u^3).
\end{aligned}
\tag{4.24}
$$

For the explicit form of $g_2^{E_8}$ and $g_3^{E_8}$, see Appendix B. As done in the $N_f = 6$ case, one can decompose the fundamental weights of E_8 into the fundamental weights of $SU(9)$. Such decomposition can be performed with help of computer programs, $e.g.$ a Mathematica

---

[10]We can also compare (4.20) to the j-invariant of $SO(16)$ manifest SW curve for E_8 [15], which reads in the massless case,

$$y^2 = x^3 + u_N^2 x^2 - 2u_N^5.$$

The corresponding j-invariant is

$$\frac{u_N^2}{54u_N - 729}.$$

We then find that the two curves are related by a constant shift in the Coulomb modulus

$$U \to 4(8u_N - 15).$$

package like LieART [29] or a computer algebra package LiE [30]. We here used a Mathematica package called 'Susyno' [31] [11] to decompose the E_8 weights into the $SU(9)$ weights. The result of the decomposition is listed in Appendix E.1. Under this decomposition, the g_2 and g_3 for (4.22) and (4.24) are in agreement with each other, thus confirming that E_8 invariance of the SW curve (4.15) obtained from the toric-like diagram for $N_f = 7$ flavors.

4.4 4d limit of 5d E_8 Seiberg-Witten curve

We start with our SW curve which is of a manifest $S[U(3) \times U(6)]$ invariant form (4.12). By redefining $-\frac{t}{S_6}$ by t, we get

$$\Big[\prod_{i=1}^{6}(w - \widetilde{m}_i)\Big]t^3 + \Big[3w^6 - 2\chi_1 w^5 + (\chi_2 + \chi_8)w^4 + Uw^3 + (\chi_1 + \chi_7)w^2 - 2\chi_8 w + 3\Big]t^2$$
$$+ \Big[\big(3w^3 - \chi_1 w^2 + \chi_8 w - 3\big)\prod_{j=7}^{9}(w - \widetilde{m}_j)\Big]t + \prod_{i=7}^{9}(w - \widetilde{m}_i)^2 = 0,$$

$$(4.25)$$

where $w = e^{-\beta v}$ and $\widetilde{m}_i = e^{-\beta m_i}$.

Upon reduction to 4d by expanding w and $\widetilde{m}_i$ in β as well as the 5d Coulomb moduli parameter U as a polynomial of β as (3.38), we obtain 4d SW curve at the order of β^6, expressed in terms of the symmetric product $D_n \equiv \sum_{i_1 < \cdots < i_n}^{9} m_{i_1} \cdots m_{i_n}$, as

$$t^3 \prod_{i=1}^{6}(v - m_i) + t^2\Big[3v^6 + 2D_2 v^4 - 2D_3 v^3 + D_4 v^2 - D_5 v + u^{4d}\Big]$$
$$+ t\Big(3v^3 + D_2 v - D_3\Big)\prod_{j=7}^{9}(v - m_j) + \prod_{j=7}^{9}(v - m_j)^2 = 0,$$

$$(4.26)$$

where

$$U = 12D_2\beta^2 - D_2^2\beta^4 + \Big(u^{4d} - \frac{1}{60}\big(24D_6 - 4D_4 D_2 + 3D_3^2 - 2D_2^3\big)\Big)\beta^6 \qquad (4.27)$$
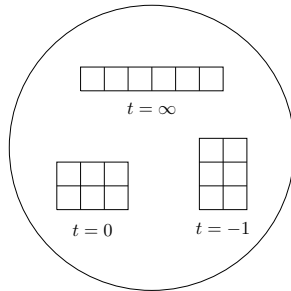

Figure 18. Sphere with three punctures which corresponds to E_8 CFT.

In the following, we check that the 4d SW curve (4.26) is exactly the SW curve for the 4d E_8 CFT found in [20, 21], which is given by the sextuple cover of the sphere with three punctures of specific type. See Figure 18. For convenience, we reparametrize the mass parameters as

$$m = \frac{1}{6}\sum_{i=1}^{6}m_i = -\frac{1}{6}\sum_{i=5}^{8}m_i,$$

$$\hat{m}_i = m_i - m \quad (i = 1,2,3,4,5,6), \qquad \hat{m}_i = m_i + 2m \quad (i = 7,8,9). \tag{4.28}$$

By changing the coordinate as

$$v = xt - m\frac{t-2}{t+1}, \tag{4.29}$$

we can write the curve in the way

$$x^6 + \sum_{n=2}^{6}\phi_n(t)x^{6-n} = 0, \tag{4.30}$$

with SW one-form $\lambda = xdt$. Here, $\phi_n(t)$ has poles at $t = 0, -1, \infty$ where the three punctures exist. The residues at each pole are given by

$$\{\hat{m}_7, \hat{m}_7, \hat{m}_8, \hat{m}_8, \hat{m}_9, \hat{m}_9\} \quad \text{at} \quad t = 0,$$
$$\{-3m, -3m, -3m, 3m, 3m, 3m\} \quad \text{at} \quad t = -1,$$
$$\{\hat{m}_1, \hat{m}_2, \hat{m}_3, \hat{m}_4, \hat{m}_5, \hat{m}_6\} \quad \text{at} \quad t = \infty, \tag{4.31}$$

which we identify as mass parameters. This is consistent with the type of each puncture. The type of each puncture can be further checked by looking at the order of the pole of ϕ_n at each puncture when we turn off the mass parameters associated with the corresponding puncture. Denoting the order of the pole of ϕ_n as p_n, we can explicitly check

$$(p_2, p_3, p_4, p_5, p_6) = (1,2,2,3,4) \quad \text{at} \quad t = 0 \quad \text{when} \quad \hat{m}_7 = \hat{m}_8 = \hat{m}_9 = 0,$$
$$(p_2, p_3, p_4, p_5, p_6) = (1,1,2,2,3) \quad \text{at} \quad t = -1 \quad \text{when} \quad m = 0,$$
$$(p_2, p_3, p_4, p_5, p_6) = (1,2,3,4,5) \quad \text{at} \quad t = \infty \quad \text{when} \quad \hat{m}_1 = \hat{m}_2 = \cdots = \hat{m}_6 = 0 \tag{4.32}$$

This is again consistent with the type of punctures. Thus, we have checked that our 4d curve (4.26) agree with that of the 4d E_8 CFT.

5 Mass decoupling limit

In this section, we discuss "mass decoupling" limit of 5d theory with E_8 ($N_f = 7$). Here masses are positions of semi-infinite $D7$ branes in (p,q) web. As in 4d, one can take large mass limit such that the flavor associated with large mass decouples which yields that rank of global symmetry group is reduced to lower one. As toric-like diagrams of E_7 theory can be naturally embedded into toric-like diagrams of E_8 theory, one expects that mass decoupling limit of E_8 toric-diagram leads to a E_7 toric-like diagram.

For mass decoupling limit from E_8 to E_7 SW curve, consider for the $SU(9)$ manifest curve for $N_f = 7$ flavors, Figure 17. We take the following scaling limit

$$\widetilde{m}_1 \to L^{-1}\,\widetilde{m}_1, \quad \widetilde{m}_9 \to L\,, \quad \widetilde{m}_i \to \widetilde{m}_i \ (i = 2, \cdots, 8), \tag{5.1}$$

and

$$U \to L\,U, \qquad w \to w, \qquad t \to t. \tag{5.2}$$

This scaling leads that the fundamental weight of $SU(9)$ scales like

$$\chi_i \ \sim \ L\,\chi_{i-1}^{U(7)} \qquad (i = 2, \cdots, 8), \tag{5.3}$$

where $\chi_0^{U(7)} \equiv 1$ and $\chi_i^{U(7)}$ are the $U(7)$ fundamental characters. For instance, $\chi_1^{U(7)} = \sum_{i=2}^8 \widetilde{m}_i$ and $\chi_7^{U(7)} = \prod_{i=2}^8 \widetilde{m}_i$. It follows from the $SU(9)$ traceless condition that in this scaling one obtains $SU(8)$ traceless condition $\prod_{i=1}^8 \widetilde{m}_i = 1$, and thus $\chi_7^{U(7)} = \widetilde{m}_1^{-1}$.

By taking large L limit, we find that the $SU(9)$ manifest SW curve (4.13) becomes

$$\left(- w + \chi_7^{U(7)} \right)T^2 + \left(- 2w^4 + (\chi_1^{U(7)} + \chi_7^{U(7)})w^3 + Uw^2 + (1 + \chi_6^{U(7)})w - 2\chi_7^{U(7)} \right)T$$
$$- w^7 + \chi_1^{U(7)}w^6 - \chi_2^{U(7)}w^5 + \chi_3^{U(7)}w^4 - \chi_4^{U(7)}w^3 + \chi_5^{U(7)}w^2 - \chi_6^{U(7)}w + \chi_7^{U(7)} = 0. \tag{5.4}$$

This has $S[U(7) \times U(1)]$ which can be also read off from the corresponding toric-like diagram below.
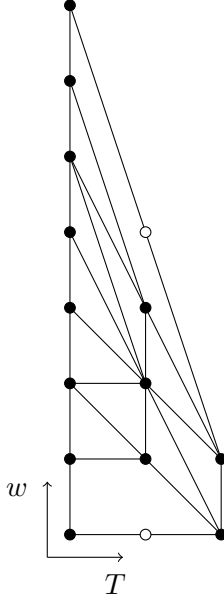

Figure 19. E_7 toric-like diagram of a manifest $S[U(7) \times U(1)]$ symmetry

We now take the Hanany-Witten transition to move the 7-brane on the right to the left. It leads to the same $SU(8)$ manifest toric-like diagram as Figure 9. As Hanany-Witten

effect is realized as a coordinate transformation, we have

$$T \to \left(-w + \chi_7^{U(7)} \right)^{-1} t, \tag{5.5}$$

which gives

$$t^2 + \left(-2w^4 + (\chi_1^{U(7)} + \chi_7^{U(7)})w^3 + Uw^2 + (1 + \chi_6^{U(7)})w - 2\chi_7^{U(7)} \right) t \tag{5.6}$$
$$+ \left(-w + \chi_7^{U(7)} \right) \left(-w^7 + \chi_1^{U(7)}w^6 - \chi_2^{U(7)}w^5 + \chi_3^{U(7)}w^4 - \chi_4^{U(7)}w^3 + \chi_5^{U(7)}w^2 - \chi_6^{U(7)}w + \chi_7^{U(7)} \right) = 0.$$

In order to compare to (3.23), we redefine the coordinate

$$t \to \widetilde{m}_1^{-1} T, \qquad w \to \widetilde{m}_1^{-\frac{1}{4}} w, \tag{5.7}$$

which leads to the the $SU(8)$ manifest curve for $N_f = 6$ (3.23) with the decomposition between the fundamental characters of $S[U(7) \times U(1)]$ and $SU(8)$

$$\chi_n^{U(7)} \widetilde{m}_1^{\frac{n}{4}} + \chi_{n-1}^{U(7)} \widetilde{m}_1^{\frac{n}{4}} = \chi_n^{SU(8)}, \tag{5.8}$$

where $\chi_0^{U(7)} = 1$, $\chi_7^{U(7)} = \widetilde{m}^{-1}$, and $n = 1, \ldots, 7$.

We note that there exits another scaling of mass parameters which is equivalent up to E_8 Weyl transformation

$$\widetilde{m}_i \to L^{\frac{2}{3}} \widetilde{m}_i \ \ (i = 1, 2, 3), \qquad \widetilde{m}_j \to L^{-\frac{1}{3}} \widetilde{m}_j \ \ (j = 4, \cdots, 9), \tag{5.9}$$

as well as

$$U \to LU, \qquad w \to L^{-\frac{1}{3}} w, \qquad T \to T. \tag{5.10}$$

As the shows two distinct scaling behaviors, it leads to the following decomposition of $SU(9)$ characters into $SU(3) \times SU(6)$ characters:

$$\chi_n \to L^{\frac{2n}{3}} \chi_n^{SU(3)} \ (n = 1, 2, 3), \qquad \chi_n \to L^{\frac{9-n}{3}} \widetilde{\chi}_{9-n}^{SU(6)} \ (n = 4, \cdots, 8), \tag{5.11}$$

satisfying $\chi_3^{SU(3)} = 1 = \widetilde{\chi}_6^{SU(6)}$. Taking large L limit, the E_8 SW curve (4.13) is expressed as

$$T^3 + \left(-\chi_1^{SU(3)}w^2 + \widetilde{\chi}_1^{SU(6)}w - 3 \right) T^2$$
$$+ \left(\chi_2^{SU(3)}w^4 + Uw^3 + (\chi_1^{SU(3)} + \widetilde{\chi}_2^{SU(6)})w^2 - 2\widetilde{\chi}_1^{SU(6)}w + 3 \right) T$$
$$- w^6 + \widetilde{\chi}_5^{SU(6)}w^5 - \widetilde{\chi}_4^{SU(6)}w^4 + \widetilde{\chi}_3^{SU(6)}w^3 - \widetilde{\chi}_2^{SU(6)}w^2 + \widetilde{\chi}_1^{SU(6)}w - 1 = 0, \tag{5.12}$$

which is of manifest $SU(6) \times SU(3)$ symmetry, a maximal compact subgroup of E_7. The corresponding toric-like diagram is given by Figure 20.
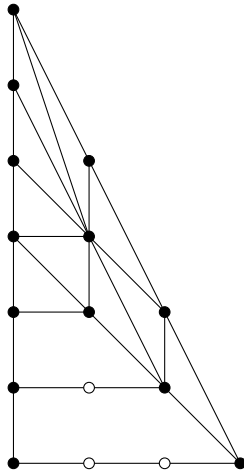
Figure 20. Toric-like diagram of E_7 theory with a manifest $SU(6) \times SU(3)$ symmetry

One can show that this diagram is equivalent to toric-like diagram for E_7 global symmetry by applying the Hanany-Witten transition several times.

The mass decoupling limit from E_7 to E_6 and to lower E_n can be done in a similar fashion, as lower E_n toric (or toric-like) diagram is embedded into higher E_n diagram. For example, E_6 rectangular shape toric-like diagram in Figure 3 is embedded to E_7 toric-like diagram, Figure 8. For $N_f \leq 4$, mass decoupling limit is straightforward and given in Appendix A.

6 Rank-N E_n curve

Toric-like diagrams for higher rank E_n theories are proposed in [20] based on symmetry, dimension of the Higgs branch as well as the Coulomb branch. As in the rank-1 case, they are embedded in T_N. More precisely, the rank-N E_6, E_7, and E_8 theories are embedded in T_{3N}, T_{4N}, and T_{6N}, respectively, such that N 5-branes are bound together with the same 7-branes as in the rank-1 case, on each side of the multi-junction. This means that the number of 7-branes does not change regardless of rank of the gauge group, $Sp(N)$, and hence global symmetry is still E_n.

In this section, we consider the SW curve for the higher rank E_n theories based on toric-like diagram. Computing the curve for the corresponding toric-like diagram is straightforward, following the properties of the white dots in the previous sections, so here we do not give details of computation, rather we sketch how the computation can be done. As explained before, to find the SW curve, it is convenient to implement the Hanany-Witten transition on the (tuned) T_N diagram so that the resultant diagram is of a rectangular shape.
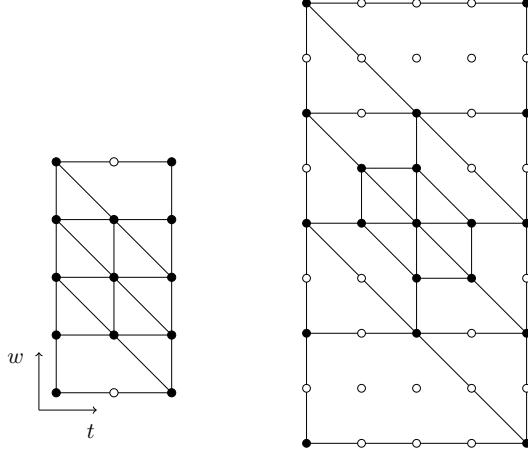
Figure 21. (Left) Rank-1 E_7 toric-like diagram, (Right) Rank-2 E_7 toric-like diagram

Consider toric-like diagram for rank-1 and rank-2 E_7 curves above. The toric-like diagram for rank-1 (on the left of Figure 21) is the same one as Figure 8. The black dot in the middle of the rank-1 diagram corresponds to the Coulomb modulus. The toric-like diagram for rank-2 (on the right of Figure 21) is obtained as follows: Given two dots which are next to each other along the outer edges of the rank-1 diagram, one inserts a white dot such that, from the point of view of (p, q)-web, the number of semi-infinite 5-branes is doubled while they are combined with the same 7-branes. The dots inside of the rank-2 diagram are introduced such that it does not break the s-rule, and dimension of the Coulomb moduli gets doubled to account for rank-2. This procedure of making multi-junction is also applicable to rank-N diagrams with any $N_f(\leq 7)$ flavors.

To compute the SW curve

$$\sum_{i=0}^{4}\sum_{j=0}^{8} c_{ij}t^i w^j = 0, \tag{6.1}$$

we write the boundary conditions

$$t \to 0 \quad : \quad \sum_{j=0}^{8} c_{0j}w^j = c_{08}\prod_{j=1}^{4}(w - \widetilde{m}_j)^2; \qquad \sum_{j=0}^{8} c_{1j}t\,w^j \propto t\prod_{j=1}^{4}(w - \widetilde{m}_j), \tag{6.2}$$

$$t \to \infty \quad : \quad \sum_{j=0}^{8} c_{4j}\,t^4 w^j = c_{48}\,t^4\prod_{j=5}^{8}(w - \widetilde{m}_j)^2; \quad \sum_{j=0}^{8} c_{3j}\,t^3 w^j \propto t^3\prod_{j=5}^{8}(w - \widetilde{m}_j), \tag{6.3}$$

and

$$w \to 0 \quad : \quad \sum_{i=0}^{4} c_{i0} t^i = c_{40}(t - t_2)^4; \qquad \sum_{i=0}^{4} c_{i1} t^i w \propto c_{41} w (t - t_2)^3;$$

$$\sum_{i=0}^{4} c_{i2} t^i w^2 \propto c_{42} w^2 (t - t_2)^2; \qquad \sum_{i=0}^{4} c_{i3} t^i w^3 \propto c_{43} w^3 (t - t_2), \qquad (6.4)$$

$$w \to \infty \quad : \quad \sum_{i=0}^{4} c_{i8} t^i w^8 = c_{48} w^8 (t - t_1)^4; \qquad \sum_{i=0}^{4} c_{i7} t^i w^7 \propto w^7 (t - t_1)^3;$$

$$\sum_{i=0}^{4} c_{i6} t^i w^6 \propto w^6 (t - t_1)^2; \qquad \sum_{i=0}^{4} c_{i1} t^i w^5 \propto w^5 (t - t_1). \qquad (6.5)$$

As explained in (3.5), not all parameters are independent but they are constrained by the same compatibility condition as for the rank-1 case

$$\frac{t_2^2}{t_1^2} = \frac{\prod_{i=5}^{8} \widetilde{m}_i}{\prod_{j=1}^{4} \widetilde{m}_j}.$$

We note that unlike rank-1 case, it turns out that there is another set of coefficients which is related each other again by this compatibility condition.

Let us count the number of the coefficients and the conditions from the boundaries. There are 45 dots (or non-vanishing coefficients) in the rank-2 E_7 toric-like diagram. For the boundary conditions $t \to 0$ and $t \to \infty$, one finds $(8 + 4) \times 2 = 24$ conditions; for the boundary conditions $w \to 0$ and $w \to \infty$, one finds $(4 + 3 + 2 + 1) \times 2 = 20$ conditions. Recall that the compatibility condition indicates that not all boundary conditions are independent. For rank-2, there are two sets of conditions, as mentioned above. The compatibility condition for rank-2 tells us that the number of independent conditions is 42 instead of 44. Hence, one is left with 3 undetermined coefficients; One of them is an overall constant (or rescaling) and the other two are two Coulomb moduli for the rank-2 theory.
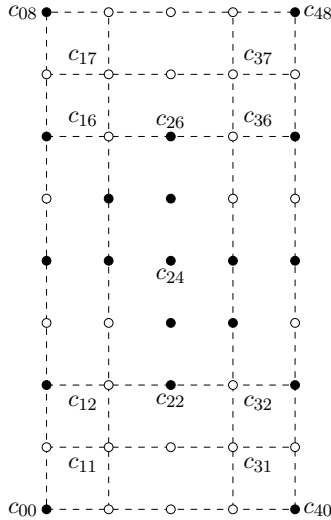

Figure 22. Rank-2 E_7 toric-like diagram

Let us give a bit more explanation for the compatibility condition. Along the four boundary edges, there are 24 dots, and we have 24 conditions from the boundary conditions above. These boundary conditions interrelate the 24 coefficients. It turns that these 24 conditions do not have solutions unless the compatibility condition is satisfied. Given this compatibility condition, 23 out of 24 conditions are independent. The undetermined coefficient is associated with choice of overall rescaling.

Now consider the dots c_{11}, c_{21}, c_{31} along the next-to-boundary edge on the bottom. As there are three dots here and we have 3 conditions from the property of the white dots, the coefficients c_{11}, c_{21}, c_{31} are all determined. The same logic applied to the dots c_{17}, c_{27}, c_{37} along the next-to-boundary edge on the top. We then consider the vertical five dots $c_{12}, \cdots, c_{16}$, we know there are only 4 conditions from the boundary conditions (6.2). Similarly, we have the vertical five dots $c_{32}, \cdots, c_{36}$ and 4 conditions (6.3). We also have three dots c_{32}, c_{22}, c_{12} and 2 conditions from (6.4). Likewise, three dots c_{36}, c_{26}, c_{16} and 2 conditions from (6.5). In total 12 dots with 12 conditions. However, here the coefficients along this rectangular are in interrelated, just like how the compatibility condition (3.5) was obtained. It thus gives another undetermined coefficient, which is related to the Coulomb moduli for the rank-2 case. Recall that the dot in the middle of the diagram is not determined, and this dot is another undetermined coefficient c_{24}. Together, these two unknown coefficients account for two Coulomb moduli of the rank-2 theory. With suitable identification of these Coulomb moduli parameters, for instance, with $U_1 + U_2$ for the first undermined coefficient and $U_1 U_2$ for c_{24}, one finds that the rank-2 SW curve is factorized as the product of the rank-1 SW curves of different Coulomb moduli parameters

$$
\left(\prod_{i=1}^{4} (w - \widetilde{m}_i)\, t^2 + \left(-2w^4 + \chi_{\mu_1}^{SU(8)}\, w^3 + U_1\, w^2 + \chi_{\mu_7}^{SU(8)}\, w - 2 \right) t + \prod_{i=5}^{8} (w - \widetilde{m}_i) \right) \quad (6.6)
$$

$$
\times \left(\prod_{i=1}^{4} (w - \widetilde{m}_i)\, t^2 + \left(-2w^4 + \chi_{\mu_1}^{SU(8)}\, w^3 + U_2\, w^2 + \chi_{\mu_7}^{SU(8)}\, w - 2 \right) t + \prod_{i=5}^{8} (w - \widetilde{m}_i) \right) = 0.
$$

We note that even though rank-2 in this case means $Sp(2)$ and the $Sp(2)$ gauge theories contain an additional antisymmetric hypermultiplet compare with $Sp(1)$ theory, the rank-2 SW curve (6.6) does not describe a generic $Sp(2)$ SW curve with antisymmetric hypermultiplet, rather it describes the $Sp(2)$ SW curve with the vanishing mass of antisymmetric hypermultiplet.

Generalization to rank-N is straightforward. Toric-like diagram for rank-N is a generalization of the rank-2 diagram. The compatibility condition is the exactly the same as that for rank-1. As in rank-2 case, N boundary conditions are redundant for rank-N case.

For instance, if the number of dots of the corresponding toric-like diagram for rank-N is n, then there are $n - 1$ conditions from the boundary conditions but taking into account the compatibility conditions, the number of independent conditions is $n - 1 - N$. Hence, among n coefficients of the SW curve, $n - 1 - N$ coefficients are fully specified by the parameters of the theory, and the undermined $N + 1$ coefficients are one overall rescaling and N Coulomb moduli parameters.

The product of SW curve for rank-1 satisfies the boundary conditions for the toric-like diagram of rank-N theory proposed by [20]. We thus claim that the SW curve for rank-N theory is also factorized as the product form of the rank-1 SW curves

$$SW_N(U_1, U_2, \cdots, U_N) = \prod_{i=1}^{N} SW_i(U_i), \qquad (6.7)$$

where we denoted SW_n as the SW curve for rank-n with E_{N_f+1} symmetry, and U_i as the corresponding Coulomb moduli parameters. This describes the $Sp(N)$ SW curve of E_{N_f+1} symmetry with the vanishing masses of antisymmetric hypermultiplet.

7 Summary and discussion

In this paper, we have proposed a systematic procedure for computing the Seiberg-Witten (SW) curve from generic toric-like diagram base on (p, q) 5-brane web diagram. Using this method, we computed the SW curve for five-dimensional $\mathcal{N} = 1$ $Sp(1)$ gauge theories with $N_f = 6, 7$ flavors, which are expected to have the UV fixed point with E_7, E_8 enhanced global symmetry, respectively. Enhancement of the global symmetry has been seen from various ways, for example, superconformal index [7, 8], topological vertex amplitudes [24, 25, 32], as well as fiber-base duality invariant Nekrasov partition functions [9]. In this paper, the enhancement also appears in the SW curve. At first sight, E_n global symmetry does not look manifest in our expression, rather only subgroup of E_n can be seen in the SW curve, and the curves with different subgroups are related by simple coordinate transformations which correspond to the Hanany-Witten transition. Our SW curves are computed using a totally different way from the method that led to the previously known E_n manifest results [16, 17], which are computed by using E-string effective action. By comparing the both j-invariants, or by performing coordinate transformation to express as the Weierstrass standard form, we find that our result agrees with the known results [15–17]. Mass decoupling limits of the curve are discussed to connect the SW curve for the theory of less flavor, and the 4d limit reproduces 4d SW curves [13, 14], as expected.

We have also computed the SW curve for five-dimensional $Sp(2)$ gauge theory with six fundamental flavors and one massless antisymmetric tensor, which is identified as rank-2 theory of E_7 symmetry, and have shown that it reduces to just the two copies of SW curve for $Sp(1)$ gauge theory with six fundamental flavors. Our result strongly implies that the SW curve for the five-dimensional $Sp(N)$ gauge theory with N_f fundamental flavors and one massless antisymmetric tensor, which is rank-N E_{N_f+1} CFT, is also factorized into N copies of the SW curve of the rank-1 E_{N_f+1} CFT.

As our method of obtaining the SW curve is applicable to any toric-like diagram, there will be more applications to various theories. One of interesting directions is to consider the five-dimensional uplift of the class S theory. The toric diagram for the five-dimensional uplift of the T_N theory was given in [20], and the corresponding SW curve was studied in [20, 24]. By replacing some of the full punctures of T_4 and T_6 with certain type of degenerate punctures, the 5d theories of E_7 and E_8 global symmetries are obtained, respectively. Degenerate punctures are nothing but white dots in toric-like diagram. It

is straightforward to write down toric-like diagram corresponding to a sphere with three punctures of arbitrary type, which is the counterpart of the "pants" in the context of pants decomposition, and thus obtaining the corresponding SW curve is also straightforward. It would be interesting to consider classification of the 5d uplifts of the pants. Moreover, it would be natural to expect that 5d uplift of the class S theories can be obtained by gluing such pants as in the 4d class S theories. The corresponding SW curve for 5d uplifts of class S theories can also be computed based on the method developed in this paper.

The 5d uplift of the degenerate punctures are studied in various recent papers in the context of, for example, the topological string partition function and the superconformal index. Especially, the way of realizing the degenerate puncture by tuning the Kähler moduli parameters of the Calabi-Yau geometry in the refined topological string is first proposed for the E_7 case in [25] and then generalized and/or applied to various cases in [9, 26, 27, 33, 34]. When we consider the limit where the Ω-deformation parameters vanish, their method is roughly translated into tuning the Coulomb moduli parameters and some of the mass parameters to be same. This tuning then reduces the genus of the SW curve as in this paper.[12] Thus, we claim that the way of tuning in this paper is consistent with the way developed in the other papers.

When we consider the 5d uplift of class S theory, an important issue is how to uplift the "$\mathcal{N} = 2$ dualities" [21], which is a generalization of the electromagnetic duality of the $SU(2)$ SW theory or Argyres-Seiberg duality for $SU(3)$ theory with six flavors. Related issue has been addressed in various papers including [24, 27, 33]. Especially, it was pointed out in [24], that the SW curve of E_6 CFT is obtained by tuning some of the parameters of the SW curve for $SU(3)$ gauge theory with six flavors with proper identification of the mass parameters, which we expect to be related to Argyres-Seiberg duality [35]. Using the result of this paper, we can find several more examples analogous to this.
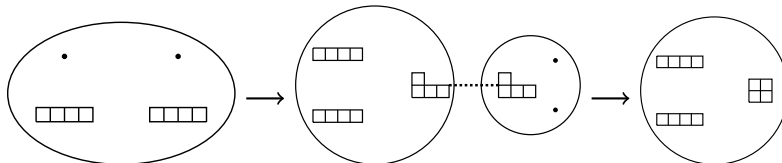

Figure 23. Construction of E_7 CFT. Start from $SU(4)$ with eight flavors, take the strong coupling limit, and Higgs one of the punctures.

As an example, 4d E_7 CFT is constructed from $SU(4)$ gauge theory with eight flavors with $\mathcal{N} = 2$ dualities and Higgsing procedure to reduce the order of a puncture. See Figure

---

[12] The tuning of mass parameters $m_I = m_J$ is equivalent to a constraint coming from the white dot, for example, the first equation in the first line of (2.11), which is straightforward to understand. The tuning of the Coulomb moduli parameters $a_i = m_J$ corresponds to another constraint coming from the white dot in the SW curve, for instance, the second equation in the first line of (2.11), which may not be obvious, because the a_i are obtained by performing A-cycle integral of the corresponding SW curve. However, by taking into account that the mass parameter is obtained by picking up the residue of the singularity, we can see that the integral over the sum of the cycle giving a_i and the path giving $-m_I$ will vanish. This implies that a certain non-trivial cycle vanishes and thus the genus of the corresponding SW curve reduces.

23. Especially, it means that the SW curve for 4d E_7 CFT is obtained from the SW curve for 4d $SU(4)$ gauge theory with eight flavors. This analogue can be seen in five dimensions. From the toric-like diagram for $Sp(1)$ theory of E_7 symmetry in Figure 11, one would find that it corresponds to the toric diagram for $SU(4)$ gauge theory with eight flavors if all the dots were black. Changing black dots to white dots corresponds to tuning the parameters in a specific way that is discussed in this paper. Therefore, we observe that the SW curve for 5d E_7 CFT is obtained from the SW curve for 5d $SU(4)$ gauge theory with eight flavors by tuning parameters. Especially, this tuning turns out to include the strong coupling limit in Figure 23. It is, therefore, natural to expect that our observation is related to the construction of 4d E_7 CFT, where the $\mathcal{N} = 2$ dualities play an essential role.
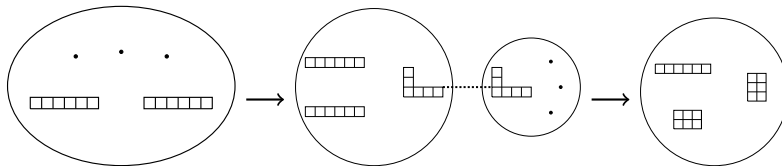

Figure 24. Construction of E_8 CFT. Start from $SU(6)^2$ theory with 6+6 flavors, take the weak coupling limit in the S-dual frame, and Higgs two of the punctures.

Another example is the construction of the E_8 CFT from $SU(6) \times SU(6)$ gauge theory with 6+6 flavors. There exists such construction in 4d level. See Figure 24. From the toric-like diagram for 5d E_8 theory in Figure 16, we observe that the SW curve for E_8 CFT is obtained from that for the $SU(6) \times SU(6)$ gauge theory with 6+6 flavors in five dimensions. This observation also implies that topological string amplitude for E_8 theory computed in [26] can be obtained as a limit of that for $N_f = 6$ $SU(6) \times N_f = 6$ $SU(6)$ theory.

Although this observation is expected to be related to the $\mathcal{N} = 2$ duality, it is not clear how this observation is connected to what is discussed in [27]. We would like clarify this point in the future.

Acknowledgement

A   Seiberg-Witten curves for $N_f \leq 4$ flavors

In this appendix, derivation of the Seiberg-Witten curve from toric-diagram is presented.

A.1 $N_f = 0$ with E_1 or $\widetilde{E}_1$ flavor symmetry
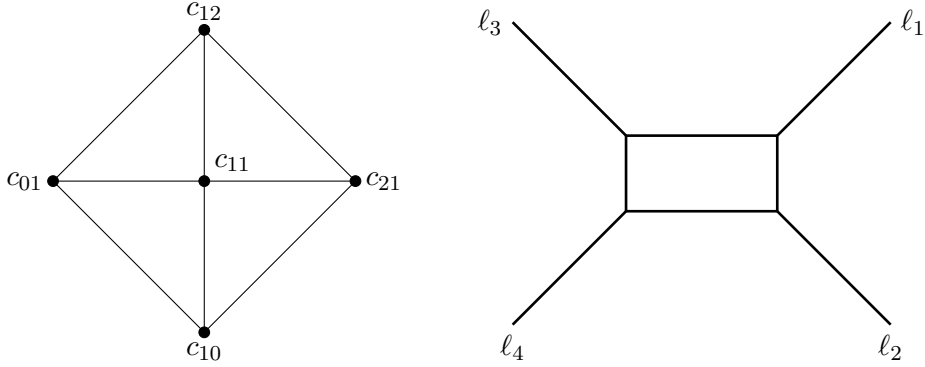
A.1.1 E_1 symmetry

Figure 25. Toric web diagram for $N_f = 0$ of E_1 flavor symmetry

The SW curve for the pure case $(N_f = 0)$ is of the form

$$c_{01}\, w + c_{10}\, t + c_{11}\, tw + c_{12}\, tw^2 + c_{21}\, t^2 w = 0. \tag{A.1}$$

Though we have thus five unknowns from the beginning, including three rescalings, one is left with only two parameters which are one Coulomb modulus and the dynamical scale Λ_0. We show how one can identify them below. We start with asymptotic boundary conditions:

$$
\begin{aligned}
|w| \sim |t| \text{ large}: & \qquad c_{12}tw^2 + c_{21}t^2 w = c_{12}tw(w + \ell_1 t) \\
|w^{-1}| \sim |t| \text{ large}: & \qquad c_{10}t + c_{21}t^2 w = c_{21}t(\ell_2 + tw) \\
|w| \sim |t^{-1}| \text{ large}: & \qquad c_{12}tw^2 + c_{01}w = c_{12}w(tw + \ell_3) \\
|w^{-1}| \sim |t^{-1}| \text{ large}: & \qquad c_{01}w + c_{10}t = c_{01}(w + \ell_4 t).
\end{aligned} \tag{A.2}
$$

The compatibility condition is then

$$\ell_1\, \ell_2 \;=\; \ell_3\, \ell_4. \tag{A.3}$$

As for three rescalings degrees of freedom, we take

$$c_{01} = c_{21} = 1, \quad c_{10} = c_{12} = \ell_2 = \ell_1^{-1} = \ell_4, \quad c_{11} \propto U, \tag{A.4}$$

and the SW curve for $N_f = 0$ is expressed in terms of two parameters, the Coulomb modulus U, and ℓ_1:

$$w + \ell_1^{-1} t\left(w^2 + Uw + 1\right) + t^2 w = 0. \tag{A.5}$$

The ℓ_1 is in fact related to the dynamical scale Λ_0. We explain how to relate it to the dynamical scale. By referring to the topological vertex results, the dynamical scale is

determined as the geometric mean of differences Δt evaluated in asymptotic values of t for given w. This is consistent with the dependence of the dynamical scale over energy scales

$$\sqrt{\left(\frac{\ell_3 w_1^{-1}}{\ell_1^{-1} w_1}\right)\left(\frac{\ell_2 w_2^{-1}}{\ell_4^{-1} w_2}\right)} = \left(\frac{\ell_1 \ell_3}{\ell_2 \ell_4}\right)^{\frac{1}{2}} w_2 w_1^{-1}\bigg|_{w_1=w_2=w_0} = \left(2\pi R \Lambda_0\right)^{2N_c - N_f}. \tag{A.6}$$

We then find

$$\ell_1 = \left(2\pi R \Lambda_0\right)^2, \tag{A.7}$$

and thus the SW curve for $N_f = 0$ is written as

$$w + \frac{t}{(2\pi R \Lambda_0)^2}\left(w^2 + Uw + 1\right) + t^2 w = 0. \tag{A.8}$$

This has E_1 flavor symmetry.

A.1.2 $\widetilde{E}_1$ symmetry
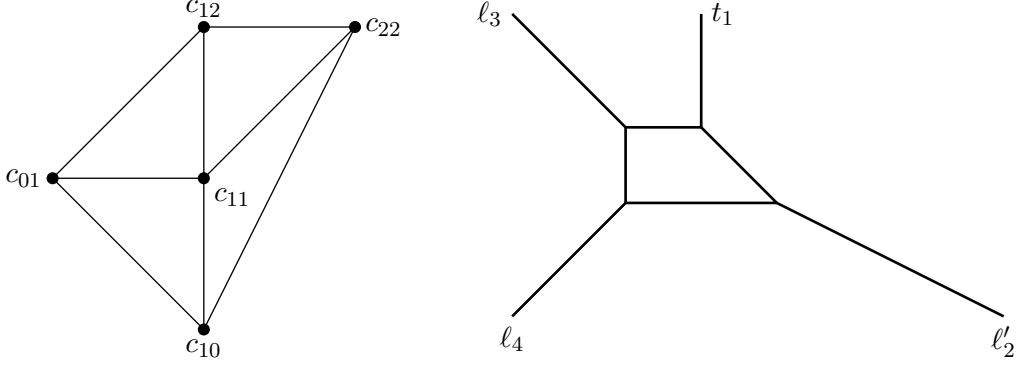
Figure 26. Toric web diagram for $N_f = 0$ of $\widetilde{E}_1$ flavor symmetry

There exits an inequivalent toric diagram which has different asymptotic boundary conditions compared with the above E_1 case. It is known as $\widetilde{E}_1$ theory. The asymptotic boundary conditions are given by

$$
\begin{aligned}
|w^{-1}| \sim |t^2| \text{ large}: \quad & c_{10}t + c_{22}t^2 w^2 = c_{22}t(tw^2 + \ell_2') && \Rightarrow && c_{10} = \ell_2' c_{22}, \\
|w| \text{ large}: \quad & c_{12}tw^2 + c_{22}t^2 w^2 = c_{22}tw^2(-t_1 + t) && \Rightarrow && c_{12} = -t_1 c_{22}, \\
|w| \sim |t^{-1}| \text{ large}: \quad & c_{12}tw^2 + c_{01}w = c_{12}w(tw + \ell_3) && \Rightarrow && c_{01} = \ell_3 c_{12}, \\
|w^{-1}| \sim |t^{-1}| \text{ large}: \quad & c_{01}w + c_{10}t = c_{01}(w + \ell_4 t) && \Rightarrow && c_{10} = \ell_4 c_{01}, \tag{A.9}
\end{aligned}
$$

subject to the compatibility condition

$$\ell_2' = -t_1 \ell_3 \ell_4. \tag{A.10}$$

We choose the three rescaling degrees of freedom to be

$$c_{12} = c_{10}, \qquad c_{22} = 1 = c_{01}, \tag{A.11}$$

The dynamical scale $\widetilde{\Lambda}_0$ is

$$\ell_4 = (2\pi R \widetilde{\Lambda}_0)^{-2}. \tag{A.12}$$

One then obtains the SW curve for $\widetilde{E}_1$ as

$$w + \frac{t}{(2\pi R \widetilde{\Lambda}_0)^2}\left(w^2 + \tilde{U}w + 1\right) + t^2 w^2 = 0. \tag{A.13}$$

We note that the 4d limit of E_1 and $\tilde{E}_1$ gives the same SW curve at $\mathcal{O}(\beta^0)$,

$$1 + t^2 + \frac{t(u + v^2)}{\Lambda_0} = 0. \tag{A.14}$$

A.1.3 E_0 Seiberg-Witten curve

It is interesting to take a limit that leads to the E_0 SW curve from the $\widetilde{E}_1$ curve. For this, we decouple the coefficient c_{12} or the tw^2-term. Instead of (A.13), we start a generic form of the $\widetilde{E}_1$ curve

$$c_{01}\left(w + \ell_4\, t + U\, tw + \frac{1}{\ell_3}\, tw^2 + \frac{\ell_4}{\ell_2'}t^2 w^2\right) = 0. \tag{A.15}$$

We then take $\ell_3 \to \infty, t_1 \to 0$ while $-t_1 \ell_3$ fixed, which gives

$$w + \ell_4\, t + U\, tw + \frac{\ell_4}{\ell_2'}t^2 w^2 = 0. \tag{A.16}$$

Using the remaining rescaling degrees of freedom associated with t and w, we can fix $\ell_4 = 1, \ell_2' = 1$, yielding the E_0 SW curve

$$w + t + U\, tw + t^2 w^2 = 0. \tag{A.17}$$
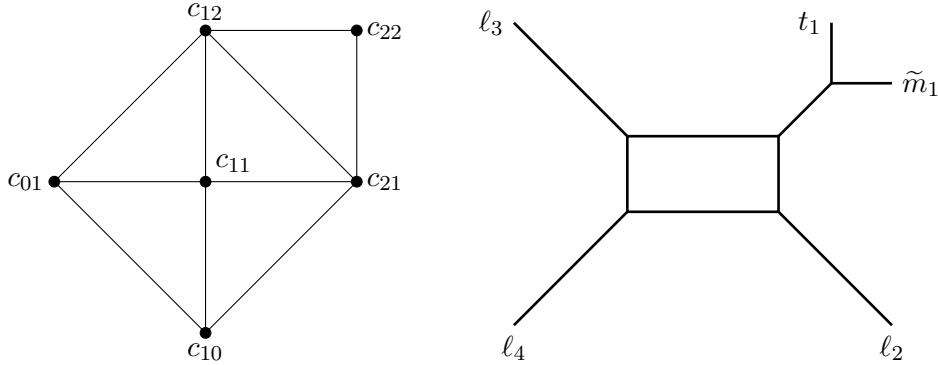
A.2 $N_f = 1$

Figure 27. Toric web diagram for $N_f = 1$ of E_2 flavor symmetry

For $N_f = 1$, we start with

$$c_{01}\, w + c_{10}\, t + c_{11}\, tw + c_{12}\, tw^2 + c_{21}\, t^2 w + c_{22}t^2 w^2 = 0. \tag{A.18}$$

The boundary conditions are

$$
\begin{array}{llll}
|w^{-1}| \sim |t| \text{ large}: & c_{10}t + c_{21}t^2 w = c_{21}t(\ell_2 + tw) & \Rightarrow & c_{10} = \ell_2 c_{21}, \\
|w| \sim |t^{-1}| \text{ large}: & c_{12}tw^2 + c_{01}w = c_{12}w(tw + \ell_3) & \Rightarrow & c_{01} = \ell_3 c_{12}, \\
|w^{-1}| \sim |t^{-1}| \text{ large}: & c_{01}w + c_{10}t = c_{01}(w + \ell_4 t) & \Rightarrow & c_{10} = \ell_4 c_{01}.
\end{array} \tag{A.19}
$$

In addition to this, there is an extra contribution from a flavor:

$$
\begin{array}{llll}
c_{21}\, t^2\, w + c_{22}\, t^2\, w^2 = c_{22}\, t^2\, w\, (-\widetilde{m}_1 + w) & \Rightarrow & c_{21} = -\widetilde{m}_1\, c_{22}, \\
c_{12}\, t\, w^2 + c_{22}\, t^2\, w^2 = c_{22}\, t\, w^2\, (-t_1 + t) & \Rightarrow & c_{12} = -t_1\, c_{22}.
\end{array} \tag{A.20}
$$

The compatibility condition is

$$
\frac{\widetilde{m}_1}{t_1}\, \ell_2 = \ell_3\, \ell_4. \tag{A.21}
$$

As in the $N_f = 0$ case, for three rescaling degrees of freedom, we take

$$
c_{01} = c_{21} = 1 \quad \text{and} \quad c_{10} = c_{12}, \tag{A.22}
$$

or equivalently,

$$
\frac{t_1}{\ell_2} = \widetilde{m}_1, \qquad t_1 \ell_3 = \widetilde{m}_1 \quad (\text{or} \quad \ell_2 = \ell_4). \tag{A.23}
$$

With dynamical scale is given by

$$
t_1^2\, \widetilde{m}_1^{-\frac{3}{2}} = \left(2\pi R_B \Lambda_1\right)^{-3}, \tag{A.24}
$$

the SW curve take the following form

$$
w + t_1\, \widetilde{m}_1^{-1}\, t\left(w^2 + U\,w + 1\right) + t^2\,w - \widetilde{m}_1^{-1}\, t^2\, w^2 = 0. \tag{A.25}
$$

A.2.1 E_1 limit
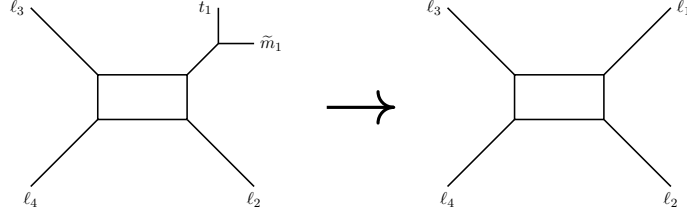
Figure 28. One obtains E_1 curve from the E_2 curve by taking $\widetilde{m}_1 \to \infty$ and $t_1 \to \infty$, while $\widetilde{m}_1 t_1^{-1} = \ell_1$ fixed.

It is clear from Figure 28 that by taking the mass decoupling limit

$$
\widetilde{m}_1 \to \infty \quad (\text{while } t_1^{-1}\widetilde{m}_1 = \ell_1 \text{ fixed}), \tag{A.26}
$$

one reproduces the $N_f = 0$, E_1 curve, (A.5). It follows that the condition (A.23) becomes the condition for $N_f = 0$, (A.4). The dynamical scale for $N_f = 1$ and $N_f = 0$ are related by

$$
\widetilde{m}_1^{\frac{1}{2}}(2\pi R\Lambda_1)^3 = (2\pi R\Lambda_0)^4, \tag{A.27}
$$

which relates (A.24) to (A.7).

A.2.2 $\widetilde{E}_1$ limit
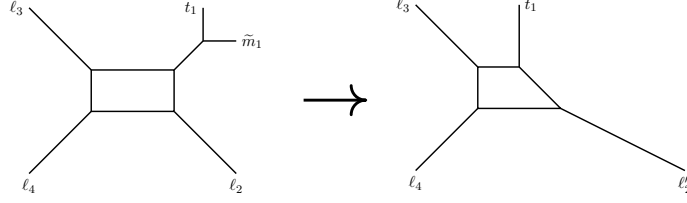
Figure 29. One obtains $\widetilde{E}_1$ curve from the E_2 curve by taking $\widetilde{m}_1 \to 0$ and $\ell_2 \to \infty$, while $-\widetilde{m}_1 \ell_2 = \ell'_2$ fixed.

We can take a distinct mass decoupling limit such that $\widetilde{m}_1 \to 0$, keeping $-\widetilde{m}_1 \ell_2 \ (= \ell'_2)$ fixed. In this case, the relation (A.21) is expressed as

$$-t_1 \ell_3 \ell_4 = -\widetilde{m}_1 \ell_2 \ (\equiv \ell'_2). \tag{A.28}$$

In this limit, the $t^2 w$-term drops out and the SW curve (A.25) becomes

$$w - t_1 \, \ell_2'^{-1} \, \ell_4 \, t \left(w^2 + \tilde{U} \, w - t_1^{-1} \ell'_2 \right) - \ell_2'^{-1} \ell_4 \, t^2 \, w^2 = 0. \tag{A.29}$$

With the choice $-t_1^{-1} \ell'_2 = 1$ and $\ell_2'^{-1} \ell_4 = 1$, or equivalently $c_{12} = c_{10}$ and $c_{01} = c_{22}$, the SW curve is written in term of two parameters, ℓ_4, $\tilde{U}$,

$$w + \ell_4 \, t \left(1 + \tilde{U} \, w + w^2 \right) + t^2 w^2 = 0, \tag{A.30}$$

which is nothing but the SW curve for $\widetilde{E}_1$, (A.13).

A.3 $N_f = 2$
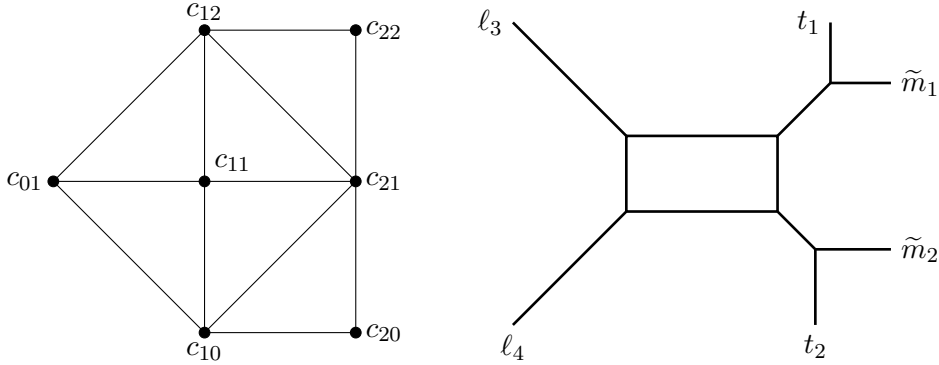
Figure 30. Toric and web diagrams for $N_f = 2$ of E_3 flavor symmetry

For $N_f = 2$, we start with

$$c_{01} \, w + c_{10} \, t + c_{11} \, tw + c_{12} \, tw^2 + c_{21} \, t^2 w + c_{22} \, t^2 w^2 + c_{20} \, t^2 = 0. \tag{A.31}$$

$$- 45 -$$

The boundary conditions are given by

$$
\begin{aligned}
|w| \text{ large}: &\qquad c_{12}tw^2 + c_{22}t^2w^2 = c_{22}tw^2(-t_1 + t) \\
|w| \text{ small}: &\qquad c_{10}t + c_{20}t^2 = c_{20}t(-t_2 + t) \\
|w| \sim |t^{-1}| \text{ large}: &\qquad c_{12}tw^2 + c_{01}w = c_{12}w(tw + \ell_3) \\
|w^{-1}| \sim |t^{-1}| \text{ large}: &\qquad c_{01}w + c_{10}t = c_{01}(w + \ell_4 t),
\end{aligned}
\tag{A.32}
$$

and the following extra boundary condition: When $|t|$ is very large,

$$
c_{20}t^2 + c_{21}t^2w + c_{22}t^2w^2 = c_{22}t^2(w - \widetilde{m}_1)(w - \widetilde{m}_2).
\tag{A.33}
$$

The compatibility condition is

$$
\widetilde{m}_1 \, t_1^{-1} \, \widetilde{m}_2 \, t_2 = \ell_3 \, \ell_4.
\tag{A.34}
$$

For three rescaling degrees of freedom, we choose

$$
c_{01} = c_{21} = 1, \quad c_{10} = c_{12},
\tag{A.35}
$$

or equivalently

$$
\frac{t_1}{t_2} = \widetilde{m}_1 \widetilde{m}_2, \qquad t_1 \ell_3 = \widetilde{m}_1 + \widetilde{m}_2.
\tag{A.36}
$$

The dynamical scale is given by

$$
\left(\frac{t_1 t_2 \ell_4}{\ell_3} \right)^{\frac{1}{2}} = \left(2\pi R_B \Lambda_2 \right)^{-2},
\tag{A.37}
$$

or equivalently,

$$
t_1^2 \, \widetilde{m}_1^{-\frac{1}{2}} \, \widetilde{m}_2^{-\frac{1}{2}} (\widetilde{m}_1 + \widetilde{m}_2)^{-1} = \left(2\pi R_B \Lambda_2 \right)^{-2}.
\tag{A.38}
$$

The SW curve for $N_f = 2$ is then

$$
w + t \frac{t_1}{\widetilde{m}_1 + \widetilde{m}_2} \left(w^2 + Uw + 1 \right) - t^2 \frac{1}{\widetilde{m}_1 + \widetilde{m}_2} \left(w - \widetilde{m}_1 \right) \left(w - \widetilde{m}_2 \right) = 0.
\tag{A.39}
$$

In the mass decoupling limit $m_2 \to \infty$, correspondingly $\widetilde{m}_2 \to 0$, while keeping $\widetilde{m}_2 t_2 = \ell_2$ fixed, it is straightforward to see that the SW curve for $N_f = 2$, (A.39), becomes that for $N_f = 1$, (A.25). The condition that we used, (A.36) becomes the condition for $N_f = 1$, (A.23), and the dynamical scales for $N_f = 2$ and $N_f = 1$ are related in this decoupling limit as

$$
\widetilde{m}_2^{-\frac{1}{2}} (2\pi R\Lambda_2)^2 = (2\pi R\Lambda_1)^3
\tag{A.40}
$$

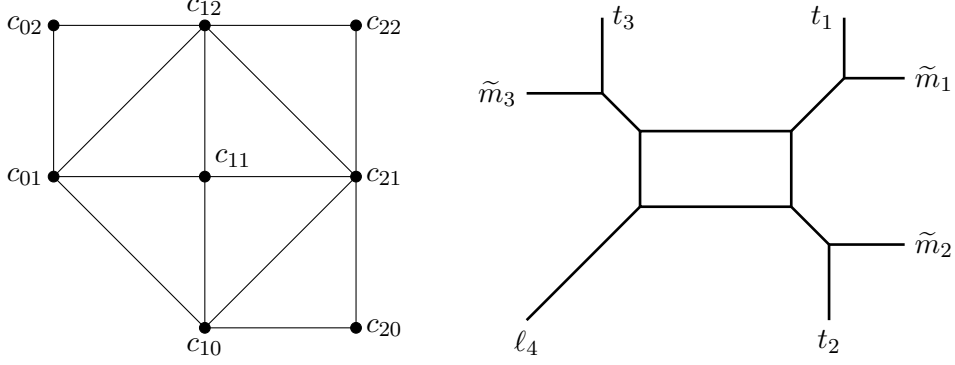which relates (A.38) to (A.24).

A.4 $N_f = 3$

Figure 31. Toric web diagram for $N_f = 3$ of E_4 flavor symmetry

For $N_f = 3$, we start with

$$c_{01}\,w + c_{10}\,t + c_{11}\,tw + c_{12}\,tw^2 + c_{21}\,t^2w + c_{22}\,t^2w^2 + c_{20}\,t^2 + c_{02}w^2 = 0. \qquad (A.41)$$

The boundary conditions are given by

$$
\begin{aligned}
&|w| \text{ small}: & c_{10}t + c_{20}t^2 &= c_{20}t(-t_2 + t), \\
&|w^{-1}| \sim |t^{-1}| \text{ large}: & c_{01}w + c_{10}t &= c_{01}(w + \ell_4 t), \\
&|t| \text{ large}: & c_{20}t^2 + c_{21}t^2w + c_{22}t^2w^2 &= c_{22}t^2(w - \widetilde{m}_1)(w - \widetilde{m}_2),
\end{aligned}
\qquad (A.42)
$$

and when $|w|$ large, the boundary condition is given by

$$c_{02}w^2 + c_{12}tw^2 + c_{22}t^2w^2 = c_{22}w^2(t - t_1)(t - t_3), \qquad (A.43)$$

and the boundary condition for $|t|$ small ($|w|$ not small) is given by

$$c_{01}w + c_{02}w^2 = c_{02}w(w - \widetilde{m}_3). \qquad (A.44)$$

The compatibility is given by

$$\widetilde{m}_1\, t_1^{-1}\, \widetilde{m}_2\, t_2 = \widetilde{m}_3\, t_3\, \ell_4. \qquad (A.45)$$

For three rescaling degrees of freedom, we choose

$$c_{01} = c_{21} = 1, \qquad c_{10} = c_{12}, \qquad (A.46)$$

or equivalently

$$\frac{t_1 + t_3}{t_2} = \widetilde{m}_1 \widetilde{m}_2, \qquad t_1 t_3 = \frac{\widetilde{m}_1 + \widetilde{m}_2}{\widetilde{m}_3}. \qquad (A.47)$$

The dynamical scale is given by

$$\left(\frac{t_1 t_2 \ell_4}{t_3}\right)^{\frac{1}{2}} = \left(2\pi R_B \Lambda_3\right)^{-1}, \qquad (A.48)$$

or

$$t_1 = \left(\frac{\widetilde{m}_1 + \widetilde{m}_2}{\widetilde{m}_3}\right)^{\frac{1}{2}} \left(\frac{(\widetilde{m}_1\widetilde{m}_2\widetilde{m}_3)^{\frac{1}{2}}}{2\pi R\Lambda_3} - 1\right)^{\frac{1}{2}}. \tag{A.49}$$

The SW curve for $N_f = 3$ is then

$$w + t\left(\frac{t_1}{\widetilde{m}_1 + \widetilde{m}_2} + \frac{1}{t_1\widetilde{m}_3}\right)\left(w^2 + Uw + 1\right) - t^2\frac{1}{\widetilde{m}_1 + \widetilde{m}_2}\left(w - \widetilde{m}_1\right)\left(w - \widetilde{m}_2\right) - \frac{1}{\widetilde{m}_3}w^2 = 0. \tag{A.50}$$

In the mass decoupling limit $\widetilde{m}_3 \to \infty$ and $t_3 \to 0$, while $\widetilde{m}_3 t_3 = \ell_3$ fixed, the SW curve for $N_f = 3$, (A.57), becomes that for $N_f = 2$, (A.50), and the condition that we used, (A.47) becomes the condition for $N_f = 3$, (A.36), and the dynamical scales for $N_f = 3$ and $N_f = 2$ are related in this decoupling limit as

$$\widetilde{m}_3^{\frac{1}{2}}(2\pi R\Lambda_3) = (2\pi R\Lambda_2)^2 \tag{A.51}$$

which relates (A.49) to (A.38).

A.5 $\quad N_f = 4$
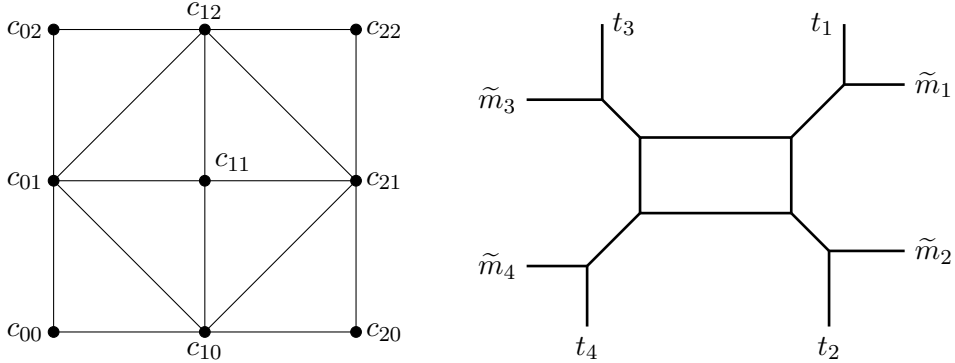
Figure 32. Toric web diagram for $N_f = 4$ of E_5 flavor symmetry

For $N_f = 4$, we start with

$$c_{01}\,w + c_{10}\,t + c_{11}\,tw + c_{12}\,tw^2 + c_{21}\,t^2w + c_{22}\,t^2w^2 + c_{20}\,t^2 + c_{02}w^2 + c_{00} = 0. \tag{A.52}$$

The boundary conditions are

$$\begin{aligned}
|w|\text{ large}: \qquad & c_{02}w^2 + c_{12}tw^2 + c_{22}t^2w^2 = c_{22}w^2(t - t_1)(t - t_3), \\
|w|\text{ small}: \qquad & c_{20}t^2 + c_{10}t + c_{00} = c_{20}(t - t_2)(t - t_4), \\
|t|\text{ large}: \qquad & c_{20}t^2 + c_{21}t^2w + c_{22}t^2w^2 = c_{22}t^2(w - \widetilde{m}_1)(w - \widetilde{m}_2), \\
|t|\text{ small}: \qquad & c_{02}w^2 + c_{01}w + c_{00} = c_{02}(w - \widetilde{m}_3)(w - \widetilde{m}_4).
\end{aligned} \tag{A.53}$$

The compatibility condition is given by

$$\widetilde{m}_1\, t_1^{-1}\, \widetilde{m}_2\, t_2 = \widetilde{m}_3\, t_3\, \widetilde{m}_4\, t_4^{-1}. \tag{A.54}$$

For three rescaling degrees of freedom, we choose

$$c_{01} = c_{21} = 1, \qquad c_{10} = c_{12}, \tag{A.55}$$

or equivalently,

$$\frac{t_1 + t_3}{t_2 + t_4} = \widetilde{m}_1 \widetilde{m}_2, \qquad t_1 t_3 = \frac{\widetilde{m}_1 + \widetilde{m}_2}{\widetilde{m}_3 + \widetilde{m}_4}. \tag{A.56}$$

The SW curve for $N_f = 4$ is then

$$-\frac{1}{\widetilde{m}_3 + \widetilde{m}_4}\big(w - \widetilde{m}_3\big)\big(w - \widetilde{m}_4\big) + t\left(\frac{t_1}{\widetilde{m}_1 + \widetilde{m}_2} + \frac{1}{t_1(\widetilde{m}_3 + \widetilde{m}_4)}\right)\big(w^2 + Uw + 1\big)$$
$$-t^2 \frac{1}{\widetilde{m}_1 + \widetilde{m}_2}\big(w - \widetilde{m}_1\big)\big(w - \widetilde{m}_2\big) = 0. \tag{A.57}$$

In this case, there is no dynamical scale but one can define the gauge coupling as geometric average of t_i

$$\left(\frac{t_1 t_2}{t_3 t_4}\right)^{\frac{1}{2}} = q^{-1}. \tag{A.58}$$

It follows from (A.54), (A.56), and (A.58) that t_1 are expressed in terms of masses and the gauge coupling as

$$t_1 = \left(\frac{\widetilde{m}_1 + \widetilde{m}_2}{\widetilde{m}_3 + \widetilde{m}_4}\right)^{\frac{1}{2}} \cdot \left(\frac{q^{-1} S^{\frac{1}{2}} - 1}{1 - q S^{\frac{1}{2}}}\right)^{\frac{1}{2}}, \quad S \equiv \widetilde{m}_1 \widetilde{m}_2 \widetilde{m}_3 \widetilde{m}_4. \tag{A.59}$$

The SW curve is also written in a symmetric way as

$$t^2\big(w - \widetilde{m}_1\big)\big(w - \widetilde{m}_2\big) - t\,(t_1 + t_3)\big(w^2 + Uw + 1\big) + t_1 t_3\big(w - \widetilde{m}_3\big)\big(w - \widetilde{m}_4\big) = 0, \tag{A.60}$$

with

$$t_1 + t_3 = \left(\frac{\widetilde{m}_1 + \widetilde{m}_2}{\widetilde{m}_3 + \widetilde{m}_4}\right)^{\frac{1}{2}} q^{-\frac{1}{2}} S^{\frac{1}{4}} \left(\frac{S^{\frac{1}{2}} - qS}{S^{\frac{1}{2}} - q}\right)^{\frac{1}{2}} \left(1 + q\frac{S^{\frac{1}{2}} - q}{1 - qS^{\frac{1}{2}}}\right). \tag{A.61}$$

In the mass decoupling limit where $\widetilde{m}_4 \to 0$ and $t_4 \to 0$, while $\widetilde{m}_4\, t_4^{-1} = \ell_4$ fixed, the SW curve for $N_f = 4$, (A.57), becomes naturally the SW curve for $N_f = 3$, (A.50), and the condition that we used, (A.56), becomes the condition for $N_f = 3$, (A.47). We note that in this mass decoupling limit, dynamical scales for $N_f = 4$ and $N_f = 3$ are related as

$$q^{-1} \widetilde{m}_4^{\frac{1}{2}} = (2\pi R \Lambda_3)^{-1}, \tag{A.62}$$

which is consistent with that (A.59) for $N_f = 4$ turns into that of $N_f = 3$, (A.49). We note that all the parameters including dynamical scales except for q are not physical. This

is due to our choice of three rescaling degrees of freedom. The choice, $c_{01} = c_{21} = 1$ and $c_{10} = c_{12}$, we have chosen, makes mass decoupling limit easier. We comment that the SW curve with unphysical parameters can be related to the SW curve with physical ones by coordinate transformation below.

SW curve with physical masses

Different choices for three rescaling degrees of freedom lead to a differently looking curve which is related by coordinate transformation. We consider a choice that the position of the exponential of masses $\widetilde{m}_i$ is measured from the center of the Coulomb branch. With $c_{22} = 1 = t_4$ in Figure 32, the SW curve is given by

$$
\mathsf{t}^2 \left(\mathsf{w} - \widetilde{m}'_1 \right) \left(\mathsf{w} - \widetilde{m}'_2 \right) - \mathsf{t} \left(\widetilde{m}'_1 \widetilde{m}'_2 (1 + qS'^{-\frac{1}{2}}) \mathsf{w}^2 + U' \mathsf{w} + (1 + qS'^{\frac{1}{2}}) \widetilde{m}'_1 \widetilde{m}'_2 \right)
$$
$$
+ qS'^{-\frac{1}{2}} \widetilde{m}'^2_1 \widetilde{m}'^2_2 \left(\mathsf{w} - \widetilde{m}'_3 \right) \left(\mathsf{w} - \widetilde{m}'_4 \right) = 0, \tag{A.63}
$$

where $S' \equiv \widetilde{m}'_1 \widetilde{m}'_2 \widetilde{m}'_3 \widetilde{m}'_4$. In the 4d limit, by expanding $\mathsf{w} \equiv e^{-\beta \mathsf{v}}$ and $\widetilde{m}'_i \equiv e^{-\beta \mathsf{m}_i}$ with respect to β while keeping t and q as they are, one finds [12, 36]

$$
\mathsf{t}^2 (\mathsf{v} - \mathsf{m}_1)(\mathsf{v} - \mathsf{m}_2) + \mathsf{t} \left(-(1+q)\mathsf{v}^2 + q\,\mathsf{v} \sum_{i=1}^{4} \mathsf{m}_i + u \right) + q(\mathsf{v} - \mathsf{m}_3)(\mathsf{v} - \mathsf{m}_4) = 0, \tag{A.64}
$$

where the masses m_i are physical masses. The coordinate transformation that connects (A.63) to (A.60) is as follows:

$$
\mathsf{w} \to Tw, \qquad \widetilde{m}'_i \to T\widetilde{m}_i, \qquad T = \left(\frac{q - S^{\frac{1}{2}}}{qS - S^{\frac{1}{2}}} \right)^{\frac{1}{2}},
$$
$$
\mathsf{t} \to \sqrt{qS^{-\frac{1}{2}} T^2 \widetilde{m}^2_1 \widetilde{m}^2_2 \left(\frac{\widetilde{m}_3 + \widetilde{m}_4}{\widetilde{m}_1 + \widetilde{m}_2} \right)} \, t, \tag{A.65}
$$

where S is the product of masses given in (A.59).

A.6   Higher rank curve

The toric-like diagram for higher rank-N with N_f flavors can be obtained in the same way as explained section 6. The corresponding SW curve is again factorized as the product of that of rank-1. As an example, we show the toric-like diagram for rank-2 E_1 theory ($N_f = 0$) and the corresponding (p, q) web in Figure 33.
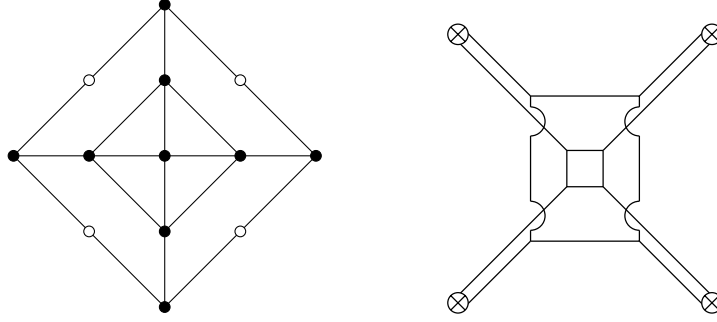
Figure 33. Toric-like diagram for rank-2 E_1 theory and corresponding web diagram.

B   The Seiberg-Witten curves from E_8 to E_0

We here list the result of decomposition of the characters of E_n into $E_{n-1} \times U(1)$ and then factoring out the $U(1)$ part, introduced in [17]:

(i) Rescale the all variables

$$(u, x, y) \rightarrow (Lu, L^2 x, L^3 y), \tag{B.1}$$

$$(\chi_{\mu_1}, \chi_{\mu_2}, \chi_{\mu_3}, \chi_{\mu_4}, \chi_{\mu_5}, \chi_{\mu_6}, \chi_{\mu_7}, \chi_{\mu_8}) \rightarrow (L^2 \chi_{\mu_1}, L^3 \chi_{\mu_2}, L^4 \chi_{\mu_3}, L^6 \chi_{\mu_4}, L^5 \chi_{\mu_5}, L^4 \chi_{\mu_6}, L^3 \chi_{\mu_7}, L^2 \chi_{\mu_8}),$$

where the power of L in the character is the *marks* of E_8.

(ii) Set χ_{μ_8} to 1 when reducing from E_8 to E_7, and take $L \rightarrow \infty$ limit, and

(iii) When reducing from E_7 to E_6, likewise the corresponding character to be unity while keeping the scaling.

The E_n manifest curve is of the standard Weierstrass form [15, 17, 28]

$$y^2 = 4x^3 - g_2^{E_n} x - g_3^{E_n}, \tag{B.2}$$

where g_2 and g_3 are given according to E_n as follows.

For E_8:

$$g_2^{E_8} = \frac{1}{12}u^4 - \left(\frac{2}{3}\chi_1^{E_8} - \frac{50}{3}\chi_8^{E_8} + 1550\right)u^2 - \left(-70\chi_1^{E_8} + 2\chi_2^{E_8} - 12\chi_7^{E_8} + 1840\chi_8^{E_8} - 115010\right)u$$
$$+ \frac{4}{3}\chi_1^{E_8}\chi_1^{E_8} - \frac{8}{3}\chi_1^{E_8}\chi_8^{E_8} - 1824\chi_1^{E_8} + 112\chi_2^{E_8} - 4\chi_3^{E_8} + 4\chi_6^{E_8}$$
$$- 680\chi_7^{E_8} + \frac{28}{3}\chi_8^{E_8}\chi_8^{E_8} + 50744\chi_8^{E_8} - 2399276,$$

$$g_3^{E_8} = \frac{1}{216}u^6 - 4u^5 - \left(\frac{1}{18}\chi_1^{E_8} + \frac{47}{18}\chi_8^{E_8} - \frac{5177}{6}\right)u^4$$
$$- \left(-\frac{107}{6}\chi_1^{E_8} + \frac{1}{6}\chi_2^{E_8} + 3\chi_7^{E_8} - \frac{1580}{3}\chi_8^{E_8} + \frac{504215}{6}\right)u^3$$
$$- \left(-\frac{2}{9}\chi_1^{E_8}\chi_1^{E_8} - \frac{20}{9}\chi_1^{E_8}\chi_8^{E_8} + \frac{5866}{3}\chi_1^{E_8} - \frac{112}{3}\chi_2^{E_8} + \frac{1}{3}\chi_3^{E_8}\right.$$
$$\left.+ \frac{11}{3}\chi_6^{E_8} - \frac{1450}{3}\chi_7^{E_8} + \frac{196}{9}\chi_8^{E_8}\chi_8^{E_8} + 39296\chi_8^{E_8} - \frac{12673792}{3}\right)u^2$$
$$- \left(\frac{94}{3}\chi_1^{E_8}\chi_1^{E_8} - \frac{2}{3}\chi_1^{E_8}\chi_2^{E_8} + \frac{718}{3}\chi_1^{E_8}\chi_8^{E_8} - \frac{270736}{3}\chi_1^{E_8} - \frac{10}{3}\chi_2^{E_8}\chi_8^{E_8} + 2630\chi_2^{E_8} - 52\chi_3^{E_8} + 4\chi_5^{E_8}\right.$$
$$\left.- 416\chi_6^{E_8} + 16\chi_7^{E_8}\chi_8^{E_8} + 25880\chi_7^{E_8} - \frac{7328}{3}\chi_8^{E_8}\chi_8^{E_8} - \frac{3841382}{3}\chi_8^{E_8} + 107263286\right)u$$
$$- \frac{8}{27}\chi_1^{E_8}\chi_1^{E_8}\chi_1^{E_8} - \frac{28}{9}\chi_1^{E_8}\chi_1^{E_8}\chi_8^{E_8} + 1065\chi_1^{E_8}\chi_1^{E_8} - \frac{118}{3}\chi_1^{E_8}\chi_2^{E_8} + \frac{4}{3}\chi_1^{E_8}\chi_3^{E_8} - \frac{4}{3}\chi_1^{E_8}\chi_6^{E_8}$$
$$+ \frac{8}{3}\chi_1^{E_8}\chi_7^{E_8} + \frac{40}{9}\chi_1^{E_8}\chi_8^{E_8}\chi_8^{E_8} + \frac{19264}{3}\chi_1^{E_8}\chi_8^{E_8} - \frac{4521802}{3}\chi_1^{E_8} + \chi_2^{E_8}\chi_2^{E_8} - \frac{572}{3}\chi_2^{E_8}\chi_8^{E_8}$$
$$+ 59482\chi_2^{E_8} + \frac{20}{3}\chi_3^{E_8}\chi_8^{E_8} - 1880\chi_3^{E_8} - 4\chi_4^{E_8} + 232\chi_5^{E_8} - \frac{8}{3}\chi_6^{E_8}\chi_8^{E_8} - 11808\chi_6^{E_8} + \frac{2740}{3}\chi_7^{E_8}\chi_8^{E_8}$$
$$+ 460388\chi_7^{E_8} - \frac{136}{27}\chi_8^{E_8}\chi_8^{E_8}\chi_8^{E_8} - \frac{205492}{3}\chi_8^{E_8}\chi_8^{E_8} - \frac{45856940}{3}\chi_8^{E_8} + 1091057493.$$

$$(B.3)$$

For E_7:

$$g_2^{E_7} = \frac{1}{12}u^4 - \left(\frac{2}{3}\chi_1^{E_7} - \frac{50}{3}\right)u^2 - \left(2\chi_2^{E_7} - 12\chi_7^{E_7}\right)u + \frac{4}{3}\chi_1^{E_7}\chi_1^{E_7} - \frac{8}{3}\chi_1^{E_7} - 4\chi_3^{E_7} + 4\chi_6^{E_7} + \frac{28}{3},$$
$$g_3^{E_7} = \frac{1}{216}u^6 - \left(\frac{1}{18}\chi_1^{E_7} + \frac{47}{18}\right)u^4 - \left(\frac{1}{6}\chi_2^{E_7} + 3\chi_7^{E_7}\right)u^3 + \left(\frac{2}{9}\chi_1^{E_7}\chi_1^{E_7} + \frac{20}{9}\chi_1^{E_7} - \frac{1}{3}\chi_3^{E_7} - \frac{11}{3}\chi_6^{E_7} - \frac{196}{9}\right)u^2$$
$$+ \left(\frac{2}{3}\chi_1^{E_7}\chi_2^{E_7} + \frac{10}{3}\chi_2^{E_7} - 4\chi_5^{E_7} - 16\chi_7^{E_7}\right)u - \frac{8}{27}\chi_1^{E_7}\chi_1^{E_7}\chi_1^{E_7} - \frac{28}{9}\chi_1^{E_7}\chi_1^{E_7} + \frac{4}{3}\chi_1^{E_7}\chi_3^{E_7}$$
$$- \frac{4}{3}\chi_1^{E_7}\chi_6^{E_7} + \frac{40}{9}\chi_1^{E_7} + \chi_2^{E_7}\chi_2^{E_7} + \frac{20}{3}\chi_3^{E_7} - 4\chi_4^{E_7} - \frac{8}{3}\chi_6^{E_7} - \frac{136}{27}.$$

$$(B.4)$$

For E_6:

$$g_2^{E_6} = \frac{1}{12}u^4 - \frac{2}{3}\chi_1^{E_6}u^2 - \left(2\chi_2^{E_6} - 12\right)u + \frac{4}{3}\chi_1^{E_6}\chi_1^{E_6} - 4\chi_3^{E_6} + 4\chi_6^{E_6},$$
$$g_3^{E_6} = \frac{1}{216}u^6 - \frac{1}{18}\chi_1^{E_6}u^4 - \left(\frac{1}{6}\chi_2^{E_6} + 3\right)u^3 + \left(\frac{2}{9}\chi_1^{E_6}\chi_1^{E_6} - \frac{1}{3}\chi_3^{E_6} - \frac{11}{3}\chi_6^{E_6}\right)u^2 + \left(\frac{2}{3}\chi_1^{E_6}\chi_2^{E_6} - 4\chi_5^{E_6}\right)u$$
$$- \frac{8}{27}\chi_1^{E_6}\chi_1^{E_6}\chi_1^{E_6} + \frac{4}{3}\chi_1^{E_6}\chi_3^{E_6} - \frac{4}{3}\chi_1^{E_6}\chi_6^{E_6} + \chi_2^{E_6}\chi_2^{E_6} - 4\chi_4^{E_6}.$$

$$(B.5)$$

For $E_5 = SO(10)$:

$$g_2^{E_5} = \frac{1}{12}u^4 - \frac{2}{3}\chi_1^{E_5}u^2 - 2\chi_2^{E_5}u + \frac{4}{3}\chi_1^{E_5}\chi_1^{E_5} - 4\chi_3^{E_5} + 4,$$

$$g_3^{E_5} = \frac{1}{216}u^6 - \frac{1}{18}\chi_1^{E_5}u^4 - \frac{1}{6}\chi_2^{E_5}u^3 + \left(\frac{2}{9}\chi_1^{E_5}\chi_1^{E_5} - \frac{1}{3}\chi_3^{E_5} - \frac{11}{3}\right)u^2 + \left(\frac{2}{3}\chi_1^{E_5}\chi_2^{E_5} - 4\chi_5^{E_5}\right)u$$
$$- \frac{8}{27}\chi_1^{E_5}\chi_1^{E_5}\chi_1^{E_5} + \frac{4}{3}\chi_1^{E_5}\chi_3^{E_5} - \frac{4}{3}\chi_1^{E_5} + \chi_2^{E_5}\chi_2^{E_5} - 4\chi_4^{E_5}. \tag{B.6}$$

For $E_4 = SU(5)$:

$$g_2^{E_4} = \frac{1}{12}u^4 - \frac{2}{3}\chi_1^{E_4}u^2 - 2\chi_2^{E_4}u + \frac{4}{3}\chi_1^{E_4}\chi_1^{E_4} - 4\chi_3^{E_4},$$

$$g_3^{E_4} = \frac{1}{216}u^6 - \frac{1}{18}\chi_1^{E_4}u^4 - \frac{1}{6}\chi_2^{E_4}u^3 + \left(\frac{2}{9}\chi_1^{E_4}\chi_1^{E_4} - \frac{1}{3}\chi_3^{E_4}\right)u^2 + \left(\frac{2}{3}\chi_1^{E_4}\chi_2^{E_4} - 4\right)u$$
$$- \frac{8}{27}\chi_1^{E_4}\chi_1^{E_4}\chi_1^{E_4} + \frac{4}{3}\chi_1^{E_4}\chi_3^{E_4} + \chi_2^{E_4}\chi_2^{E_4} - 4\chi_4^{E_4}. \tag{B.7}$$

For $E_3 = SU(3) \times SU(2)$:

$$g_2^{E_3} = \frac{1}{12}u^4 - \frac{2}{3}\chi_1^{E_3}u^2 - 2\chi_2^{E_3}u + \frac{4}{3}\chi_1^{E_3}\chi_1^{E_3} - 4\chi_3^{E_3},$$

$$g_3^{E_3} = \frac{1}{216}u^6 - \frac{1}{18}\chi_1^{E_3}u^4 - \frac{1}{6}\chi_2^{E_3}u^3 + \left(\frac{2}{9}\chi_1^{E_3}\chi_1^{E_3} - \frac{1}{3}\chi_3^{E_3}\right)u^2 + \frac{2}{3}\chi_1^{E_3}\chi_2^{E_3}u$$
$$- \frac{8}{27}\chi_1^{E_3}\chi_1^{E_3}\chi_1^{E_3} + \frac{4}{3}\chi_1^{E_3}\chi_3^{E_3} + \chi_2^{E_3}\chi_2^{E_3} - 4. \tag{B.8}$$

For $E_2 = SU(2) \times U(1)$:

$$g_2^{E_2} = \frac{1}{12}u^4 - \frac{2}{3}\chi_1^{E_2}u^2 - 2\chi_2^{E_2}u + \frac{4}{3}\chi_1^{E_2}\chi_1^{E_2} - 4, \tag{B.9}$$

$$g_3^{E_2} = \frac{1}{216}u^6 - \frac{1}{18}\chi_1^{E_2}u^4 - \frac{1}{6}\chi_2^{E_2}u^3 + \left(\frac{2}{9}\chi_1^{E_2}\chi_1^{E_2} - \frac{1}{3}\right)u^2 + \frac{2}{3}\chi_1^{E_2}\chi_2^{E_2}u - \frac{8}{27}\chi_1^{E_2}\chi_1^{E_2}\chi_1^{E_2} + \frac{4}{3}\chi_1^{E_2} + \chi_2^{E_2}\chi_2^{E_2}.$$

For $\widetilde{E}_1 = U(1)$:

$$g_2^{\widetilde{E}_1} = \frac{1}{12}u^4 - \frac{2}{3}u^2 - 2\chi_2^{\widetilde{E}_1}u + \frac{4}{3},$$

$$g_3^{\widetilde{E}_1} = \frac{1}{216}u^6 - \frac{1}{18}u^4 - \frac{1}{6}\chi_2^{\widetilde{E}_1}u^3 + \frac{2}{9}u^2 + \frac{2}{3}\chi_2^{\widetilde{E}_1}u - \frac{8}{27} + \chi_2^{\widetilde{E}_1}\chi_2^{\widetilde{E}_1}. \tag{B.10}$$

For $E_1 = SU(2)$:

$$g_2^{E_1} = \frac{1}{12}u^4 - \frac{2}{3}\chi_1^{E_1}u^2 + \frac{4}{3}\chi_1^{E_1}\chi_1^{E_1} - 4, \tag{B.11}$$

$$g_3^{E_1} = \frac{1}{216}u^6 - \frac{1}{18}\chi_1^{E_1}u^4 + \left(\frac{2}{9}\chi_1^{E_1}\chi_1^{E_1} - \frac{1}{3}\right)u^2 - \frac{8}{27}\chi_1^{E_1}\chi_1^{E_1}\chi_1^{E_1} + \frac{4}{3}\chi_1^{E_1}.$$

Here we note that the E_1 curve is obtained only by setting $\chi_2 \to 0$ from the E_2 curve, which does not involve the scaling.

For E_0: (from $\widetilde{E}_1$)

$$g_2^{E_0} = \frac{1}{12}u^4 - 2u, \qquad g_3^{E_0} = \frac{1}{216}u^6 - \frac{1}{6}u^3 + 1. \tag{B.12}$$

In summary, one stars from E_8 curve and obtains lower E_n curves:

$$E_8 \to E_7 \to E_6 \to E_5 \to E_4 \to E_3 \to E_2 \to \widetilde{E}_1 \to E_0$$
$$\to E_1. \tag{B.13}$$

All the holomorphic SW one form is of the standard form:

$$\omega_{SW} = \frac{dx}{y}. \tag{B.14}$$

C   The j-invariant

The Weierstrass form for elliptic curve is given

$$y^2 = 4z^3 - g_2 z - g_3, \tag{C.1}$$

then the j-invariant which is $SL(2, \mathbb{Z})$ invariant is define by

$$j(\tau) = \frac{g_2^3}{g_2^3 - 27g_3^2}, \tag{C.2}$$

where the denominator is proportional to the discriminant of the Weierstrass form. For (C.1), $\Delta = 16(g_2^3 - 27g_3^2)$, and thus the denominator of the j-invariant is $\frac{\Delta}{16}$.

For an elliptic curve given by

$$y^2 = Ax^3 + Bx^2 + Cx + D, \tag{C.3}$$

let us find how the j-invariant is given. It is straightforward to rewrite (C.3) into the standard Weierstrass form

$$\tilde{y}^2 = 4\tilde{x}^3 - \frac{4}{3A^2}\left(B^2 - 3AC\right)\tilde{x} - \frac{4}{27A^3}\left(9ABC - 2B^3 - 27A^2D\right), \tag{C.4}$$

where $\tilde{y} = \frac{y}{\sqrt{A}/2}$, $\tilde{x} = x + \frac{B}{3A}$, yielding

$$g_2 = \frac{4}{3A^2}\left(B^2 - 3AC\right), \quad g_3 = \frac{4}{27A^3}\left(9ABC - 2B^3 - 27A^2D\right). \tag{C.5}$$

As the discriminant Δ for a cubic equation $Ax^3 + Bx^2 + Cx + D = 0$ is given by

$$\Delta = B^2C^2 - 4AC^3 - 4B^3D - 27A^2D^2 + 18ABCD, \tag{C.6}$$

one finds that

$$g_2^3 - 27g_3^2 = \frac{16}{A^4}\Delta. \tag{C.7}$$

An elliptic curve may also be expressed as a quartic polynomial

$$y^2 = ax^4 + bx^3 + cx^2 + dx + e. \tag{C.8}$$

The forms of g_2 and g_3 for the curve are given by

$$g_2 = \frac{4}{a^3}(c^2 - 3bd + 12ae), \qquad g_2^3 - 27g_3^2 = \frac{16}{a^6}\Delta, \tag{C.9}$$

where the discriminant for the quartic equation is given by

$$\Delta = 256a^3e^3 - 192a^2bde^2 - 128a^2c^2e^2 + 144a^2cd^2e - 27a^2d^4 + 144ab^2ce^2 - 6ab^2d^2e - 80abc^2de$$
$$+ 18abcd^3 + 16ac^4e - 4ac^3d^2 - 27b^4e^2 + 18b^3cde - 4b^3d^3 - 4b^2c^3e + b^2c^2d^2.$$

D The Weierstrass from for $SU(8)$ manifest curve of E_7 theory

Following [28], we rewrite (3.26) into the standard Weierstrass form

$$y^2 = 4x^3 - g_2 x - g_3, \tag{D.1}$$

where

$$
\begin{aligned}
g_2 = -\frac{4}{3}\Big(& -64 - 48\chi_1\chi_3 + 64\chi_4 - 16\chi_4^2 + 48\chi_3\chi_5 + 48\chi_1^2\chi_6 - 192\chi_2\chi_6 + 16\chi_1\chi_7 \\
& + 16\chi_1\chi_4\chi_7 - 48\chi_5\chi_7 - 16\chi_1^2\chi_7^2 + 48\chi_2\chi_7^2 + 24\chi_1^2 u - 192\chi_2 u + 24\chi_1\chi_5 u \\
& - 192\chi_6 u + 24\chi_3\chi_7 u + 24\chi_7^2 u - 208 u^2 + 8\chi_4 u^2 + 8\chi_1\chi_7 u^2 - u^4 \Big),
\end{aligned} \tag{D.2}
$$

and

$$
\begin{aligned}
g_3 =\frac{8}{27}\Big(& -512 - 216\chi_1^4 + 864\chi_1^2\chi_2 - 576\chi_1\chi_3 + 768\chi_4 + 288\chi_1\chi_3\chi_4 - 384\chi_4^2 \\
& + 64\chi_4^3 + 432\chi_1^3\chi_5 - 1728\chi_1\chi_2\chi_5 + 576\chi_3\chi_5 - 288\chi_3\chi_4\chi_5 - 216\chi_1^2\chi_5^2 + 864\chi_2\chi_5^2 \\
& - 1152\chi_1^2\chi_6 + 4608\chi_2\chi_6 + 864\chi_3^2\chi_6 + 576\chi_1^2\chi_4\chi_6 - 2304\chi_2\chi_4\chi_6 + 192\chi_1\chi_7 \\
& - 144\chi_1^2\chi_3\chi_7 + 96\chi_1\chi_4\chi_7 - 96\chi_1\chi_4^2\chi_7 - 576\chi_5\chi_7 + 144\chi_1\chi_3\chi_5\chi_7 + 288\chi_4\chi_5\chi_7 \\
& - 288\chi_1^3\chi_6\chi_7 + 1152\chi_1\chi_2\chi_6\chi_7 - 1728\chi_3\chi_6\chi_7 + 336\chi_1^2\chi_7^2 - 1152\chi_2\chi_7^2 - 216\chi_3^2\chi_7^2 \\
& - 96\chi_1^2\chi_4\chi_7^2 + 576\chi_2\chi_4\chi_7^2 - 144\chi_1\chi_5\chi_7^2 + 864\chi_6\chi_7^2 + 64\chi_1^3\chi_7^3 - 288\chi_1\chi_2\chi_7^3 \\
& + 432\chi_3\chi_7^3 - 216\chi_7^4 - 576\chi_1^2 u + 4608\chi_2 u + 864\chi_3^2 u + 720\chi_1^2\chi_4 u - 2304\chi_2\chi_4 u \\
& - 1440\chi_1\chi_5 u - 144\chi_1\chi_4\chi_5 u + 864\chi_5^2 u + 4608\chi_6 u + 864\chi_1\chi_3\chi_6 u - 2304\chi_4\chi_6 u \\
& - 144\chi_1^3\chi_7 u + 288\chi_1\chi_2\chi_7 u - 1440\chi_3\chi_7 u - 144\chi_3\chi_4\chi_7 u - 144\chi_1^2\chi_5\chi_7 u \\
& + 864\chi_2\chi_5\chi_7 u + 288\chi_1\chi_6\chi_7 u - 576\chi_7^2 u - 144\chi_1\chi_3\chi_7^2 u + 720\chi_4\chi_7^2 u - 144\chi_1\chi_7^3 u \\
& + 4416 u^2 + 792\chi_1\chi_3 u^2 - 2112\chi_4 u^2 - 48\chi_4^2 u^2 + 72\chi_3\chi_5 u^2 + 72\chi_1^2\chi_6 u^2 + 576\chi_2\chi_6 u^2 \\
& - 456\chi_1\chi_7 u^2 - 24\chi_1\chi_4\chi_7 u^2 + 792\chi_5\chi_7 u^2 - 48\chi_1^2\chi_7^2 u^2 + 72\chi_2\chi_7^2 u^2 + 36\chi_1^2 u^3 \\
& + 576\chi_2 u^3 + 36\chi_1\chi_5 u^3 + 576\chi_6 u^3 + 36\chi_3\chi_7 u^3 + 36\chi_7^2 u^3 + 552 u^4 + 12\chi_4 u^4 + 12\chi_1\chi_7 u^4 - u^6 \Big).
\end{aligned} \tag{D.3}
$$

D.1 Decomposition of the E_7 characters into $SU(8)$

We list decomposition of the characters $\chi_i^{E_7} \equiv \chi_{\mu_i}^{E_7}$ of E_7 fundamental weights into the characters χ_i of $SU(8)$ fundamental weights

$$E_7 \text{ Dynkin diagram}$$

$$\chi_1^{E_7} = -1 + \chi_1\chi_7 + \chi_4$$

$$\chi_2^{E_7} = \chi_1^2 + \chi_7^2 + \chi_3\chi_7 + \chi_1\chi_5 - 2\chi_2 - 2\chi_6$$

$$\chi_3^{E_7} = 1 - 2\chi_4 + \chi_3\chi_5 + \chi_1^2\chi_6 - 3\chi_2\chi_6 - \chi_1\chi_7 + \chi_1\chi_4\chi_7 + \chi_2\chi_7^2$$

$$\chi_4^{E_7} = -2 + \chi_2^2 - \chi_1\chi_3 + 2\chi_4 - \chi_4^2 + \chi_1^3\chi_5 - 3\chi_1\chi_2\chi_5 + 2\chi_3\chi_5 + \chi_2\chi_5^2 - \chi_1^2\chi_6$$
$$+ 3\chi_2\chi_6 + \chi_3^2\chi_6 + \chi_1^2\chi_4\chi_6 - 4\chi_2\chi_4\chi_6 - \chi_1\chi_5\chi_6 + \chi_6^2 + 2\chi_1\chi_7 - \chi_2\chi_3\chi_7$$
$$- \chi_5\chi_7 + \chi_1\chi_3\chi_5\chi_7 - 3\chi_3\chi_6\chi_7 - \chi_2\chi_7^2 + \chi_2\chi_4\chi_7^2 + \chi_3\chi_7^3$$

$$\chi_5^{E_7} = \chi_3^2 + \chi_1^2\chi_4 - 3\chi_2\chi_4 - \chi_1\chi_5 + \chi_5^2 + \chi_1\chi_3\chi_6 - 3\chi_4\chi_6 - \chi_3\chi_7 + \chi_2\chi_5\chi_7 + \chi_4\chi_7^2$$

$$\chi_6^{E_7} = -1 + \chi_1\chi_3 - 2\chi_4 + \chi_2\chi_6 + \chi_5\chi_7$$

$$\chi_7^{E_7} = \chi_2 + \chi_6. \tag{D.4}$$

E   The Weierstrass from for $SU(9)$ manifest curve of E_8 theory

Following [28], we rewrite (4.15) with $U \to u - 60$ into the standard Weierstrass form

$$y^2 = 4x^3 - g_2 x - g_3, \tag{E.1}$$

where

$$
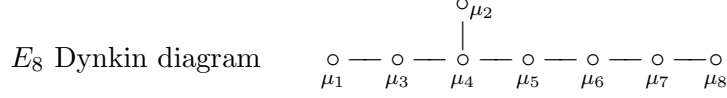\begin{aligned}
g_2 =\ & \frac{1}{972}\Big(16(\chi_1^2 - 3\chi_2 + 3\chi_8)^2(3\chi_1 - 3\chi_7 + \chi_8^2)^2 \\
& + 16(3\chi_1 - 3\chi_7 + \chi_8^2)\big[2\chi_1^2\chi_8 + 3(3\chi_4 - 3\chi_7 - \chi_2\chi_8 + \chi_8^2) + 3\chi_1(-57 + u)\big]^2 \\
& - 8(\chi_1^2 - 3\chi_2 + 3\chi_8)(3\chi_1 - 3\chi_7 + \chi_8^2)\big(2\chi_1\chi_8 + 3(-54 + u)\big)^2 + (-162 + 2\chi_1\chi_8 + 3u)^4 \\
& - 16(\chi_1^2 - 3\chi_2 + 3\chi_8)\big[2\chi_1^2\chi_8 + 3(3\chi_4 - 3\chi_7 - \chi_2\chi_8 + \chi_8^2) + 3\chi_1(-57 + u)\big] \\
& \times (-1539 + 27\chi_6 + 9\chi_1\chi_8 - 9\chi_7\chi_8 + 2\chi_8^3 + 27u) \\
& - 8\big[2\chi_1^2\chi_8 + 3(3\chi_4 - 3\chi_7 - \chi_2\chi_8 + \chi_8^2) + 3\chi_1(-57 + u))(2\chi_1\chi_8 + 3(-54 + u)\big] \\
& \times (3\chi_1^2 - 9\chi_2 + 9\chi_5 - 3\chi_1\chi_7 - 171\chi_8 + 2\chi_1\chi_8^2 + 3\chi_8 u) \\
& + 16(\chi_1^2 - 3\chi_2 + 3\chi_8)(3\chi_1^2 - 9\chi_2 + 9\chi_5 - 3\chi_1\chi_7 - 171\chi_8 + 2\chi_1\chi_8^2 + 3\chi_8 u)^2 \\
& + 8\big(2\chi_1\chi_8 + 3(-54 + u)\big)\big[-1539 + 27\chi_6 + 9\chi_1\chi_8 - 9\chi_7\chi_8 + 2\chi_8^3 + 27u) \\
& \times (2\chi_1^3 - 9\chi_1(\chi_2 - \chi_8) + 27(-57 + \chi_3 + u)\big] - 16(3\chi_1 - 3\chi_7 + \chi_8^2)(3\chi_1^2 - 9\chi_2 + 9\chi_5 \\
& - 3\chi_1\chi_7 - 171\chi_8 + 2\chi_1\chi_8^2 + 3\chi_8 u)\big[2\chi_1^3 - 9\chi_1(\chi_2 - \chi_8) + 27(-57 + \chi_3 + u)\big]\Big), \tag{E.2}
\end{aligned}
$$

and

$$g_3 = \frac{1}{157464}\Big(-64(\chi_1^2 - 3\chi_2 + 3\chi_8)^3(3\chi_1 - 3\chi_7 + \chi_8^2)^3 + 192(\chi_1^2 - 3\chi_2 + 3\chi_8) \quad\text{(E.3)}$$

$$\times (3\chi_1 - 3\chi_7 + \chi_8^2)^2\Big[2\chi_1^2\chi_8 + 3(3\chi_4 - 3\chi_7 - \chi_2\chi_8 + \chi_8^2) + 3\chi_1(-57 + u)\Big]^2$$

$$+ 48(\chi_1^2 - 3\chi_2 + 3\chi_8)^2(3\chi_1 - 3\chi_7 + \chi_8^2)^2(2\chi_1\chi_8 + 3(-54 + u))^2$$

$$+ 24(3\chi_1 - 3\chi_7 + \chi_8^2)\Big[2\chi_1^2\chi_8 + 3(3\chi_4 - 3\chi_7 - \chi_2\chi_8 + \chi_8^2) + 3\chi_1(-57 + u)\Big]^2$$

$$\times (2\chi_1\chi_8 + 3(-54 + u))^2 - 12(\chi_1^2 - 3\chi_2 + 3\chi_8)(3\chi_1 - 3\chi_7 + \chi_8^2)(-162 + 2\chi_1\chi_8 + 3u)^4$$

$$+ (-162 + 2\chi_1\chi_8 + 3u)^6 - 96(\chi_1^2 - 3\chi_2 + 3\chi_8)^2$$

$$\times (3\chi_1 - 3\chi_7 + \chi_8^2)\Big[2\chi_1^2\chi_8 + 3(3\chi_4 - 3\chi_7 - \chi_2\chi_8 + \chi_8^2) + 3\chi_1(-57 + u)\Big]$$

$$\times (-1539 + 27\chi_6 + 9\chi_1\chi_8 - 9\chi_7\chi_8 + 2\chi_8^3 + 27u)$$

$$- 32\Big[2\chi_1^2\chi_8 + 3(3\chi_4 - 3\chi_7 - \chi_2\chi_8 + \chi_8^2) + 3\chi_1(-57 + u)\Big]^3$$

$$\times (-1539 + 27\chi_6 + 9\chi_1\chi_8 - 9\chi_7\chi_8 + 2\chi_8^3 + 27u) + 72(\chi_1^2 - 3\chi_2 + 3\chi_8)$$

$$\times \Big[2\chi_1^2\chi_8 + 3(3\chi_4 - 3\chi_7 - \chi_2\chi_8 + \chi_8^2) + 3\chi_1(-57 + u)\Big](2\chi_1\chi_8 + 3(-54 + u))^2$$

$$\times (-1539 + 27\chi_6 + 9\chi_1\chi_8 - 9\chi_7\chi_8 + 2\chi_8^3 + 27u) + 32(\chi_1^2 - 3\chi_2 + 3\chi_8)^3$$

$$\times (-1539 + 27\chi_6 + 9\chi_1\chi_8 - 9\chi_7\chi_8 + 2\chi_8^3 + 27u)^2 - 240(\chi_1^2 - 3\chi_2 + 3\chi_8)(3\chi_1 - 3\chi_7 + \chi_8^2)\times$$

$$\times \Big[2\chi_1^2\chi_8 + 3(3\chi_4 - 3\chi_7 - \chi_2\chi_8 + \chi_8^2) + 3\chi_1(-57 + u)\Big]$$

$$\times (2\chi_1\chi_8 + 3(-54 + u))(3\chi_1^2 - 9\chi_2 + 9\chi_5 - 3\chi_1\chi_7 - 171\chi_8 + 2\chi_1\chi_8^2 + 3\chi_8 u)$$

$$- 12\Big[2\chi_1^2\chi_8 + 3(3\chi_4 - 3\chi_7 - \chi_2\chi_8 + \chi_8^2) + 3\chi_1(-57 + u)\Big](2\chi_1\chi_8 + 3(-54 + u))^3$$

$$\times (3\chi_1^2 - 9\chi_2 + 9\chi_5 - 3\chi_1\chi_7 - 171\chi_8 + 2\chi_1\chi_8^2 + 3\chi_8 u) - 96(\chi_1^2 - 3\chi_2 + 3\chi_8)^2$$

$$\times (2\chi_1\chi_8 + 3(-54 + u))(-1539 + 27\chi_6 + 9\chi_1\chi_8 - 9\chi_7\chi_8 + 2\chi_8^3 + 27u)$$

$$\times (3\chi_1^2 - 9\chi_2 + 9\chi_5 - 3\chi_1\chi_7 - 171\chi_8 + 2\chi_1\chi_8^2 + 3\chi_8 u) + 192(\chi_1^2 - 3\chi_2 + 3\chi_8)^2(3\chi_1 - 3\chi_7 + \chi_8^2)$$

$$\times (3\chi_1^2 - 9\chi_2 + 9\chi_5 - 3\chi_1\chi_7 - 171\chi_8 + 2\chi_1\chi_8^2 + 3\chi_8 u)^2 + 24(2\chi_1^2\chi_8 + 3(3\chi_4 - 3\chi_7 - \chi_2\chi_8 + \chi_8^2)$$

$$+ 3\chi_1(-57 + u))^2(3\chi_1^2 - 9\chi_2 + 9\chi_5 - 3\chi_1\chi_7 - 171\chi_8 + 2\chi_1\chi_8^2 + 3\chi_8 u)^2 + 24(\chi_1^2 - 3\chi_2 + 3\chi_8)$$

$$\times (2\chi_1\chi_8 + 3(-54 + u))^2(3\chi_1^2 - 9\chi_2 + 9\chi_5 - 3\chi_1\chi_7 - 171\chi_8 + 2\chi_1\chi_8^2 + 3\chi_8 u)^2$$

$$- 96(3\chi_1 - 3\chi_7 + \chi_8^2)^2\Big[2\chi_1^2\chi_8 + 3(3\chi_4 - 3\chi_7 - \chi_2\chi_8 + \chi_8^2) + 3\chi_1(-57 + u)\Big](2\chi_1\chi_8 + 3(-54 + u))$$

$$\times (2\chi_1^3 - 9\chi_1(\chi_2 - \chi_8) + 27(-57 + \chi_3 + u)) + 48(\chi_1^2 - 3\chi_2 + 3\chi_8)(3\chi_1 - 3\chi_7 + \chi_8^2)$$

$$\times (2\chi_1\chi_8 + 3(-54 + u))(-1539 + 27\chi_6 + 9\chi_1\chi_8 - 9\chi_7\chi_8 + 2\chi_8^3 + 27u)$$

$$\times \Big[2\chi_1^3 - 9\chi_1(\chi_2 - \chi_8) + 27(-57 + \chi_3 + u)\Big] - 20(2\chi_1\chi_8 + 3(-54 + u))^3$$

$$\times (-1539 + 27\chi_6 + 9\chi_1\chi_8 - 9\chi_7\chi_8 + 2\chi_8^3 + 27u)\Big[2\chi_1^3 - 9\chi_1(\chi_2 - \chi_8) + 27(-57 + \chi_3 + u)\Big]$$

$$- 96(\chi_1^2 - 3\chi_2 + 3\chi_8)(3\chi_1 - 3\chi_7 + \chi_8^2)^2(3\chi_1^2 - 9\chi_2 + 9\chi_5 - 3\chi_1\chi_7 - 171\chi_8 + 2\chi_1\chi_8^2 + 3\chi_8 u)$$

$$\times (2\chi_1^3 - 9\chi_1(\chi_2 - \chi_8) + 27(-57 + \chi_3 + u)) + 72(3\chi_1 - 3\chi_7 + \chi_8^2)(2\chi_1\chi_8 + 3(-54 + u))^2$$

$$\times (3\chi_1^2 - 9\chi_2 + 9\chi_5 - 3\chi_1\chi_7 - 171\chi_8 + 2\chi_1\chi_8^2 + 3\chi_8 u)(2\chi_1^3 - 9\chi_1(\chi_2 - \chi_8) + 27(-57 + \chi_3 + u))$$

$$+ 48\Big[2\chi_1^2\chi_8 + 3(3\chi_4 - 3\chi_7 - \chi_2\chi_8 + \chi_8^2) + 3\chi_1(-57 + u)\Big](-1539 + 27\chi_6 + 9\chi_1\chi_8 - 9\chi_7\chi_8 + 2\chi_8^3 + 27u)$$

$$\times (3\chi_1^2 - 9\chi_2 + 9\chi_5 - 3\chi_1\chi_7 - 171\chi_8 + 2\chi_1\chi_8^2 + 3\chi_8 u)\Big[2\chi_1^3 - 9\chi_1(\chi_2 - \chi_8) + 27(-57 + \chi_3 + u)\Big]$$

$$- 32(3\chi_1^2 - 9\chi_2 + 9\chi_5 - 3\chi_1\chi_7 - 171\chi_8 + 2\chi_1\chi_8^2 + 3\chi_8 u)^3\Big[2\chi_1^3 - 9\chi_1(\chi_2 - \chi_8) + 27(-57 + \chi_3 + u)\Big]$$

$$+ 32(3\chi_1 - 3\chi_7 + \chi_8^2)^3(2\chi_1^3 - 9\chi_1(\chi_2 - \chi_8) + 27(-57 + \chi_3 + u))^2$$

$$- 8(-1539 + 27\chi_6 + 9\chi_1\chi_8 - 9\chi_7\chi_8 + 2\chi_8^3 + 27u)^2\Big[2\chi_1^3 - 9\chi_1(\chi_2 - \chi_8) + 27(-57 + \chi_3 + u)\Big]^2\Big).$$

E.1 Decomposition of the E_8 characters into $SU(9)$

We list decomposition of the characters $\chi_i^{E_8} \equiv \chi_{\mu_i}^{E_8}$ of E_8 fundamental weights into the characters χ_i of $SU(9)$ fundamental weights. As mentioned in section 4.3, χ_4 and χ_5 are determined such that (E.4) agrees with (B.3).

$$E_8 \text{ Dynkin diagram}$$

$$
\begin{array}{c}
\overset{\displaystyle\circ\,\mu_2}{\underset{\displaystyle|}{}} \\
\circ\!-\!\circ\!-\!\circ\!-\!\circ\!-\!\circ\!-\!\circ\!-\!\circ \\
\mu_1 \quad \mu_3 \quad \mu_4 \quad \mu_5 \quad \mu_6 \quad \mu_7 \quad \mu_8
\end{array}
$$

$$
\chi_1^{E_8} = -1 + \chi_1\chi_2 - 2\chi_3 + \chi_1\chi_5 - 2\chi_6 + \chi_2\chi_7 + \chi_4\chi_8 + \chi_7\chi_8 \tag{E.4}
$$

$$
\begin{aligned}
\chi_2^{E_8} = {}& \chi_1{}^3 + \chi_1{}^2\chi_4 - 4(\chi_1\chi_2 - \chi_3) + \chi_1\chi_2\chi_6 - 2(\chi_2\chi_7 - \chi_1\chi_8) + \chi_1\chi_2 \\
& - \chi_1\chi_3\chi_8 + \chi_1\chi_4\chi_7 - 4(\chi_1\chi_5 - \chi_6) + 3\chi_1\chi_5 - \chi_1\chi_6\chi_8 + \chi_1(\chi_7)^2 \\
& + \chi_1\chi_8 - 4(\chi_1\chi_8 - 1) + \chi_2{}^2\chi_8 - 2\chi_2\chi_4 + \chi_2\chi_5\chi_8 + 2\chi_2\chi_7 \\
& - 4(\chi_4\chi_8 - \chi_3) - 3\chi_3\chi_6 + \chi_3\chi_7\chi_8 - 5\chi_3 + \chi_4\chi_5 + \chi_4\chi_8 + \chi_5(\chi_8)^2 \\
& - 4(\chi_7\chi_8 - \chi_6) - 5\chi_6 + \chi_7\chi_8 + \chi_8{}^3 - 3 + \chi_2\chi_4 - \chi_1\chi_5 - \chi_5\chi_7 + \chi_4\chi_8
\end{aligned} \tag{E.5}
$$

$$
\begin{aligned}
\chi_3^{E_8} = {}& \chi_2{}^3 + \chi_1{}^3\chi_3 - 5\chi_1\chi_2\chi_3 + 5\chi_3{}^2 - \chi_2\chi_4 + \chi_1\chi_5 + \chi_1{}^2\chi_2\chi_5 - \chi_2{}^2\chi_5 \\
& - \chi_1\chi_3\chi_5 - \chi_4\chi_5 + \chi_2\chi_5{}^2 - 2\chi_1\chi_2\chi_6 + 5\chi_3\chi_6 + \chi_1{}^2\chi_4\chi_6 - 2\chi_2\chi_4\chi_6 \\
& - 3\chi_1\chi_5\chi_6 + 5\chi_6{}^2 + \chi_2\chi_7 + \chi_1\chi_2{}^2\chi_7 - \chi_1{}^2\chi_3\chi_7 - \chi_2\chi_3\chi_7 + \chi_1\chi_4\chi_7 \\
& + \chi_4{}^2\chi_7 - \chi_5\chi_7 + \chi_1\chi_2\chi_5\chi_7 - 2\chi_3\chi_5\chi_7 - \chi_2\chi_6\chi_7 - \chi_1\chi_7{}^2 + \chi_1\chi_3\chi_7{}^2 \\
& - \chi_4\chi_7{}^2 + \chi_7{}^3 - \chi_2{}^2\chi_8 + \chi_1\chi_3\chi_8 + \chi_4\chi_8 + \chi_1\chi_2\chi_4\chi_8 - 3\chi_3\chi_4\chi_8 \\
& - (\chi_1)^2\chi_5\chi_8 + \chi_2\chi_5\chi_8 + \chi_1\chi_4\chi_5\chi_8 + \chi_1\chi_6\chi_8 + (\chi_2)^2\chi_6\chi_8 \\
& - 2\chi_1\chi_3\chi_6\chi_8 - \chi_4\chi_6\chi_8 - 2\chi_3\chi_7\chi_8 + \chi_2\chi_4\chi_7\chi_8 + \chi_1\chi_5\chi_7\chi_8 - 5\chi_6\chi_7\chi_8 \\
& + \chi_2(\chi_7)^2\chi_8 - \chi_1\chi_4(\chi_8)^2 + \chi_3\chi_5(\chi_8)^2 - \chi_2\chi_6(\chi_8)^2 + \chi_4\chi_7(\chi_8)^2 + \chi_6(\chi_8)^3
\end{aligned} \tag{E.6}
$$

$$
\begin{aligned}
\chi_5^{E_8} = {}& 3 + 2\chi_2\chi_4 + \chi_4^3 + \chi_1^2\chi_5 + \chi_2^2\chi_5 - 2\chi_4\chi_5 + \chi_2\chi_5^2 + \chi_5^3 - 3\chi_6 + \chi_2^3\chi_6 - 3\chi_2\chi_4\chi_6 \\
& + \chi_2^2\chi_5\chi_6 - 4\chi_4\chi_5\chi_6 - 4\chi_2\chi_7 - 2\chi_2^2\chi_4\chi_7 + \chi_4^2\chi_7 + 2\chi_5\chi_7 + \chi_2\chi_4\chi_5\chi_7 \\
& + 2\chi_2\chi_6\chi_7 + \chi_2^2\chi_7^2 + \chi_4\chi_7^2 - 2\chi_2\chi_5\chi_7^2 + \chi_1^3(-1 + (-1 + \chi_3)\chi_6 + \chi_6^2 - \chi_5\chi_7) - \chi_2^2\chi_8 \\
& - \chi_2\chi_4^2\chi_8 - 2\chi_2\chi_5\chi_8 - \chi_5^2\chi_8 - 2\chi_2^2\chi_6\chi_8 + 6\chi_4\chi_6\chi_8 + 2\chi_7\chi_8 + 2\chi_2\chi_4\chi_7\chi_8 \\
& + \chi_4\chi_5\chi_7\chi_8 - \chi_2\chi_7^2\chi_8 + 2\chi_2\chi_8^2 + \chi_2^2\chi_4\chi_8^2 - \chi_4^2\chi_8^2 + \chi_2\chi_6\chi_8^2 - 4\chi_4\chi_7\chi_8^2 \\
& + \chi_2\chi_5\chi_7\chi_8^2 - \chi_8^3 - \chi_2\chi_4\chi_8^3 + \chi_4\chi_8^4 + \chi_3^2(8\chi_6 - 4\chi_7\chi_8 + \chi_8^3) + \chi_1^2(-\chi_5^2 + \chi_4\chi_6 + 2\chi_7 \\
& + \chi_3\chi_7 + \chi_3\chi_6\chi_7 + \chi_4^2\chi_8 - \chi_4\chi_7\chi_8 - \chi_3\chi_8^2 - \chi_6\chi_8^2 + \chi_2(-4\chi_5 + \chi_4\chi_7 + \chi_8) \\
& + \chi_5(\chi_7^2 - (-2 + 2\chi_3 + \chi_6)\chi_8)) + \chi_3(-3 + 8\chi_6^2 + 2\chi_2\chi_7 - 3\chi_5\chi_7 + \chi_7^3 + \chi_5^2\chi_8 + 4\chi_7\chi_8 + \chi_5\chi_8^2 \\
& - \chi_8^3 + \chi_4(-4\chi_5 + \chi_7^2 + 3\chi_8 - 2\chi_6\chi_8) + \chi_6(-3 - 2\chi_2\chi_7 - 6\chi_7\chi_8 + \chi_2\chi_8^2 + \chi_8^3)) \\
& + \chi_1(6\chi_3\chi_5 + \chi_4^2(-1 + \chi_6) + 3\chi_5\chi_6 - 2\chi_3\chi_5\chi_6 - \chi_5^2\chi_7 - \chi_7^2 - 2\chi_3\chi_7^2 - 3\chi_8 + \chi_3\chi_8 + \chi_6\chi_8 \\
& + \chi_3\chi_6\chi_8 - 2\chi_5\chi_7\chi_8 + \chi_3\chi_5\chi_7\chi_8 + \chi_5^2\chi_8^2 + \chi_7^2\chi_8^2 + \chi_2^2(-\chi_7 + \chi_5\chi_8) \\
& + \chi_4(-2\chi_7 + \chi_7^2\chi_8 - \chi_8(\chi_5 + (-2 + \chi_3 + 2\chi_6)\chi_8)) + \chi_2(2 - 4\chi_6^2 + 2\chi_5\chi_7 - \chi_7\chi_8 \\
& + \chi_3\chi_7\chi_8 - \chi_5\chi_8^2 + \chi_4(\chi_5 + (-2 + \chi_6)\chi_8) + \chi_6(4 - 6\chi_3 + \chi_7\chi_8)))
\end{aligned} \tag{E.7}
$$

$$
\begin{aligned}
\chi_6^{E_8} = {}& -1 + 3\chi_3 - \chi_2\chi_4 + \chi_1\chi_4^2 + \chi_1\chi_5 + \chi_2^2\chi_5 - 2\chi_1\chi_3\chi_5 - 2\chi_4\chi_5 + 3\chi_6 + \chi_1^3\chi_6 - 4\chi_1\chi_2\chi_6 \\
& + 6\chi_3\chi_6 + \chi_2\chi_4\chi_6 - \chi_1\chi_5\chi_6 + \chi_1^2\chi_3\chi_7 - 2\chi_2\chi_3\chi_7 - \chi_5\chi_7 + \chi_3\chi_5\chi_7 + \chi_1^2\chi_6\chi_7 - 2\chi_2\chi_6\chi_7 \\
& + \chi_4\chi_7^2 + 2\chi_1\chi_8 - 2\chi_1\chi_3\chi_8 + \chi_4\chi_8 + \chi_1\chi_2\chi_4\chi_8 - \chi_3\chi_4\chi_8 - \chi_1^2\chi_5\chi_8 + \chi_5^2\chi_8 - 2\chi_1\chi_6\chi_8 \\
& + \chi_1\chi_3\chi_6\chi_8 - 2\chi_4\chi_6\chi_8 + \chi_1\chi_2\chi_7\chi_8 - 4\chi_3\chi_7\chi_8 + \chi_1\chi_5\chi_7\chi_8 - \chi_1^2\chi_8^2 + \chi_2\chi_3\chi_8^2 \\
& - \chi_1\chi_4\chi_8^2 + \chi_2\chi_6\chi_8^2 + \chi_3\chi_8^3
\end{aligned} \tag{E.8}
$$

$$\chi_7^{E_8} = \chi_1{}^2\chi_7 + \chi_1\chi_3\chi_8 - 2\chi_1\chi_5 + \chi_1\chi_6\chi_8 + 2\chi_1\chi_8 - 4(\chi_1\chi_8 - 1) + 2\chi_2\chi_4$$
$$- 2\chi_2\chi_7 + \chi_2\chi_8{}^2 + \chi_3\chi_6 - \chi_3 - \chi_6 - 2 - \chi_2\chi_4 + \chi_1\chi_5 + \chi_5\chi_7 - \chi_4\chi_8 \tag{E.9}$$

$$\chi_8^{E_8} = -1 + \chi_3 + \chi_6 + \chi_1\chi_8 \tag{E.10}$$

$$\chi_4^{E_8} = -3 + 6\chi_3 - \chi_3^3 + \chi_1^5\chi_4 + \chi_4^3 + 5\chi_4\chi_5 - 3\chi_3\chi_4\chi_5 + \chi_5^3 + \chi_3\chi_5^3 + 6\chi_6 + 9\chi_3\chi_6 - 7\chi_3^2\chi_6$$
$$+ \chi_4^3\chi_6 - 3\chi_4\chi_5\chi_6 - 6\chi_3\chi_4\chi_5\chi_6 - 7\chi_3\chi_6^2 + 9\chi_3^2\chi_6^2 - \chi_6^3 + \chi_2^4\chi_7 + \chi_3\chi_4^2\chi_7$$
$$+ \chi_5\chi_7 + 2\chi_3\chi_5\chi_7 - 2\chi_3^2\chi_5\chi_7 - 2\chi_4^2\chi_6\chi_7 - 4\chi_5\chi_6\chi_7 + 4\chi_3\chi_5\chi_6\chi_7 + 3\chi_3\chi_4\chi_7^2$$
$$+ 2\chi_4\chi_6\chi_7^2 - \chi_7^3 - \chi_3\chi_7^3 + \chi_3^2\chi_7^3 - 4\chi_4\chi_8 - \chi_3\chi_4\chi_8 + 2\chi_3^2\chi_4\chi_8 - \chi_4^2\chi_5\chi_8$$
$$- 3\chi_5^2\chi_8 + \chi_3\chi_5^2\chi_8 - 7\chi_4\chi_6\chi_8 + 5\chi_3\chi_4\chi_6\chi_8 + 4\chi_4\chi_6^2\chi_8 - 3\chi_7\chi_8 - 6\chi_3\chi_7\chi_8$$
$$+ \chi_3^2\chi_7\chi_8 - \chi_4\chi_5\chi_7\chi_8 + \chi_3\chi_4\chi_5\chi_7\chi_8 + \chi_6\chi_7\chi_8 + 6\chi_3\chi_6\chi_7\chi_8 - 6\chi_3^2\chi_6\chi_7\chi_8$$
$$+ 5\chi_5\chi_7^2\chi_8 - 2\chi_3\chi_5\chi_7^2\chi_8 + \chi_4^2\chi_8^2 - \chi_3\chi_4^2\chi_8^2 + 2\chi_5\chi_8^2 - \chi_3\chi_5\chi_8^2 + \chi_3^2\chi_5\chi_8^2$$
$$+ \chi_4^2\chi_6\chi_8^2 + 5\chi_5\chi_6\chi_8^2 - 2\chi_3\chi_5\chi_6\chi_8^2 + 4\chi_4\chi_7\chi_8^2 - 3\chi_3\chi_4\chi_7\chi_8^2 - 4\chi_4\chi_6\chi_7\chi_8^2$$
$$+ \chi_7^2\chi_8^2 + \chi_8^3 + \chi_3\chi_8^3 + \chi_3^2\chi_8^3 - 2\chi_6\chi_8^3 - \chi_3\chi_6\chi_8^3 + \chi_3^2\chi_6\chi_8^3 - 5\chi_5\chi_7\chi_8^3 + \chi_3\chi_5\chi_7\chi_8^3$$
$$- \chi_4\chi_8^4 + \chi_4\chi_6\chi_8^4 + \chi_5\chi_8^5 + \chi_1^4((-1 + \chi_3)\chi_5 + \chi_7^2 - (1 + \chi_6)\chi_8) + \chi_2^2(3\chi_5\chi_6 - 3\chi_4\chi_7$$
$$+ \chi_5^2\chi_7 - 2\chi_4\chi_6\chi_7 + 3\chi_7^2 + \chi_6\chi_7^2 + 2\chi_8 - \chi_4\chi_5\chi_8 + \chi_6\chi_8 - 2\chi_6^2\chi_8 + \chi_4\chi_6\chi_8^2 - 4\chi_7\chi_8^2$$
$$+ \chi_8^4 + \chi_3(2\chi_5 + \chi_7^2 + \chi_8 - 2\chi_6\chi_8)) + \chi_2^3(-1 - \chi_6 + \chi_6^2 + \chi_5(-2\chi_7 + \chi_8^2)) + \chi_1^3(1 + \chi_6 + \chi_6^2$$
$$+ \chi_4^2\chi_7 - \chi_5\chi_7 - \chi_4\chi_8 - \chi_5^2\chi_8 - \chi_7\chi_8 + \chi_5\chi_8^2 + \chi_3(-2 - \chi_6 + \chi_6^2 - 2\chi_5\chi_7 + \chi_7\chi_8)$$
$$+ \chi_2(\chi_4(-5 + \chi_6) - \chi_6\chi_7 + \chi_8(\chi_5 + \chi_8))) + \chi_1^2(\chi_5^2 + \chi_3\chi_5^2 - \chi_5^2\chi_6 + 2\chi_3\chi_7 + 2\chi_3^2\chi_7$$
$$+ 3\chi_3\chi_6\chi_7 + \chi_3\chi_5\chi_7^2 + 2\chi_5\chi_8 + 3\chi_3\chi_5\chi_8 + \chi_4^2(-2 + \chi_6)\chi_8 + 4\chi_5\chi_6\chi_8 - 2\chi_3\chi_5\chi_6\chi_8$$
$$- \chi_7^2\chi_8 - \chi_3\chi_7^2\chi_8 - \chi_8^2 - 2\chi_3\chi_8^2 - 2\chi_6\chi_8^2 - \chi_5\chi_7\chi_8^2 + \chi_7\chi_8^3 + \chi_2^2(1 + \chi_5\chi_7 - \chi_7\chi_8)$$
$$+ \chi_4(2 + \chi_6^2 - 2\chi_5\chi_7 + \chi_7^2 - 2\chi_7\chi_8 + \chi_5\chi_8^2 + \chi_8^3 - \chi_3(-5 + 2\chi_6 + \chi_7\chi_8) - \chi_6(1 + 2\chi_7\chi_8))$$
$$+ \chi_2(-4\chi_7^2 + \chi_8 + 3\chi_3\chi_8 + 5\chi_6\chi_8 - 2\chi_3\chi_6\chi_8 + \chi_7\chi_8^2 + \chi_5(4 - 4\chi_3 - 3\chi_6 + \chi_4\chi_8 - \chi_7\chi_8)$$
$$+ \chi_4((2 + \chi_6)\chi_7 - \chi_8^2))) + \chi_2(\chi_5^2\chi_6 + 4\chi_3^2\chi_7 - 6\chi_6\chi_7 + 4\chi_6^2\chi_7 - 3\chi_5\chi_7^2 + \chi_7^4 - \chi_5\chi_8$$
$$- 3\chi_5\chi_6\chi_8 - 2\chi_5^2\chi_7\chi_8 + \chi_7^2\chi_8 - 4\chi_6\chi_7^2\chi_8 + 2\chi_6\chi_8^2 + 2\chi_6^2\chi_8^2 + 2\chi_5\chi_7\chi_8^2 + \chi_5^2\chi_8^3$$
$$+ \chi_4^2(\chi_7^2 + \chi_8 - 2\chi_6\chi_8) + \chi_4(1 - 2\chi_6^2 + 3\chi_5\chi_7 - 2\chi_7^3 + \chi_5^2\chi_8 + 4\chi_7\chi_8 - 2\chi_5\chi_8^2 + \chi_7^2\chi_8^2$$
$$- \chi_8^3 + \chi_3(-4 + 4\chi_6 - 2\chi_7\chi_8) + \chi_6(2 + 4\chi_7\chi_8 - 2\chi_8^3)) + \chi_3(-2\chi_5^2 + 2\chi_7^2\chi_8 + 3\chi_6\chi_8^2$$
$$+ \chi_5(-2\chi_7^2 + 3\chi_8 + \chi_7\chi_8^2) - \chi_7(6 + 5\chi_6 + \chi_8^3))) + \chi_1(-4\chi_5 - 7\chi_3\chi_5 + 4\chi_3^2\chi_5 - \chi_5\chi_6 + 5\chi_3\chi_5\chi_6$$
$$+ 2\chi_5\chi_6^2 + \chi_5^2\chi_7 - 2\chi_3\chi_5^2\chi_7 + 2\chi_7^2 + \chi_3\chi_7^2 - 2\chi_3^2\chi_7^2 + \chi_6\chi_7^2 - 2\chi_3\chi_6\chi_7^2 + 4\chi_8$$
$$- 2\chi_3\chi_8 - 5\chi_3^2\chi_8 + \chi_2^3(-1 + \chi_6)\chi_8 - 2\chi_6\chi_8 - 10\chi_3\chi_6\chi_8 + 4\chi_3^2\chi_6\chi_8 - 5\chi_6^2\chi_8$$
$$+ 4\chi_3\chi_6^2\chi_8 + \chi_5\chi_7\chi_8 - \chi_7^3\chi_8 + \chi_3\chi_7^3\chi_8 - 2\chi_5^2\chi_8^2 + \chi_3\chi_5^2\chi_8^2 + \chi_7\chi_8^3 + 5\chi_3\chi_7\chi_8^3$$
$$+ 3\chi_6\chi_7\chi_8^3 - 2\chi_3\chi_6\chi_7\chi_8^3 - \chi_5\chi_8^3 - \chi_8^4 - \chi_3\chi_8^4 + \chi_4^2(-3 + \chi_6 + \chi_5\chi_7 + \chi_7\chi_8 - \chi_8^3)$$
$$+ \chi_2^2((1 - 4\chi_3 + 2\chi_6)\chi_7 - \chi_8(5\chi_5 - \chi_5\chi_6 + \chi_8 + \chi_6\chi_8) + \chi_4(5 - 2\chi_6 + \chi_7\chi_8)) - \chi_4(\chi_5^2 - (-5 + \chi_3)\chi_7^2\chi_8$$
$$+ (-2 + 2\chi_3(-2 + \chi_6) - 3\chi_6)\chi_8^2 + \chi_5(\chi_7^2 + 2(-2 + \chi_3 + \chi_6)\chi_8 - \chi_7\chi_8^2) + \chi_7(1 + 3\chi_3 - 3\chi_6 - \chi_8^3))$$
$$+ \chi_2(-3 - 6\chi_6 + \chi_6^2 - 2\chi_4^2\chi_7 + 4\chi_5\chi_7 - 2\chi_5\chi_6\chi_7 + \chi_5^2\chi_8 + 4\chi_7\chi_8 + \chi_6\chi_7\chi_8 + \chi_5\chi_7^2\chi_8$$
$$- 2\chi_5\chi_8^2 - \chi_5\chi_6\chi_8^2 - \chi_7^2\chi_8^2 - \chi_8^3 + \chi_6\chi_8^3 + \chi_3(1 - 6\chi_6^2 + 4\chi_5\chi_7 + \chi_7\chi_8 - 2\chi_5\chi_8^2$$
$$+ \chi_6(6 + \chi_7\chi_8)) + \chi_4(\chi_8 - \chi_7\chi_8^2 + \chi_5(-1 + \chi_6 + \chi_7\chi_8)))). \tag{E.11}$$

F Relation among the parameters for E_7 SW curve

In this section, we clarify the the relation among various parameters appearing in the E_7 SW curve. They are basically related by change of the basis of the simple roots. First,

we would like to write E_7 parameters in terms of 6 masses m'_i, $(i = 1, \cdots 6)$ and 1 gauge coupling $m'_0 = 1/(2g^2)$. Here we put prime so that we distinguish them with the parameters m_i related to $SU(8)$. Since the mass parameters are related to $SO(12)$ subgroup of E_7, we should decompose E_7 into $SO(12) \times SU(2)$. In this case, it is convenient to choose the simple roots as

$$
\begin{aligned}
&\alpha_1 = \mathbf{e}_1 - \mathbf{e}_2, \qquad \alpha_2 = \mathbf{e}_2 - \mathbf{e}_3, \qquad \alpha_3 = \mathbf{e}_3 - \mathbf{e}_4, \\
&\alpha_4 = \mathbf{e}_4 - \mathbf{e}_5, \qquad \alpha_5 = \mathbf{e}_5 + \mathbf{e}_6, \qquad \alpha_6 = \mathbf{e}_5 - \mathbf{e}_6, \\
&\alpha_7 = -\frac{1}{2}\left(\mathbf{e}_1 + \mathbf{e}_2 + \mathbf{e}_3 + \mathbf{e}_4 + \mathbf{e}_5 - \mathbf{e}_6 + \sqrt{2}\mathbf{e}_7\right), \\
&\alpha_{-\gamma} = \sqrt{2}\mathbf{e}_7.
\end{aligned}
\tag{F.1}
$$

where $\mathbf{e}_i$ are the orthonormal basis of the root lattice. The root $\alpha_{-\gamma}$ corresponds to the extra node of the extended Dynkin diagram. The $SO(12) \times SU(2)$ subgroup is given by removing the root α_7. In this convention, the weights of the fundamental representation of $SO(12)$ are given by $\pm\mathbf{e}_i$ $(i = 1, \cdots, 6)$. When we compute the character, it is possible to parametrize the element of the Cartan subalgebra in such a way that the state with the weight $\pm\mathbf{e}_i$ has the eigenvalue $\pm m'_i$. In this sense, we can identify the vector $\mathbf{e}_i$ with the mass parameter m'_i $(i = 1, \cdots, 6)$. Analogously, we identify the vector $\mathbf{e}_7$ with the gauge coupling m'_0.

On the other hand, when we decompose E_7 into its subgroup $SU(8)$, it is natural to choose the simple roots as

$$
\begin{aligned}
&\alpha_1 = \mathbf{e}'_1 - \mathbf{e}'_2, \qquad \alpha_2 = \mathbf{e}'_2 - \mathbf{e}'_3, \qquad \alpha_3 = \mathbf{e}'_3 - \mathbf{e}'_4, \qquad \alpha_4 = \mathbf{e}'_4 - \mathbf{e}'_5, \\
&\alpha_5 = -\frac{1}{2}\left(\mathbf{e}'_1 + \mathbf{e}'_2 + \mathbf{e}'_3 + \mathbf{e}'_4 - \mathbf{e}'_5 - \mathbf{e}'_6 - \mathbf{e}'_7 - \mathbf{e}'_8\right), \\
&\alpha_6 = \mathbf{e}'_5 - \mathbf{e}'_6, \qquad \alpha_7 = \mathbf{e}'_6 - \mathbf{e}'_7, \qquad \alpha_{-\gamma} = \mathbf{e}'_7 - \mathbf{e}'_8.
\end{aligned}
\tag{F.2}
$$

where we used the different orthonormal basis $\mathbf{e}'_i$. The $SU(8)$ subgroup is obtained by removing the root α_5. We identify the vector $\mathbf{e}'_i$ with the parameters m_i.

Still another choice is the case when we decompose E_7 into its subgroup $SU(4) \times SU(4) \times SU(2)$;

$$
\begin{aligned}
&\alpha_1 = \mathbf{e}''_1 - \mathbf{e}''_2, \qquad \alpha_2 = \mathbf{e}''_2 - \mathbf{e}''_3, \qquad \alpha_3 = \mathbf{e}''_3 - \mathbf{e}''_4, \\
&\alpha_4 = -\frac{1}{4}\left(\mathbf{e}''_1 + \mathbf{e}''_2 + \mathbf{e}''_3 - 3\mathbf{e}''_4 + 2\mathbf{e}''_5 - 2\mathbf{e}''_6 + 3\mathbf{e}''_7 - \mathbf{e}''_8 - \mathbf{e}''_9 - \mathbf{e}''_{10}\right) \\
&\alpha_5 = \mathbf{e}''_5 - \mathbf{e}''_6, \quad \alpha_6 = \mathbf{e}''_7 - \mathbf{e}''_8, \quad \alpha_7 = \mathbf{e}''_8 - \mathbf{e}''_9, \quad \alpha_{-\gamma} = \mathbf{e}''_9 - \mathbf{e}''_{10}.
\end{aligned}
\tag{F.3}
$$

where we used the still different orthonormal basis $\mathbf{e}''_i$. We find the correspondence between the orthonormal basis $\mathbf{e}''_i$ and the parameters L_i, M_j and N_k as

$$
L_i : \mathbf{e}''_i, \qquad N_i : \mathbf{e}''_{i+4}, \qquad M_i : \mathbf{e}''_{i+6}.
\tag{F.4}
$$

The relation between these parameters is obtained by equating the parameters corresponding to the corresponding simple roots. For example, α_1 corresponds to $m'_1 - m'_2$ in the $SO(12) \times SU(2)$ parameters and $m_1 - m_2$ in the $SU(8)$ parameters, respectively, and

thus we equate these two. In this way, we find 7 independent equations in total and the relation between them are obtained by solving them.

The parameters used in the Seiberg-Witten curve is actually the exponentiated values. Therefore, we define $\widetilde{m}_i = \exp(-\beta m_i)$, $q = \exp(-\beta m_0')$ and so on, where β is the circumference of the compactified circle. Then, the relation between $SU(8)$ parameters $\widetilde{m}_i$ and the $SO(12) \times SU(2)$ parameters $\widetilde{m}_i'$, q are

$$\widetilde{m}_i = \frac{\widetilde{m}_i'}{\prod_{i=1}^{6} \widetilde{m}_i'^{\frac{1}{4}}} \quad (i = 1, \cdots 6)$$

$$\widetilde{m}_7 = q^{\frac{1}{2}} \prod_{i=1}^{6} \widetilde{m}_i'^{\frac{1}{4}}, \qquad \widetilde{m}_8 = q^{-\frac{1}{2}} \prod_{i=1}^{6} \widetilde{m}_i'^{\frac{1}{4}}. \tag{F.5}$$

The relation between $SU(8)$ parameters $\widetilde{m}_i$ and the $SU(4) \times SU(4) \times SU(2)$ parameters L_i, M_i, N_i are

$$\widetilde{m}_i = N_2^{\frac{1}{2}} L_i, \qquad \widetilde{m}_{i+4} = N_1^{\frac{1}{2}} M_i \qquad (i = 1, 2, 3, 4). \tag{F.6}$$

This is exactly what we have already obtained in (3.19).

G Maximal Compact Subgroups via Hanany-Witten transitions

Here we discuss various toric like diagrams for $5 \leq N_f \leq 7$ flavors showing maximal compact subgroups for E_{N_f+1} via the Hanany-Witten transition which we mentioned in the main text[13]. Since we use (p, q) 5-brane web diagram, maximal compact subgroups of E_{N_f+1} are restricted to those of type A_N. As there are many ways of getting to diagram showing the subgroup symmetry, we simply list a representative toric-like diagram of type A_N below.

G.1 $N_f = 5$ or E_6 case

The $N_f = 5$ case has two maximal compact subgroups of type A_N, which are

$$E_6 \supset SU(3) \times SU(3) \times SU(3), \tag{G.1}$$

$$E_6 \supset SU(6) \times SU(2). \tag{G.2}$$

As already discussed, the first one is dictated from the T_3 diagram as in Figure 1. A toric-like diagram for the second maximal subgroup is given in Figure 34.

G.2 $N_f = 6$ or E_7 case

The $N_f = 6$ case has three maximal compact subgroups of type A_N, which are

$$E_7 \supset SU(4) \times SU(4) \times SU(2), \tag{G.3}$$

$$E_7 \supset SU(8), \tag{G.4}$$

$$E_7 \supset SU(6) \times SU(3), \tag{G.5}$$

whose toric-like diagrams are given in Figure 7, in Figure 9 and in Figure 20, respectively.

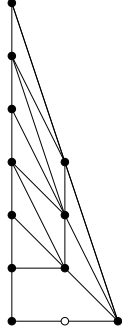[13]The authors thank Amihay Hanany suggesting to explore all possible subgroups.

Figure 34. A toric-like diagram for the $SU(2)$ theory with $N_f = 5$ flavors of $SU(6) \times SU(2) \subset E_6$ symmetry

G.3 $N_f = 7$ or E_8 case

The $N_f = 8$ case has four maximal compact subgroups of type A_N, which are

$$E_8 \supset SU(6) \times SU(3) \times SU(2), \tag{G.6}$$
$$E_8 \supset SU(9), \tag{G.7}$$
$$E_8 \supset SU(8) \times SU(2), \tag{G.8}$$
$$E_8 \supset SU(5) \times SU(5). \tag{G.9}$$

The first two are given in Figure 15 and in Figure 17, respectively. The toric-like diagram for (G.8) is given in Figure 35:
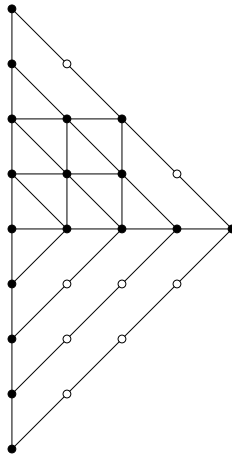

Figure 35. A toric-like diagram of $SU(2)$ theory with $N_f = 7$ flavors of $SU(8) \times SU(2) \subset E_8$ symmetry

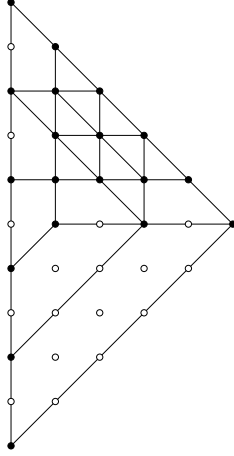The toric-like diagram for (G.9) is given in Figure 36:

Figure 36. A toric-like diagram of $SU(2)$ theory with $N_f = 7$ flavors of $SU(5) \times SU(5) \subset E_8$ symmetry

.

References

[1] E. Witten, "Solutions of four-dimensional field theories via M theory," *Nucl.Phys.* **B500** (1997) 3–42, `arXiv:hep-th/9703166 [hep-th]`.

[2] A. Brandhuber, N. Itzhaki, J. Sonnenschein, S. Theisen, and S. Yankielowicz, "On the M theory approach to (compactified) 5-D field theories," *Phys.Lett.* **B415** (1997) 127–134, `arXiv:hep-th/9709010 [hep-th]`.

[3] O. Aharony, A. Hanany, and B. Kol, "Webs of (p,q) five-branes, five-dimensional field theories and grid diagrams," *JHEP* **9801** (1998) 002, `arXiv:hep-th/9710116 [hep-th]`.

[4] I. Brunner and A. Karch, "Branes and six-dimensional fixed points," *Phys.Lett.* **B409** (1997) 109–116, `arXiv:hep-th/9705022 [hep-th]`.

[5] O. Aharony and A. Hanany, "Branes, superpotentials and superconformal fixed points," *Nucl.Phys.* **B504** (1997) 239–271, `arXiv:hep-th/9704170 [hep-th]`.

[6] N. Seiberg, "Five-dimensional SUSY field theories, nontrivial fixed points and string dynamics," *Phys.Lett.* **B388** (1996) 753–760, `arXiv:hep-th/9608111 [hep-th]`.

[7] H.-C. Kim, S.-S. Kim, and K. Lee, "5-dim Superconformal Index with Enhanced En Global Symmetry," *JHEP* **1210** (2012) 142, `arXiv:1206.6781 [hep-th]`.

[8] C. Hwang, J. Kim, S. Kim, and J. Park, "General instanton counting and 5d SCFT," `arXiv:1406.6793 [hep-th]`.

[9] V. Mitev, E. Pomoni, M. Taki, and F. Yagi, "Fiber-Base Duality and Global Symmetry Enhancement," `arXiv:1411.2450 [hep-th]`.

[10] S. Katz, P. Mayr, and C. Vafa, "Mirror symmetry and exact solution of 4-D N=2 gauge theories: 1.," *Adv.Theor.Math.Phys.* **1** (1998) 53–114, `arXiv:hep-th/9706110 [hep-th]`.

[11] L. Bao, E. Pomoni, M. Taki, and F. Yagi, "M5-Branes, Toric Diagrams and Gauge Theory Duality," *JHEP* **1204** (2012) 105, `arXiv:1112.5228 [hep-th]`.

[12] L. Bao, E. Pomoni, M. Taki, and F. Yagi, "M5-branes, toric diagrams and gauge theory duality," *Int.J.Mod.Phys.Conf.Ser.* **21** (2013) 136–137.

[13] J. A. Minahan and D. Nemeschansky, "An N=2 superconformal fixed point with E(6) global symmetry," *Nucl.Phys.* **B482** (1996) 142–152, `arXiv:hep-th/9608047 [hep-th]`.

[14] J. A. Minahan and D. Nemeschansky, "Superconformal fixed points with E(n) global symmetry," *Nucl.Phys.* **B489** (1997) 24–46, `arXiv:hep-th/9610076 [hep-th]`.

[15] J. Minahan, D. Nemeschansky, and N. Warner, "Investigating the BPS spectrum of noncritical E(n) strings," *Nucl.Phys.* **B508** (1997) 64–106, `arXiv:hep-th/9705237 [hep-th]`.

[16] T. Eguchi and K. Sakai, "Seiberg-Witten curve for the E string theory," *JHEP* **0205** (2002) 058, `arXiv:hep-th/0203025 [hep-th]`.

[17] T. Eguchi and K. Sakai, "Seiberg-Witten curve for E string theory revisited," *Adv.Theor.Math.Phys.* **7** (2004) 419–455, `arXiv:hep-th/0211213 [hep-th]`.

[18] N. C. Leung and C. Vafa, "Branes and toric geometry," *Adv.Theor.Math.Phys.* **2** (1998) 91–118, `arXiv:hep-th/9711013 [hep-th]`.

[19] T. Eguchi and H. Kanno, "Five-dimensional gauge theories and local mirror symmetry," *Nucl.Phys.* **B586** (2000) 331–345, `arXiv:hep-th/0005008 [hep-th]`.

[20] F. Benini, S. Benvenuti, and Y. Tachikawa, "Webs of five-branes and N=2 superconformal field theories," *JHEP* **0909** (2009) 052, `arXiv:0906.0359 [hep-th]`.

[21] D. Gaiotto, "N=2 dualities," *JHEP* **1208** (2012) 034, `arXiv:0904.2715 [hep-th]`.

[22] O. DeWolfe, A. Hanany, A. Iqbal, and E. Katz, "Five-branes, seven-branes and five-dimensional E(n) field theories," *JHEP* **9903** (1999) 006, `arXiv:hep-th/9902179 [hep-th]`.

[23] M. Taki, "Seiberg Duality, 5d SCFTs and Nekrasov Partition Functions," `arXiv:1401.7200 [hep-th]`.

[24] L. Bao, V. Mitev, E. Pomoni, M. Taki, and F. Yagi, "Non-Lagrangian Theories from Brane Junctions," *JHEP* **1401** (2014) 175, `arXiv:1310.3841 [hep-th]`.

[25] H. Hayashi, H.-C. Kim, and T. Nishinaka, "Topological strings and 5d T_N partition functions," *JHEP* **1406** (2014) 014, `arXiv:1310.3854 [hep-th]`.

[26] H. Hayashi and G. Zoccarato, "Exact partition functions of Higgsed 5d T_N theories," `arXiv:1409.0571 [hep-th]`.

[27] O. Bergman and G. Zafir, "Lifting 4d dualities to 5d," `arXiv:1410.2806 [hep-th]`.

[28] M.-X. Huang, A. Klemm, and M. Poretschkin, "Refined stable pair invariants for E-, M- and $[p,q]$-strings," *JHEP* **1311** (2013) 112, `arXiv:1308.0619 [hep-th]`.

[29] R. Feger and T. W. Kephart, "LieART - A Mathematica Application for Lie Algebras and Representation Theory," `arXiv:1206.6379 [math-ph]`.

[30] LiE: http://wwwmathlabo.univ-poitiers.fr/∼maavl/LiE/
LieLink: https://github.com/teake/LieLink

[31] R. M. Fonseca, "Calculating the renormalisation group equations of a SUSY model with Susyno," *Comput.Phys.Commun.* **183** (2012) 2298–2306, `arXiv:1106.5016 [hep-ph]`.

[32] A. Iqbal and C. Vafa, "BPS Degeneracies and Superconformal Index in Diverse Dimensions," *Phys.Rev.* **D90** (2014) no. 10, 105031, `arXiv:1210.3605 [hep-th]`.

[33] H. Hayashi, Y. Tachikawa, and K. Yonekura, "Mass-deformed T_N as a linear quiver," `arXiv:1410.6868 [hep-th]`.

[34] M. Isachenkov, V. Mitev, and E. Pomoni, "Toda 3-Point Functions From Topological Strings II," `arXiv:1412.3395 [hep-th]`.

[35] P. C. Argyres and N. Seiberg, "S-duality in N=2 supersymmetric gauge theories," *JHEP* **0712** (2007) 088, `arXiv:0711.0054 [hep-th]`.

[36] T. Eguchi and K. Maruyoshi, "Penner Type Matrix Model and Seiberg-Witten Theory," *JHEP* **1002** (2010) 022, `arXiv:0911.4797 [hep-th]`.